SEEPAGE NEAR FOUNDATIONS AND OTHER IMPERMEABLE BARRIERS

by

Arthur Will Warrick

A Dissertation Submitted to the
Graduate Faculty in Partial Fulfillment of
The Requirements for the Degree of
DOCTOR OF PHILOSOPHY

Major Subject: Soil Physics

Approved:

Signature was redacted for privacy.

In Charge of Major Work

Signature was redacted for privacy.

Head of Major Department

Signature was redacted for privacy.

Dean of Graduate College

Iowa State University
Of Science and Technology
Ames, Iowa

1967

TABLE OF CONTENTS

I. INTRODUCTION

This thesis solves theoretical problems of soil water seepage to drains near foundations and other impermeable barriers. Although many solutions in the past have been presented for seepage below dams and around cutoffs, little work has been completed on flow to drains near foundations or basements. Here, solutions are obtained for 14 foundation problems and two related problems in agricultural field drainage. In these problems the flow regions are rectilinear. Angles at the corners of the regions are either 90 or 270 degrees. Some of the boundary lines of the flow regions extend to infinity. In the 14 foundation problems, one, two or more tile drains are situated near the foundation base or side. In the two field drainage problems, seepage of ponded water to ditch drains is investigated.

In solving the problems Schwartz-Christoffel conformal transformations are used. It is assumed that the reader has some knowledge of complex variable theory. Nevertheless, a brief description of the Schwartz-Christoffel transformation is given as well as numerous references to help the reader with details in the theoretical developments.

Exact analytical expressions are obtained for all problems studied, although in some cases the inverse transformations of the analytical expressions are not found in an explicit form. In some cases numerical calculations are carried out. To avoid unnecessary tedious hand calculations, frequent use of a digital computer (IBM, model 50) was made.

The primary objective here is to provide exact solutions to a variety of seepage problems which apparently up to now have not been solved. A

secondary objective is to stimulate interest in using conformal transformations to solve soil water flow problems. Types of flow problems that can be solved will be illustrated and methods for solving them will be given.

II. LITERATURE REVIEW

Literature of drainage and ground water flow is plentiful. Luthin (1957) edited a book in which more than 600 references to drainage literature were cited; van Schilfgaarde, Kirkham, and Frevert (1956) gave 61; more recently Kirkham (1966) gave 62 and Luthin (1966) gave more than 150. Numerous references treating ground water seepage are given by Muskat (1946) in his classical treatise on flow of homogeneous fluids through porous media. Harr (1962), Leliavsky (1955), and Polubarinova-Kochina (1962) give many references related to ground water flow, especially as regards hydraulic structures. Each of the last three books contains many references to the Russian literature.

Ground water seepage and drainage problems may be divided into steady and nonsteady-state problems. In the strictest sense, all flow systems are dependent on time and therefore exist in a nonsteady state. Many flow systems, however, vary slowly with time and may be treated as idealized steady-state problems. Because we have chosen to solve problems of steady-state seepage, the literature review will be primarily on steady-state theories.

Two approaches are commonly used to study flow problems: direct mathematical analysis and utilization of models. In most cases Darcy's law is assumed valid, that is, the flow velocity is assumed to be related to the hydraulic gradient by

$$v = ki \tag{1}$$

where v is the amount of flow taking place per unit time per unit area perpendicular to flow, k is the hydraulic conductivity and i is the hydraulic gradient. The hydraulic gradient is the negative change in

hydraulic head, ϕ, per unit length in the direction of flow. Harr (1962) illustrates how Darcy's law may be deduced from Bernoulli's equation by accounting for the loss of energy due to the viscous resistance of individual pores and neglecting the velocity head relative to the pressure head and elevation head. The range of validity of Darcy's law is closely associated with the Reynolds number R defined by

$$R = vD\rho/N \tag{2}$$

where v is the discharge velocity, D the average of diameters of soil particles, ρ the density of fluid, and N the coefficient of viscosity. It is generally accepted that for R less than unity the flow in soils is laminar and that Darcy's law is valid. A detailed discussion of the "law of flow" and a summary of investigations are found in Muskat (1946). It is pointed out by Harr (1962) that it is unlikely that the range of Darcy's law will be exceeded in natural seepage flow situations and that the laminar flow encountered in soil water movement under saturated flow conditions represents one of the few valid examples of laminar flow in all hydraulic engineering.

The velocity potential $\bar{\phi}$ is defined by

$$\bar{\phi}(x,y,z) = k\bar{\phi} \tag{3}$$

where ϕ is the hydraulic head given by

$$\phi = p/\rho g - y \tag{4}$$

where ρ is the unit density of water, g is the acceleration constant and y is taken to be vertically downward. The flow velocities in the x, y, and z direction are respectively

$$v_x = -k\partial\phi/\partial x \tag{5a}$$

$$v_y = -k\partial\phi/\partial y \tag{5b}$$

$$v_z = -k\partial\phi/\partial z \tag{5c}$$

For saturated steady-state flow of a non-compressible fluid through an isotropic medium it follows from continuity of mass considerations that Laplace's equation is satisfied by the hydraulic head (as well as by the velocity potential):

$$\partial^2\phi/\partial x^2 + \partial^2\phi/\partial y^2 + \partial^2\phi/\partial z^2 = 0 \tag{6}$$

For a two-dimensional problem Laplace's equation is also satisfied by the stream function $\psi(x,y)$, that is

$$\partial^2\psi/\partial x^2 + \partial^2\psi/\partial y^2 = 0 \tag{7}$$

where $\psi(x,y)$ is the conjugate harmonic of $k\,\phi(x,y)$ and can be defined by the Cauchy-Riemann relations

$$k\,\partial\phi/\partial x = \partial\psi/\partial y \tag{8a}$$

$$k\,\partial\phi/\partial y = -\partial\psi/\partial x \tag{8b}$$

Darcy's law for isotropic saturated flow leads to a reduction of the problems to forms to which apply the classical methods of potential theory. It follows that there are analogies to ground water flow problems in other areas of mathematical physics and that the results from studies of the other physical systems can be applied to saturated flow problems. The analogies allow a variety of systems for model studies. Muskat (1946) tabulates the correspondence between the hydrodynamics of the steady-state fluid flow through porous media and the problems of steady-state heat flow, electrostatics, and current flow in continuous conductors. Table 1 is a tabulation of five corresponding systems including gas diffusion and steady-state ground water flow. To this list could be added magnetism, gravitational fields, and elasticity as noted on page 26 of Bewley (1948).

Table 1. Correspondences between five analogous potential problems

Steady-state ground water flow	Heat conduction	Electrostatics	Current conduction	Diffusion
Hydraulic head: ϕ	Temperature: u	Electrostatic potential: ϕ	Voltage potential: V	Concentration: c
Negative hydraulic gradient: $-\text{grad}\ \phi$	Negative temperature gradient: $-\text{grad}\ u$	Field-strength vector: $-\text{grad}\ \phi$	Negative potential gradient: $-\text{grad}\ V$	Negative concentration gradient: $-\text{grad}\ c$
Hydraulic conductivity: k	Thermal conductivity: k	(Dielectric constant)/4π: $\varepsilon/4\pi$	Specific conductivity: σ	Diffusion coefficient: D
Velocity vector: $\bar{v} = -k\ \text{grad}\ \phi$ (Darcy's law)	Rate of heat transfer: $\bar{q} = -k\ \text{grad}\ u$ (Fourier's law)	Dielectric displacement: $(\varepsilon/4\pi)\bar{E} = -(\varepsilon/4\pi)\text{grad}\ \phi$ (Maxwell's law of dielectric displacement)	Current vector: $\bar{I} = -\sigma\ \text{grad}\ V$ (Ohm's law)	Rate of diffusion: $\bar{q} = -D\ \text{grad}\ c$ (Fick's law)
Equipotential surface: $\phi = \text{const.}$	Isothermal surface: $u = \text{const.}$	Equipotential surface: $\phi = \text{const.}$	Equipotential surface: $v = \text{const.}$	Lines of equal concentration: $c = \text{const.}$
Impermeable barrier or streamline: $\partial\phi/\partial n = 0$	Insulated surface or line of heat flow: $\partial u/\partial n = 0$	A tube or line of force: $\partial\phi/\partial n = 0$	Insulated surface or tube or line of flow: $\partial V/\partial n = 0$	Impermeable barrier or tube or line of flow: $\partial c/\partial n = 0$

Most rigorous mathematical analyses of flow problems are based on the potential theory as just introduced. Potential problems may be solved utilizing methods such as Fourier analysis, conformal transformations, image methods, or numerical analysis.

Fourier analysis includes use of infinite series of orthogonal functions and the use of integral transforms. Kirkham (1958) presents formulas and flow nets for steady rainfall or excess irrigation seeping into drains in soil underlain by a barrier. He first solved for the stream function using Fourier sine and cosine series and then for the potential function using the Cauchy-Riemann relations. Toksoz and Kirkham (1961) have developed nomographs and tables giving maximum water table heights where the water table intercepts the drain tube. Wesseling (1964) and Warrick (1966) give tables to evaluate maximum water table heights for continually submerged drain tubes. Hinesly and Kirkham (1966) solved the same problem using Fourier series, but where the rainfall water was reinforced with the simultaneous upward seepage of artesian water. Warrick (1964) used a Fourier sine transform to solve the same problem for drains which were completely below the water table and where the depth of the aquifer or an impermeable barrier was at a great depth. Powers, et al. (1967, 1968) used generalized orthonormal functions to solve the problem of surface water moving into and through water-saturated soil bedding and also for steady rainfall seeping through soil into drainage ditches of unequal height. The last two references are unique in that for each, the flow medium for which the boundary conditions were set up was not a rectangle, but was a quadrilateral with two right angles only.

The technique of conformal mapping has proved to be a powerful tool for solving two-dimensional ground water flow problems. The basic principal is to use analytic functions of complex variables to mathematically transform flow regions to simpler geometries from which the solution is easier to determine. The complex potential functions defined by

$$w(z) = k\phi + i\psi \tag{9}$$

where

$$z = x + iy \tag{10}$$

is of fundamental importance. Once $w(z)$ is determined, the basic flow characteristics such as streamlines, flow velocities, and pressure distributions can, at least in principle, be obtained. Churchill (1960) uses conformal transformations to solve several examples of elementary heat conduction, electrostatic potential, and fluid flow problems.

Three special mapping techniques as described in Harr (1962) have proved useful and valuable in conformal mappings of flow regions. They are the velocity hodograph, the Zhukovsky functions, and the Schwartz-Christoffel transformation.

The complex velocity W may be defined by

$$W = dw/dz \tag{11}$$

or

$$W = -v_x + iv_y \tag{12}$$

where w is the previously defined complex potential function, the physical flow region is the z-plane (x,y-plane), and v_x and v_y are the previously defined velocities in the x and y directions respectively. The transformation of the region of flow from the z-plane into the W-plane is called the velocity hodograph and is found to be particularly useful in

solving problems with a free water surface. Although the shape of the free water surface is often unknown originally, the hodograph in the W-plane may be completely defined. Numerous examples using the hodograph are worked out in Polubarinova-Kochina (1962), Harr (1962), and Muskat (1946), many dealing with seepage through porous dams and from canal ditches or other hydraulic structures. Van Deemter (1949, 1950) used a velocity hodograph in solving a tile drainage problem where rainfall and or deep artesian flow maintained a curved water table above the level of parallel drains and where the permeable soil was assumed to extend to a great depth. Fukuda (1957) utilizes a hodograph in determining theoretical equations for the quantity of water in saturated soil seeping per unit time from a plane water table into equally spaced ditches with vertical walls. For purposes of his analysis, he assumed that the depth of water in the ditches was zero and that the width of the ditches was zero. DeJong (1965), in using the hodograph method for determining patterns of flow of ground water in a coastal aquifer to a drain, found that the hodograph was double valued; nevertheless, he solved the two-fluid case of fresh water flowing over stationary salt water.

The Zhukovsky function Z as defined by Harr (1962) and Polubarinova-Kochina (1962) is

$$Z = C(w - ikz) \qquad (13)$$

where C is an arbitrary constant. Others such as Van Deemter (1949) have used the same function, but have not referred to it by a special name. If the constant C is taken to be unity and the real and imaginary parts of the right-hand-side (r.h.s.) of Equation 13 are separated, we have

$$Z = k(\phi + y) + i(\psi - kx) \qquad (14)$$

We observe that along a free surface if ϕ is $-y$ then the real part of Z is zero. As pointed out by Polubarinova-Kochina (1962), Zhukovsky functions are useful for a system where in addition to a free surface, we have horizontal equipotential and vertical streamlines for flow boundaries. This is verified by observing for horizontal equipotentials, the real part of Z in Equation 14 is a constant and for vertical streamlines the imaginary part is constant. Thus, all of the boundaries for such a system would transform to rectangular regions in the Z-plane. Polubarinova-Kochina solves several free-water surface problems with the aid of Zhukovsky functions.

The Schwartz-Christoffel transformation is a well known and powerful technique useful in conformal transformations to map a polygon of n sides of one plane onto the upper half of a second plane. Let πk_A, πk_B,... be exterior angles of the polygon at points A, B,... as in Figure 1. Then the transformation which maps the interior of the polygon ABCDE of the z-plane of Figure 1 conformally onto the upper half of the t-plane is

$$z(t) = M \int (t - a)^{-k_A}(t - b)^{-k_B}(t - c)^{-k_C}(t - d)^{-k_D}(t - e)^{-k_E}\, dt + N \qquad (15)$$

The points A, B, C, D, and E in the z-plane correspond to the points a, b, c, d, and e respectively in the t-plane. Any of the points a, b, c, d, or e can be taken at infinity in the t-plane by leaving the corresponding factor, say $(t - a)^{-k_A}$, out of the transformation. It can be shown as in Churchill (1960) that three of the numbers a, b, c, etc. for any polygon, or three independent conditions on these numbers, may be chosen arbitrarily. Often the limitation in applying Equation 15 is in carrying out

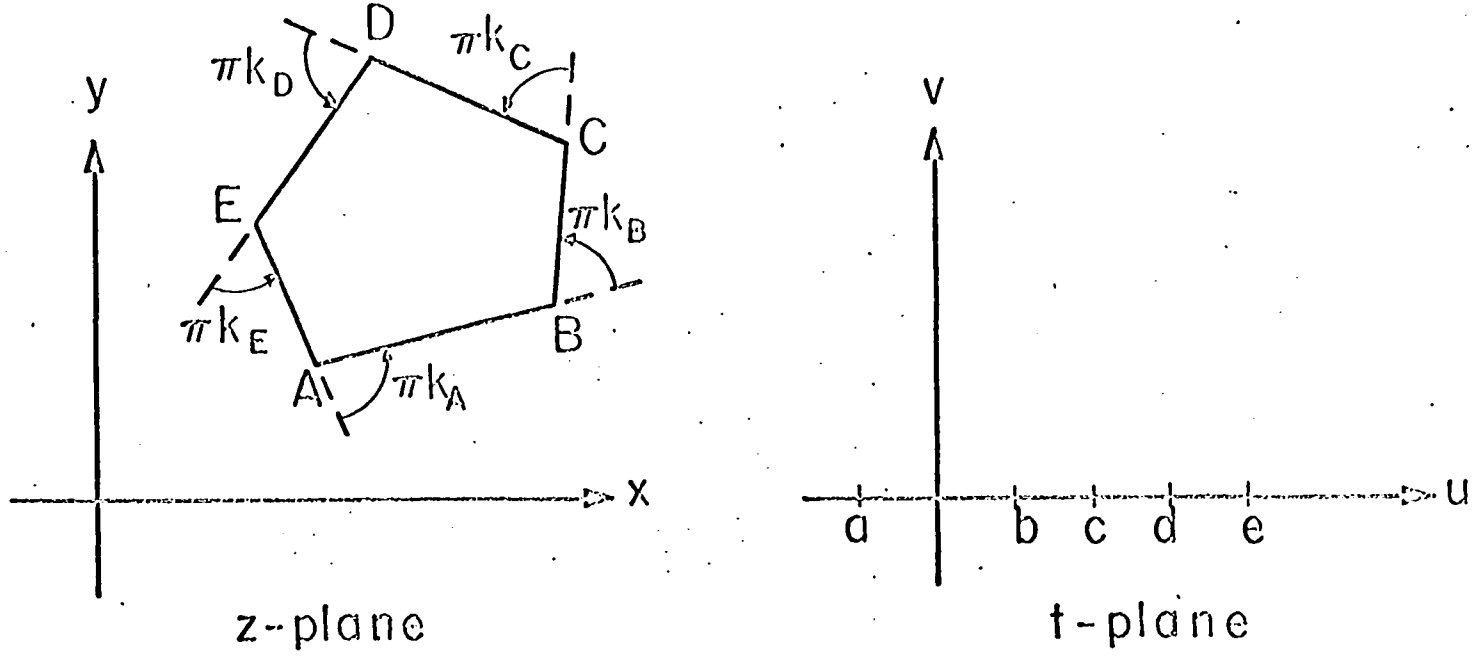

Figure 1. The z and t-planes considered in the Schwartz-Christoffel transformation. The interior of the polygon ABCDEA of the z-plane is mapped on the upper half of the t-plane.

the integration. If the integration of Equation 15 can be made successfully it is often difficult or impossible to obtain an explicit form of the inverse, that is, obtain t as a function of z. Examples of Schwartz-Christoffel transformations are given by Churchill (1960) and Kober (1957).

The method of images has been used to solve steady-state water flow problems. Kirkham (1949) solved the problem of flow from ponded water into tile drains overlying an impermeable barrier by summing the potentials due to an infinite array of image drains. List (1964) utilized images in obtaining an approximate solution of seepage of steady rainfall into drains above an impermeable barrier.

The use of strictly numerical methods has become feasible for a large number of flow problems due to the accessibility and popularity of high speed digital computers. Harr (1962) illustrates how a finite difference scheme may be used to solve Laplace's equation. Van Deemter (1949, 1950) uses a relaxation method to solve problems where the permeability is not homogeneous. Numerical methods are especially valuable in working with unsaturated flow problems such as infiltration where in general the differential equations involved are non-linear.

Model studies have been used to study many drainage problems, many of which are very difficult to treat mathematically. Soil, sand and glass beads have been used as porous materials. Electric analogues have also been useful. Grover and Kirkham (1964) used a glassbead-glycerol model to measure drawdown rates for water tables. Asseed and Kirkham (1966) used a similar model to study drawdown rates and steady-state cases. Childs (1943, 1945a, 1945b, 1946) used electric analogues to develop theories of soil drainage.

Most of the theoretical investigations cited above have been for steady-state flow for an isotropic soil. In some cases steady-state theories have been adapted or useful in analyzing non-steady state problems. Ligon, Kirkham, and Johnson (1964) assumed that a falling water table could be approximated by a series of steady-state water tables and found results agreeable with model data. Bouwer and van Schilfgaarde (1963) used a similar technique to predict the fall of the highest point of a water table between parallel tile drains. Maasland (1953) transformed, mathematically, certain anisotropic soils into apparent isotropic soils and hence obtained some solutions for anisotropic flow media.

III. TWO-DIMENSIONAL THEORY FOR SEEPAGE FROM A STATIONARY PLANE WATER TABLE TO TILE DRAINS NEAR A FOUNDATION BARRIER

A. The Foundation Problem: Objectives

Water seepage through walls, cracks, and porous material is a serious problem in many structures. One approach towards a solution is to attempt to make the wall or base impermeable to water by using the highest quality of workmanship, waterproofing agents, and materials; see, for example, Creasy (1963), Lazarr (1965), and Tice (1965). Although extreme care may be used in construction, the water head may be sufficiently high to cause a leakage. Beer et al. (1963) points out that a pressure head of three feet is sufficient to raise a six inch thick slab of concrete. The second approach to avoid or minimize leakage is to provide some sort of artificial drain in close proximity to the foundation to give a pressure relief; see, for example DeBoer (1963) and Beer et al. (1963). It is difficult to assess intermediate conditions of the water table, but, as pointed out by Creasy (1963), the maximum pressure head is equal to the full depth of the structure below the ground level provided there is no ponded water on the soil surface. If there is ponded water, its head must be added.

We shall solve analytically the problem of seepage from a stationary plane water table to a single tile drain or to a pair of symmetrically placed tile drains near a basement or foundation of a structure such as a farm building or house. We shall consider only two-dimensional flow and shall assume that for a defined saturated soil flow medium Laplace's equation is satisfied by both a potential function and a stream function as in Equations 6 and 7. After we have determined the potential and

stream functions, we will then have relationships from which flow nets can be drawn, pressures can be calculated, and the flow velocities will be known.

B. Geometry of the Flow Medium

Figure 2 is a sketch of the two-dimensional flow medium considered. A saturated layer of very coarse gravel of thickness δ and width S in the region DD'E'ED overlies a permeable soil of saturated hydraulic conductivity k and of thickness (H + h) in the region ABCO'DEFA. The prime is used on "O'" to avoid confusion with zero. The loss of hydraulic head across the coarse gravel is assumed negligible relative to the loss of head in the remainder of the system. A basement or foundation of width 2s (where little s and capital S of Figure 2 are not to be confused) extends to a depth H. An origin of coordinates is located at O' with the y-axis vertically downward. The x-axis is directed to the left in order to give a right-hand system. The origin is chosen at O' since in examples to follow one or more of the points A, B, E and F are at infinity. The center of a tile drain of radius r is located at point C which for purposes of the illustration is located on the line O'B, but could just as well be anywhere along the border EFABO'D, excluding points along the line DE. The coordinates of C are denoted by x_t, y_t where the subscript "t" refers to "tile." For cases with the tile center placed along the foundation base O'B as shown in Figure 2, we denote the distance of the tile center from the origin by R which is equal to $-x_t$. The flow medium is symmetric with respect to the vertical lines AB and EF. This implies that if a tile is located at C as shown, then a second tile drain must be located to the right of point B as shown in Figure 2.

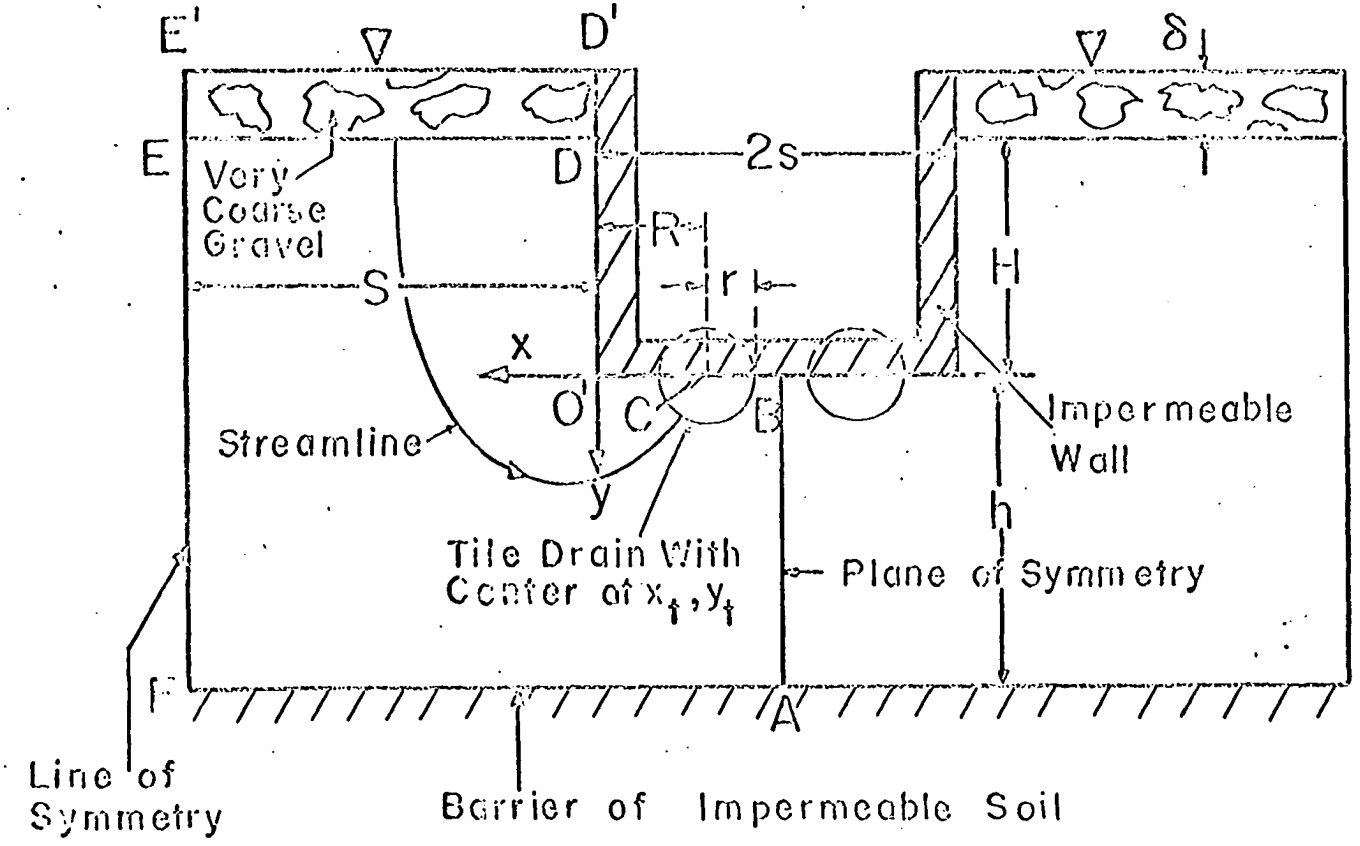

Figure 2. The geometry of the flow medium considered for the two-dimensional theory for seepage from a stationary plane water table to tile drains near a foundation barrier.

1. Shape of drain tubes

For cases with a drain tube situated in contact with an impermeable horizontal or vertical plane barrier such as along DO' or O'B of Figure 2, it is convenient for analytic purposes to assume the tube is of semicircular cross-section with the diameter in contact with the barrier. In practice, however, a tube having the cross-section of a complete circle would normally be used and placed such that its outside surface would come in contact with the impermeable barrier. In Appendix 1 a comparison is made of a circular drain tube whose outside surface is in contact with an impermeable barrier to a semicircular drain whose diameter lies along the barrier. The result found is that a circular drain tube of radius r whose outside surface is in contact with a barrier is equivalent to a semicircular drain tube of larger radius 1.57r whose diameter is along the impermeable barrier.

The problem will be solved for 12 cases by choosing special values of the parameters δ, H, h, s, and S. For example, $h = \infty$ corresponds to a soil extending to a great depth. For $S = \infty$ the water table E'D' extends in the x-direction infinitely. For $\delta = 0$ there is no layer of coarse gravel, but an infinitesimally thick layer of water is assumed. Table 2 indicates the ranges of the parameters for the 12 cases solved. In this section we shall also examine seepage around a sheetpile and seepage to a multiple drain system, problems not indicated in Table 2.

C. General Transformation of the z and w-planes to the t-plane

If we rotate the flow region ABO'DEFA of Figure 2 by 180 degrees, then we have the y-axis vertically upward and the x-axis extending to the right and a hexagonal flow medium ABO'DEFA as shown in the z-plane of Figure 3.

Table 2. The range of values for H, h, S and s of Figure 2 used in the 12 cases of the stationary plane water table. The finite values are taken to be greater than zero

Case	H	h	S	s
1	finite	finite	infinite	finite
2	finite	infinite	infinite	finite
3	finite	finite	infinite	infinite
4	finite	infinite	infinite	infinite
5	finite	infinite	finite	finite
6	finite	infinite	finite	infinite
7	zero	finite	finite	finite
8	zero	infinite	finite	finite
9	zero	finite	infinite	finite
10	zero	finite	finite	infinite
11	zero	infinite	infinite	finite
12	zero	infinite	infinite	infinite

We will now discuss a Schwartz-Christoffel transformation of the interior of the hexagon onto the upper half of the auxiliary t-plane of Figure 3. Also, we will discuss the related region CDEC shown in Figure 3 of the complex potential plane w and develop the transformation mapping the interior of CDEC of the w-plane to the upper half of the same auxiliary t-plane on which we mapped the flow medium of the z-plane. If the transformations of the z to t-plane and the w to t-plane are known, then the relationship of z to w will be known, although it may be an implicit

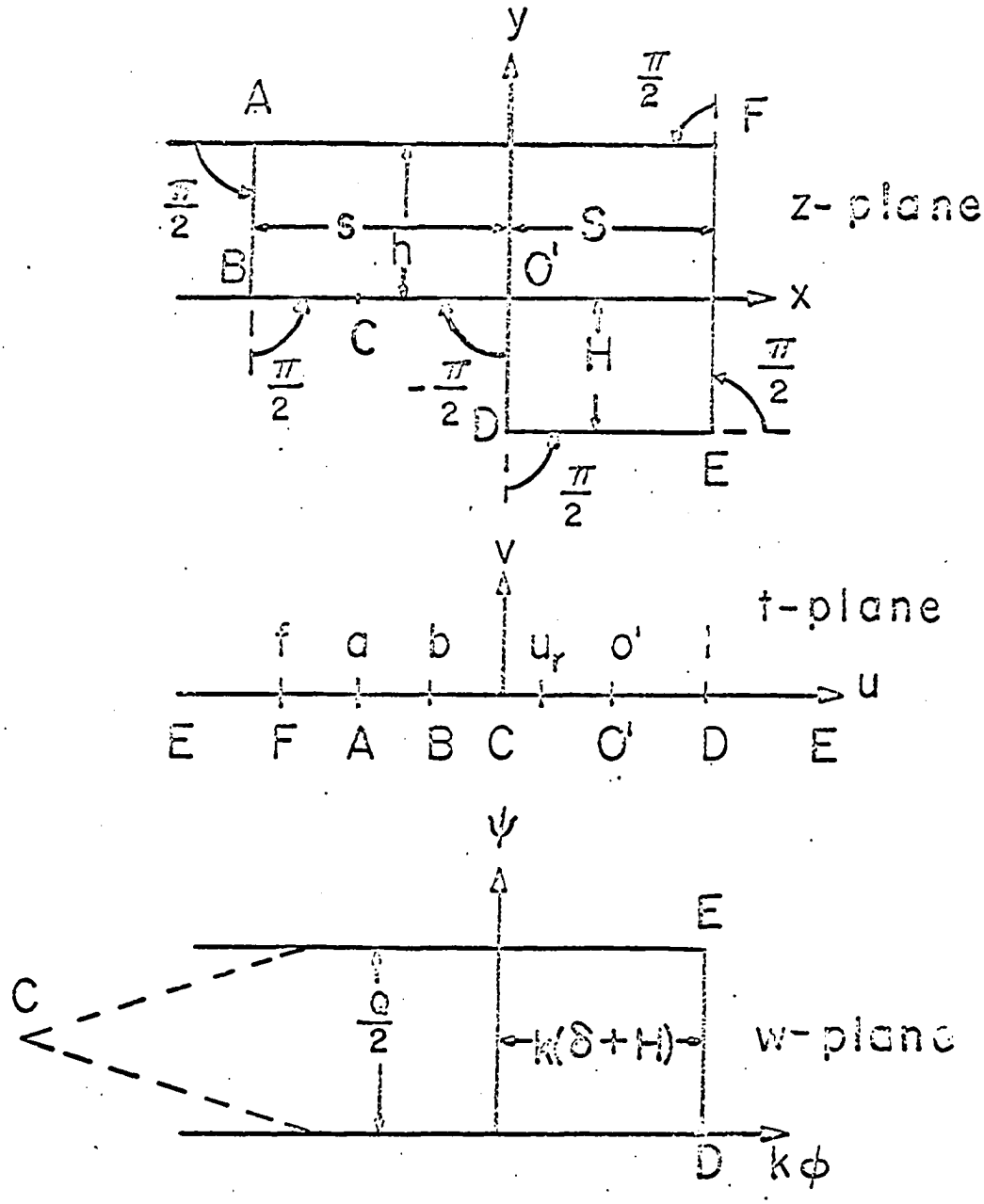

Figure 3. The z-plane, the auxilliary t-plane and the complex potential w-plane for the geometry of Figure 2.

relationship only.

Examining the z-plane of Figure 3, we observe that the exterior angles of the hexagonal flow region ABO'DEFA are each $\pi/2$ except at the origin O' where the exterior angle is $-\pi/2$. Mapping the hexagonal flow region to the upper half of the t-plane gives by Equation 15

$$z(t) = M' \int (t - f)^{-1/2}(t - a)^{-1/2}(t - b)^{-1/2}(t - o')^{1/2}(t - 1)^{-1/2} dt + N \tag{16}$$

where f, a, b, o' and 1 of the t-plane correspond to the points F, A, B, O', and D respectively of the z-plane and point E of the z-plane is mapped at ∞ (infinity) of the t-plane. The symbol "o'" is to be considered as an algebraic symbol and not zero-prime. The image of the "tile center" which is at C and has coordinates x_t and y_t in the z-plane is at the origin of the t-plane. The point C in the z and t-planes is for the illustration taken to be along BO' but need not be in the sequence A, B,... The point C could just as well be taken anywhere along EFABO'D. The integral of Equation 16 is a hyperelliptic integral as defined below eq. 575.00 of Byrd and Friedman (1954). To demonstrate the integral in the r.h.s. of Equation 16 is a hyperelliptic integral, we define quantities

$$T = t - o' \tag{17}$$

$$P(T) = (T - r_1)(T - r_2)(T - r_3)(T - r_4)(T - r_5) \tag{18}$$

where

$$r_1 = 0 \tag{19a}$$

$$r_2 = f - o' \tag{19b}$$

$$r_3 = a - o' \tag{19c}$$

$$r_4 = b - o' \tag{19d}$$

$$r_5 = 1 - o' \tag{19e}$$

and these give for z in terms of T by Equation 16, the result

$$z(T) = M'' \int \frac{T\,dT}{[P(T)]^{1/2}} + N \qquad (20)$$

where M" and N are constants. The integral in the last equation is identical to that in 575.09 of Byrd and Friedman with his i and p both equal to 1. Byrd and Friedman state that hyperelliptic integrals, except for special cases, must be evaluated by direct numerical methods or complicated series expansions.

Although it is possible the integral in Equation 20 may be expressible in terms of elliptic integrals and elementary functions, it is more expedient to examine simpler cases for which one or more of the parameters h, S, and s approach infinity. We will do this for the 12 cases of Table 2 after we examine boundary conditions in the z-plane and develop the w to t-plane transformation.

In order to show the correspondence between the boundary of the flow medium of the z and w-planes of Figure 3, we first must examine the values of ϕ and Φ along the boundary of ABO'DEFA of Figure 2 (or Figure 3). We define arbitrarily the stream function ϕ as zero along DO'C of Figure 2. We define Q/2 as the amount of water seeping across ED from the coarse gravel at the left, per unit time per unit length of the flow system perpendicular to the plane of Figure 2. The stream function ϕ will then be Q/2 along EFABC. Since the value of the stream function changes abruptly at C from 0 to Q/2, the potential must approach $-\infty$ at C. If the reference level of the potential is chosen as the x-axis, the potential along ED will be $\Phi = \delta + H$, since we have assumed the hydraulic head loss across the saturated gravel layer is negligible. Thus, the boundary

conditions are

Boundary Condition 1: $\psi = Q/2$ along EFABC
Boundary Condition 2: $\psi = 0$ along DO'C
Boundary Condition 3: $\phi = -\infty$ at C
Boundary Condition 4: $\phi = \delta + H$ along DE

Use of the four boundary conditions gives the correspondence of boundary values in the z and w-planes of Figure 3. The flow medium of the z-plane corresponds to a semi-infinite strip in the w-plane. For purposes of the analysis, we consider the semi-infinite strip as the degenerate triangle CDEC with the vertex C at infinity. The base of the triangle DE is of length Q/2 and is at $k\phi = k(\delta + H)$. The two infinitely long sides of the triangle are along $\psi = 0$ and $\psi = Q/2$. The exterior angles πk_B, πk_C, and πk_D for the triangle are $\pi/2$, π, and $\pi/2$, respectively. We choose c and d of Equation 15 to have the values of 0 and 1, since the points C and D in the w-plane must correspond to 0 and 1 of the t-plane to agree with the z to t-plane correspondences we have already established. Similarly, D of the w-plane must be mapped to infinity in the t-plane. Thus, Equation 15 gives for the transformation of the interior of the degenerate triangle BCDB of the w-plane onto the upper half the t-plane

$$w(t) = M' \int t^{-1}(t - 1)^{-1/2} dt + N$$

Use of eq. 104 of Peirce (1956) to evaluate the integral yields

$$w(t) = M \tan^{-1}(t - 1)^{1/2} + N$$

where M and N are constants to be determined from the boundary conditions. Since $t = 1$ corresponds to $w = k(\delta + H)$ we have from the last equation, the relation,

$$k(\delta + H) = M \tan^{-1} 0 + N$$

from which we can solve for N giving

$$N = k(\delta + H) \tag{21}$$

Similarly, as t approaches infinity, w approaches the value $k(\delta + H) + iQ/2$ which may be written as

$$k(\delta + H) + iQ/2 = M \lim_{t \to \infty} \tan^{-1}(t - 1)^{1/2} + N$$

The limiting value of $\tan^{-1}(t - 1)^{1/2}$, as t approaches infinity, is $\pi/2$. Using $\pi/2$ for the limit in the last equation and the value for N from Equation 21, we can solve for M giving

$$M = iQ/\pi \tag{22}$$

The desired transformation is using Equations 21 and 22

$$w(t) = i(Q/\pi) \tan^{-1}(t - 1)^{1/2} + k(S + H) \tag{23}$$

The inverse of Equation 23 is useful to calculate points for flow nets. Using

$$t = u + iv \tag{24}$$

and defining α and β by

$$\alpha = \pi\phi/Q \tag{25a}$$

$$\beta = (\pi k/Q)(\delta + H)[1 - \phi/(\delta + H)] \tag{25b}$$

one can verify that Equation 23 is equivalent to

$$\tan^{-1}(t - 1)^{1/2} = \alpha + i\beta \tag{26a}$$

Taking the tangent of each side of the last equation and squaring the results gives

$$t - 1 = \tan^2(\alpha + i\beta) \tag{26b}$$

Squaring both sides of eq. 408.18 of Dwight (1961) gives

$$\tan^2(\alpha + i\beta) = \frac{\sin^2 2\alpha - \sinh^2 2\beta + 2i \sin 2\alpha \sinh 2\beta}{(\cos 2\alpha + \cosh 2\beta)^2} \tag{27}$$

Substituting the r.h.s. of Equation 27 into Equation 26b, adding 1 to each side, putting the resulting r.h.s. over a common denominator and simplifying leads to

$$t = \frac{2(1 + \cos 2\alpha \cosh 2\beta) + 2i \sin 2\alpha \sinh 2\beta}{(\cos 2\alpha + \cosh 2\beta)^2} \tag{28}$$

The real part u and the imaginary part v of t are by inspection

$$u = \frac{2(1 + \cos 2\alpha \cosh 2\beta)}{(\cos 2\alpha + \cosh 2\beta)^2} \tag{29a}$$

$$v = \frac{2 \sin 2\alpha \sinh 2\beta}{(\cos 2\alpha + \cosh 2\beta)^2} \tag{29b}$$

where α and β are defined by Equations 25a and 25b and are both real.

The volume of water Q/2 seeping from the coarse gravel layer across the line ED per unit time per unit length of the flow system perpendicular to Figure 2 will now be found. Q/2 can be determined by specifying a value for an equipotential in the z-plane or t-plane. Since it is necessary to identify a resulting equipotential enclosing the tile center as the surface of the tile itself, it is convenient to define in the z-plane a distance from the tile center at C to a nearby equipotential as the "tile radius" r. This nearby equipotential will be very nearly circular in shape for small choices of r since we chose the point C of the z-plane a certain distance u_r as shown by the coordinate u_r in the t-plane of Figure 3. The length u_r is necessarily less than 1 because the point D was mapped to unity on the t-plane. For u values between C and D on the t-plane, we have $\psi = 0$ by Boundary Condition 1. If the potential at the tile surface, that is, at u_r has a value of ϕ_r, we have from Equation 23 the relation

$$k\phi_r = i(Q/\pi)\ \tan^{-1}(u_r - 1)^{1/2} + k(\delta \div H) \tag{30}$$

If we use the relationship

$$\tan^{-1}(u_r - 1)^{1/2} = i\ \tanh^{-1}(1 - u_r)^{1/2} \tag{31}$$

we can solve Equation 30 for Q/2, finding that

$$Q/2 = \frac{\pi k(\delta + H - \phi_r)}{2\ \tanh^{-1}(1 - u_r)^{1/2}} \tag{32}$$

An alternate form of Equation 32 is obtained by use of eq. 702 of Dwight (1961):

$$Q/2 = \pi k(\delta + H - \phi_r)/\ln\left[\frac{1 + (1 - u_r)^{1/2}}{1 - (1 - u_r)^{1/2}}\right] \tag{33}$$

For u_r much less than 1, it may be more convenient to write Equation 33 as

$$Q/2 = \pi k(\delta + H - \phi_r)/\ln[(2 - T)/T] \tag{34}$$

where T is obtained by expanding $(1 - u_r)^{1/2}$ in the numerator and denominator of Equation 33 by the binomial theorem and simplifying, the result for T being

$$T = u_r/2 + u_r^2/4 + (3/48)u_r^3 + (15/384)u_r^4 + \ldots \tag{35}$$

For u_r very small compared to unity, Equations 34 and 35 give

$$Q/2 = \pi k(\delta + H - \phi_r)/\ln(4/u_r), \qquad 0 < u_r << 1 \tag{36}$$

1. Pressure distribution along the foundation walls in terms of the parameters of the t-plane

A comparison of the z and t-planes of Figure 3 shows that along the base of the foundation u is always less than 1. For u between 0 and 1, ψ will be 0 and α of Equation 25a will be 0. Solving for β in terms of u with $\alpha = 0$ in Equation 26a gives

$$\beta = \cosh^{-1}(1/u)^{1/2}, \qquad 0 \leq u \leq 1\ (\psi = 0) \tag{37a}$$

Similarly, for negative values of u, ψ will be $Q/2$ and α will be $\pi/2$ giving from Equation 26a

$$\beta = \sinh^{-1}(-1/u)^{1/2}, \qquad u < 0 \ (\psi = Q/2) \tag{37b}$$

Using the right-hand-side (r.h.s.) of Equation 25b for β in Equations 37a and 37b and solving for $p/\rho g = \phi - y$ from Equation 4 gives two results. For positive u the result is

$$p/\rho g = y + (\delta + H)\{1 - Q/[k\pi(\delta + H)] \cosh^{-1}(1/u)^{1/2}\}, \qquad 0 \leq u \leq 1 \tag{38a}$$

and for negative u the result is

$$p/\rho g = y + (\delta + H)\{1 - Q/[\pi k(\delta + H)] \sinh^{-1}(-1/u)^{1/2}\}, \qquad u < 0 \tag{38b}$$

Equations 38a and 38b pertain to the 12 cases studied in relation to Figure 2 as well as to the vertical sheetpile problem later to be discussed. These last two equations give the pressure head along the foundation side and base as a function of the elevation y and the t-plane coordinate u.

The pressure head may be obtained, independent of Q, by introducing the parameter u_r from Equation 33 into the last two equations. Dividing each side of Equation 33 by $\pi k(\delta + H)$ and setting ϕ_r equal to zero gives

$$Q/[\pi k(\delta + H)] = 2/\ln\left[\frac{1 + (1 - u_r)^{1/2}}{1 - (1 - u_r)^{1/2}}\right], \qquad \phi_r = 0 \tag{39}$$

which when substituted into Equations 38a and 38b gives

$$p/\rho g = y + (\delta + H)\{1 - 2 \cosh^{-1}(1/u)^{1/2}/\ln\left[\frac{1 + (1 - u_r)^{1/2}}{1 - (1 - u_r)^{1/2}}\right]\},$$

$$0 \leq u \leq 1, \ \phi_r = 0 \tag{40a}$$

$$p/\rho g = y + (\delta + H)\{1 - 2 \sinh^{-1}(-1/u_r)^{1/2}/\ln\left[\frac{1 + (1 - u_r)^{1/2}}{1 - (1 - u_r)^{1/2}}\right]\},$$

$$u < 0, \ \phi_r = 0 \tag{40b}$$

Figure 4. The normalized potential distribution for points along the foundation in terms of the auxilliary t-plane coordinate u. The values of u_r correspond to the size of the drain tube. For $y = 0$ the curves give the pressure head.

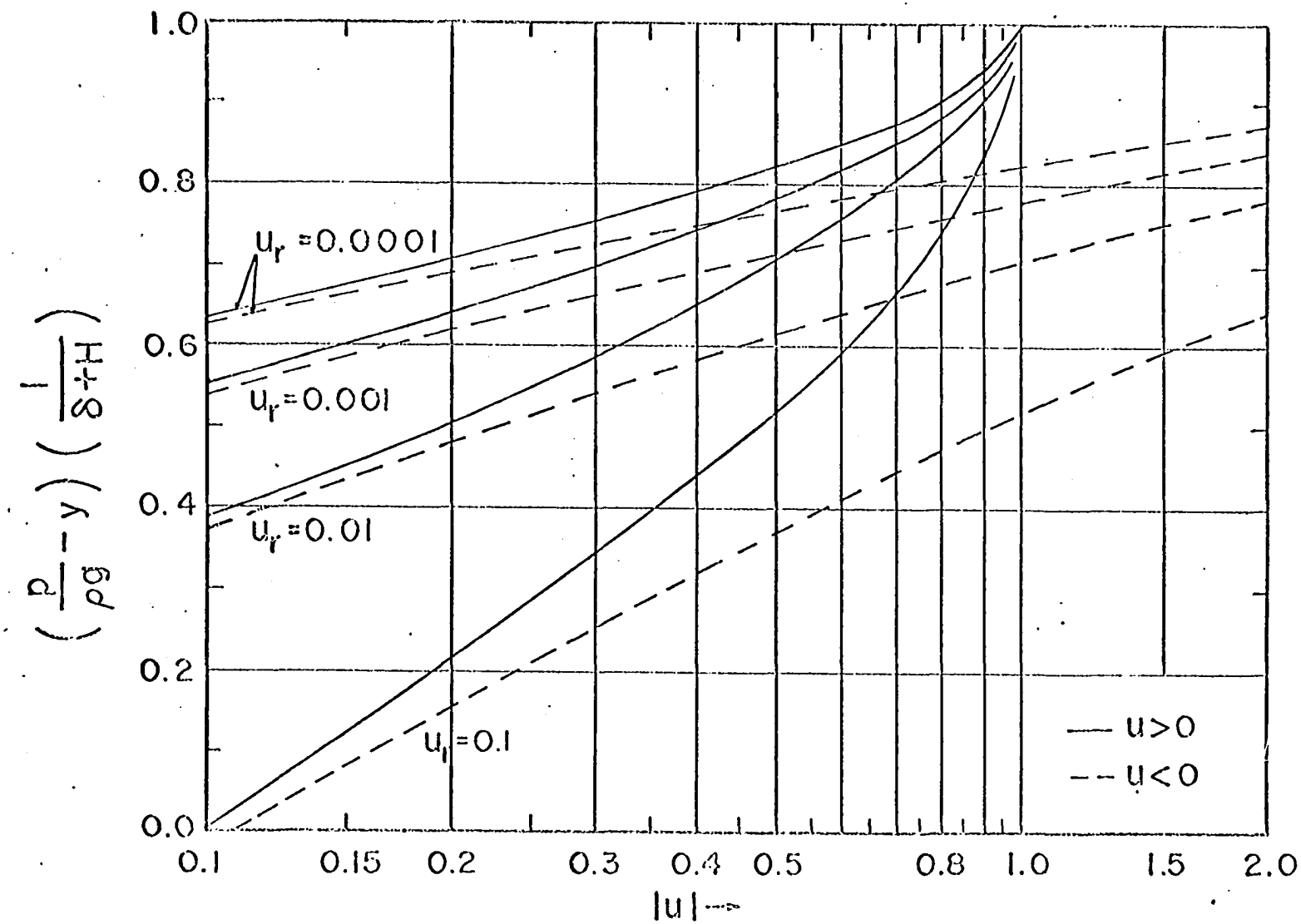
1.0
0.8
0.6
0.4
0.2
0.0
0.1
0.15
0.2
0.3
0.4
0.5
0.8
1.0
1.5
2.0
|u|→
$\left(\frac{\partial}{\rho g}\right)\left(\frac{1}{\delta+H}\right)$
$u_r = 0.0001$
$u_r = 0.001$
$u_r = 0.01$
$u_r = 0.1$
u>0
u<0

where u_r is the length in the t-plane corresponding to the tile radius of the z-plane.

Figure 4 gives the normalized potential $[(p/\rho g) - y]/(\delta + H)$ as a function of u for u_r equal to 0.0001, 0.001, 0.01, and 0.1. Since the basement or foundation floor is on the x-axis, y is zero and the ordinate of Figure 4 is a plot of the normalized pressure head when the floor is considered. An example of the use of Figure 4 will be given later.

D. Coarse Gravel Layer Not Extending to the Depth of the Foundation

1. Case 1: Foundation of finite width, water table of infinite width and soil below the foundation of finite depth

If in the z-plane of Figure 3, the water table DE becomes very wide, S approaches infinity and the image point f in the t-plane will approach infinity also. The Schwartz-Christoffel transformation mapping the interior of the resulting pentagon ABO'DEA in the z-plane to the upper half of the t-plane differs from Equation 16 only in that the $(t - f)^{-1/2}$ term is not included:

$$z(t) = M' \int (t - a)^{-1/2}(t - b)^{-1/2}(t - o')^{1/2}(t - 1)^{-1/2}\, dt + N \qquad (41)$$

Use of eq. 258.02 of Byrd and Friedman (1954) to evaluate the integral gives

$$z(t) = M\, \pi(m,n,\sigma) + N, \qquad \sigma = \sigma(t) \qquad (42)$$

where $\pi(m,n,\sigma)$ is an elliptic integral of the third kind of Legendre's canonical form with modulus m, parameter n, and amplitude σ defined as in the notation of Appendix B of Harr (1962) by

$$\pi(m,n,\sigma) = \int_0^{\sigma} \frac{d\sigma}{(1 + n \sin \sigma)(1 - m^2 \sin^2 \sigma)^{1/2}} \qquad (43)$$

For Equation 42 we have

$$m^2 = \frac{(o' - b)(1 - a)}{(1 - b)(o' - a)} \tag{44}$$

$$n = -\frac{1 - a}{o' - a} \tag{45}$$

$$\sigma = \arcsin\left[\frac{(o' - a)(t - 1)}{(1 - a)(t - o')}\right]^{1/2} \tag{46}$$

For a less than b less than o' and o' less than 1, it can be shown that m^2 lies between 0 and 1 and that n is less than -1. For n less than -1, the function $\pi(m,n,\sigma)$ is the hyperbolic case as discussed by Abramowitz and Stegun (1964) under eq. 17.7.7 with their n equal to our -n.

Examining the correspondence between points of the t-plane and those of the z-plane of Figure 3 we find:

$$z(1) = -iH \tag{47a}$$

$$z(a) = -s + iH \tag{47b}$$

$$z(b) = -s \tag{47c}$$

$$z(o') = 0 \tag{47d}$$

Use of the last four equations along with Equations 43, 44, and 46 gives

$$M\,\pi(m,n,0) + N = -iH \tag{48a}$$

$$M\,\pi(m,n,\pi/2) + N = -s + ih \tag{48b}$$

$$M\,\pi(m,n,\sin^{-1}[1/m]) + N = -s \tag{48c}$$

$$M\,\pi(m,n,\sin^{-1}\infty) + N = 0 \tag{48d}$$

where $\pi(m,n,\sin^{-1}\infty)$ is the limiting value of $\pi(m,n,\sigma)$ as sin σ approaches infinity.

From Equation 43, for $\sigma = 0$, we have

$$\pi(m,n,0) = 0 \tag{49}$$

which along with Equation 48a gives the value of N as

$$N = -iH \tag{50}$$

With Harr (1962, eq. 26b, Appendix B), we define the complete elliptic integral of the third kind $\pi_o(m,n)$ by

$$\pi_o(m,n) = \pi(m,n,\pi/2) \tag{51}$$

The function $\pi_o(m,n)$ has an imaginary part for the hyperbolic case (n less than -1). Eq. 27b of Appendix B of Harr is

$$\pi_o(m,n) = -\pi_o(m,m^2/n) + K + (\pi/2)/[(1 + n)(1 + m^2/n)]^{1/2} \tag{52}$$

where $\pi_o(m,m^2/n)$ is the complete elliptic integral of the first kind of modulus m and parameter m^2/n and K is the complete elliptic integral of the first kind of parameter m. Both $\pi_o(m,m^2/n)$ and K are real. As n in Equation 45 is less than -1, we observe that the last term on the r.h.s. of Equation 52 is imaginary. Factoring out an i^2 from the last term gives, for Equation 52, the relation

$$\pi_o(m,n) = -\pi_o(m,m^2/n) + K + i(\pi/2)/[-(1 + n)(1 + m^2/n)] \tag{53}$$

Equation 28b of Appendix B of Harr is

$$\pi(m,n,\arcsin[1/m]) = \pi_o(m,n) + im^2\pi_o(m',n')/(n + m^2) \tag{54}$$

where m' and n' are

$$m' = (1 - m^2)^{1/2} \tag{55}$$

$$n' = -\frac{n(m')^2}{m^2 + n} \tag{56}$$

and $\pi_o(m',n')$ will be real.

Subtracting Equation 48b from Equation 48c gives

$$M\{\pi(m,n,\sin^{-1}[1/m]) - \pi_o(m,n)\} = -ih \tag{57}$$

Use of Equation 54 and the last equation yields

$$Mm^2\pi_o(m',n')/(n + m^2) = -h \tag{58}$$

from which we conclude M is real.

Use of -iH for N in Equation 48b, along with Equation 53, leads to

$$M\{-\pi_o(m,m^2/n) + K + i(\pi/2)/[-(1 + n)(1 + m^2/n)]^{1/2} - iH = -s + ih \qquad (59)$$

Equating real and imaginary parts of the last equation gives

$$M(\pi/2)/[-(1 + n)(1 + m^2/n)]^{1/2} = H + h \qquad (60)$$

$$M[\pi_o(m,m^2/n) - K] = s \qquad (61)$$

From Equations 58, 60, and 61, we can determine the useful ratios

$$h/s = -\left(\frac{m^2}{n + m^2}\right)\left[\frac{\pi_o(m',n')}{\pi_o(m,m^2/n) - K}\right] \qquad (62)$$

$$H/s = \left\{\frac{\pi}{2[-(1 + n)(1 + m^2/n)]^{1/2}} + \frac{m^2\pi_o(m',n')}{n + m^2}\right\}/[\pi_o(m,m^2/n) - K] \qquad (63)$$

$$H/h = -1 - \frac{(n + m^2)\pi}{2m^2\pi_o(m',n')[-(1 + n)(1 + m^2/n)]^{1/2}} \qquad (64)$$

Two of the last three equations are independent and can be used to solve for m and n when any two of the ratios h/s, H/s, or H/h are specified. The constant M can be solved for by using Equation 61, for instance, to give

$$M = s/[\pi_o(m,m^2/n) - K] \qquad (65)$$

once m and n have been determined.

Substituting the r.h.s. of Equation 65 for M in Equation 42 and using Equation 50 gives the t to z-plane transformation

$$z(t) = \frac{s\,\pi(m,n,\sigma)}{\pi_o(m,m^2/n) - K} - iH, \qquad \sigma = \sigma(t) \qquad (66)$$

where σ is given by Equation 46. If the coordinates of the tile center are x_t and y_t and it is mapped to the origin of the t-plane, we have

from Equation 66

$$M\,\pi(m,n,\arcsin[(o' - a)/o'(1 - a)]^{1/2}) - iH = x_t + iy_t \qquad (67)$$

If m, n and M are previously determined, the last equation may be used along with Equation 45 to determine a and o'. The value of b can then be determined from Equation 44 although it is unneeded to apply Equation 66. The determination of constants a and o' will be difficult except for special cases such as when the tile center is at a corner or center of the foundation base. For example, when the tile center is at x = -s, y = 0, b of Equation 44 will be zero and o' and a can be easily evaluated for given m and n values by Equations 44 and 45.

2. Case 2: Foundation of finite width, water table of infinite width and soil below the foundation of infinite depth

If in the z-plane of Figure 3 the depth h to the impermeable soil layer approaches infinity, correspondingly a will approach infinity in the t-plane. Thus, as h approaches infinity, a approaches infinity in Equations 44, 45, and 46 giving

$$\lim_{h \to \infty} m^2 = \frac{o' - b}{1 - b} \qquad (68)$$

$$\lim_{h \to \infty} n = -1 \qquad (69)$$

$$\lim_{h \to \infty} \sigma = \arcsin\left(\frac{t - 1}{t - o'}\right)^{1/2} \qquad (70)$$

Eq. 111.06 of Byrd and Friedman (1954) in our notation is

$$\pi(m,-1,\sigma) = [m'^2 F(m,\sigma) - E(m,\sigma) + \tan\sigma\,(1 - m^2\sin^2\sigma)^{1/2}]/m'^2 \qquad (71)$$

where $F(m,\sigma)$ and $E(m,\sigma)$ are elliptic integrals of the first and second kinds. The definitions of $F(m,\sigma)$ and $E(m,\sigma)$ are given in Harr (1962) by

his eq. 3 and 14b of Appendix B and in our notation are

$$F(m,\sigma) = \int_0^{\sigma} (1 - m^2\sin^2\sigma)^{-1/2} d\sigma \tag{72}$$

$$E(m,\sigma) = \int_0^{\sigma} (1 - m^2\sin^2\sigma)^{1/2} d\sigma \tag{73}$$

As h approaches infinity, we have for Equation 42, using Equations 50, 69, and 71

$$z(t) = (Mm'^2)[m'^2F(m,\sigma) - E(m,\sigma) + \tan\sigma\,(1 - m^2\sin^2\sigma)^{1/2}] - iH, \quad \sigma = \sigma(t) \tag{74}$$

where m^2 and σ are given by Equations 68 and 70 as

$$m^2 = \frac{o' - b}{1 - b} \tag{75}$$

$$\sigma = \arcsin\left(\frac{t - 1}{t - o'}\right)^{1/2} \tag{76}$$

In order to evaluate the constant M for the limit as h approaches infinity, we first use eq. 111.06 of Byrd and Friedman (1954) which is

$$\pi(m,-m^2,\sigma) = [E(m,\sigma) - m^2\sin\sigma\cos\sigma/(1 - m^2\sin^2\sigma)]/m'^2 \tag{77}$$

For $\sigma = \pi/2$ the last equation reduces to

$$\pi_o(m,-m^2) = E/m'^2 \tag{78}$$

where E is the complete elliptic integral of the second kind

$$E = E(m,\pi/2) \tag{79}$$

Substitution of E/m'^2 for $\pi_o(m,m^2/n)$ in Equation 65 yields

$$M = s\,m'^2/(E - m'^2K) \tag{80}$$

which when substituted into Equation 74 gives

$$z(t) = \frac{s[m'^2F(m,\sigma) - E(m,\sigma) + \tan\sigma\,(1 - m^2\sin^2\sigma)^{1/2}]}{E - m'^2K} - iH, \quad \sigma = \sigma(t) \tag{81}$$

Replacement of m and n by m' and n' respectively in Equation 52 gives

$$\pi_o(m',n') = -\pi_o(m',m'^2/n') + K' + (\pi/2)/[(1 + n')(1 + m'^2/n')]^{1/2} \quad (82)$$

To simplify Equation 63 we also need an identity. By use of Equations 55 and 56 for m' and n', one may verify for n less than -1 the following equation

$$(\frac{m^2}{n + m^2})/[(1 + n')(1 + m'^2/n')]^{1/2} = -1/[-(1 + n)(1 + m^2/n)]^{1/2} \quad (83)$$

and this is the needed identity. Use of Equations 82 and 83 in Equation 63 gives

$$H/s = (\frac{m^2}{n + m^2})[\frac{-\pi_o(m',m'^2/n) + K'}{\pi_o(m,m^2/n) - K}] \quad (84)$$

In the limit as n approaches -1, the last equation becomes by Equation 78

$$H/s = \frac{E' - m^2K'}{E - (1 - m^2)K} \quad (85)$$

which can be used to solve for m. Figure 5 is a graphical relationship of H/s and s/H versus m as calculated using Equation 85. If a very accurate value of m is desired we may use Equation 85 directly to solve for m using numerical techniques.

In order to apply Equation 81 we also need to evaluate o' of Equation 76. For the special case when the tile center is located at coordinates x = -s, y = 0 which is point B of the z-plane of Figure 3, b of the t-plane will be zero and o' is given by substituting b = 0 in Equation 75. The result is

$$o' = m^2, \qquad x_t = -s, y_t = 0 (b = 0) \quad (86)$$

For another special case, the tile center may be at the origin of the

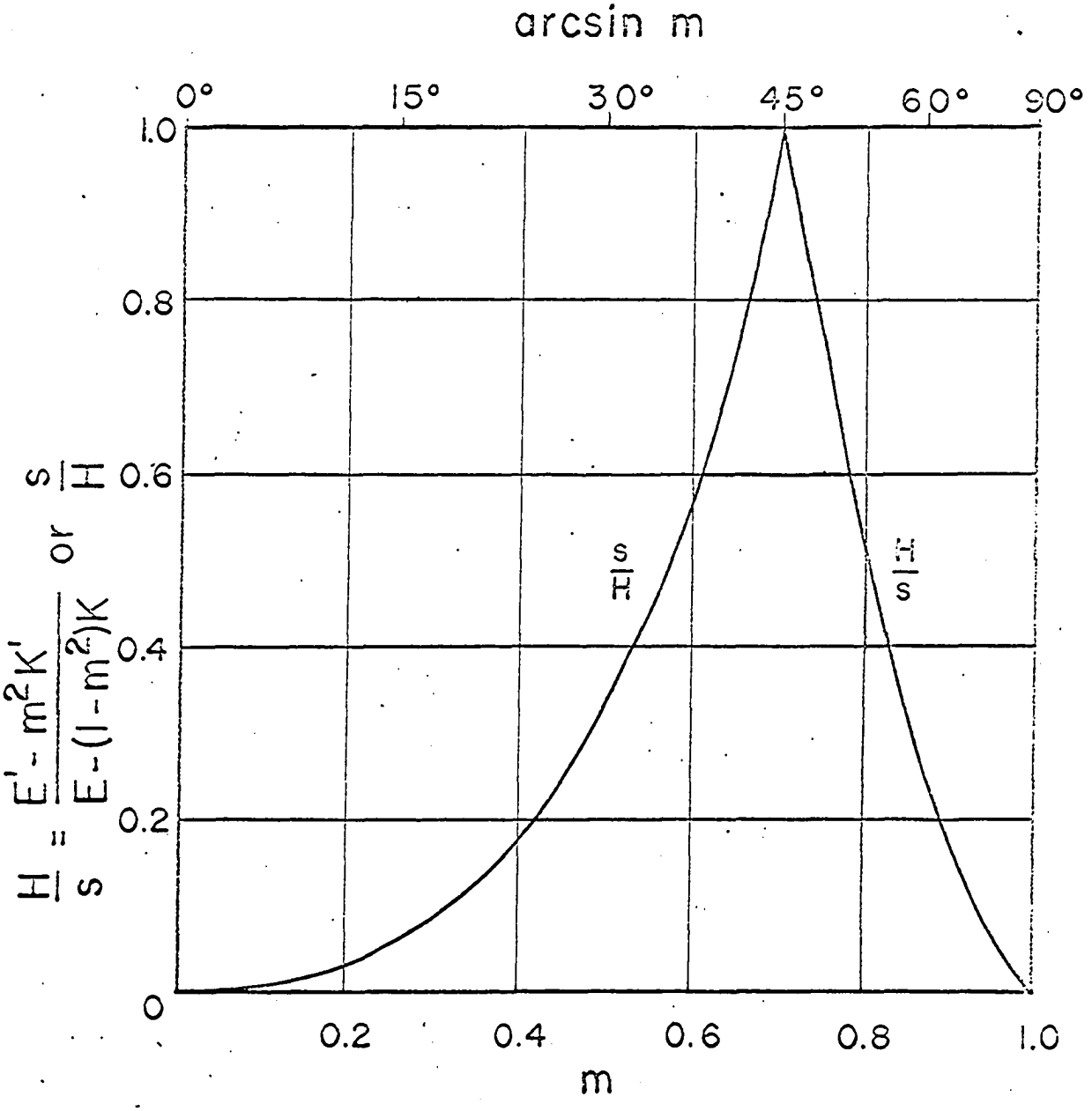

Figure 5. The graphical relationship of the elliptic modulus m to the ratio $(E' - m^2K')/[E - (1 - m^2)K]$ used for Case 2.

z-plane. We compare the z and t-planes of Figure 3 finding when the tile center is at the origin of the z-plane the result

$$o' = 0, \qquad x_t = y_t = 0 \tag{87}$$

More generally, if the tile center coordinates are x_t, y_t in the z-plane of Figure 3 and the tile center corresponds to the origin of the t-plane, we have, by Equation 81, the relationship

$$x_t + iy_t = s\{m'^2 F(m,\sin^{-1}[1/o']^{1/2}) - E(m,\sin^{-1}[1/o']^{1/2} + (o' - 1)^{-1/2}(1 - m^2/o')^{1/2}\}/(E - m'^2 K) - iH \tag{88}$$

The last relationship may be solved for o' for cases not covered by Equation 86 or 87.

3. Case 3: Foundation of infinite width, water table of infinite width and soil below the foundation of finite depth

If in the z-plane of Figure 3 we let the semi-width of the foundation s approach infinity, the image of the foundation midpoint b of the t-plane will approach a. We need to simplify Equation 42 for this case.

Assuming Equation 42 is valid in the limit as b approaches a, we find from Equation 44 with b and a equal:

$$\lim_{s \to \infty} m^2 = 1 \tag{89}$$

Eq. 111.04 of Byrd and Friedman (1954) gives $\pi(m,n,\sigma)$ for a modulus of one in terms of elementary functions and in our notation as

$$\pi(1,n,\sigma) = \frac{1}{1+n}\{\ln(\tan\sigma + \sec\sigma) - (-n)^{1/2}\ln[\frac{1 + (-n)^{1/2}\sin\sigma}{1 - (-n)^{1/2}\sin\sigma}]^{1/2}\} \tag{90}$$

For m = 1, m' and n' from Equations 55 and 56 become

$$\lim_{s \to \infty} m' = 0 \tag{91}$$

$$\lim_{s \to \infty} n' = 0 \tag{92}$$

If n and m are both zero in Equation 43, we observe

$$\pi(0,0,\sigma) = \sigma$$

from which

$$\pi_o(0,0) = \pi/2 \tag{93}$$

Solving for M from Equation 58 with m and $\pi_o(m',n')$ equal to 1 and $\pi/2$ respectively gives

$$M = -(2h/\pi)(1 + n) \tag{94}$$

Use of Equations 50, 90 and 94 in Equation 42 gives for s approaching infinity

$$z(t) = -(2h/\pi)\{\ln(\tan\sigma + \sec\sigma) - (-n)^{1/2}\ln[\frac{1 + (-n)^{1/2}\sin\sigma}{1 - (-n)^{1/2}\sin\sigma}]^{1/2}\} - iH \tag{95}$$

where σ and n are identical to those in Equations 46 and 45, namely

$$\sigma = \arcsin[\frac{(o' - a)(t - 1)}{(1 - a)(t - o')}]^{1/2} \tag{96}$$

$$n = -(\frac{1 - a}{o' - a}) \tag{97}$$

The parameters n, o', and a of the last two equations can be evaluated for m approaching 1 as follows. Use of Equation 64 with m and $\pi_o(m',n')$ equal to 1 and $\pi/2$ respectively gives

$$H/h = -1 - \frac{n + 1}{[-(1 + n)(1 + 1/n)]^{1/2}}$$

Since our n is less than -1, we can show

$$[-(1 + n)(1 + 1/n)]^{1/2} = -(n + 1)/(-n)^{1/2}, \qquad n < -1 \tag{98}$$

which gives for H/h from above

$$H/h = (-n)^{1/2} - 1 \tag{99}$$

or which when solved for n gives

$$n = -(1 + H/h)^2 \tag{100}$$

our needed result for n.

Assuming n to be known, we can now obtain a and o' in implicit form by observing the z and t-planes corresponding for point C of Figure 3. The relationship obtained will be

$$z(0) = x_t + iy_t \tag{101}$$

where x_t and y_t are the z-plane coordinates of the "tile center." Equation 101 along with Equation 95 give one equation with a and o' as unknowns. The definition of n given by Equation 97 gives a second equation in a and o' which may be used along with Equation 101 to obtain a and o'. For the special case that the tile center is at the origin O' of the z-plane, the resulting image point o' of the t-plane will be zero as in Figure 3. Use of zero for o' in Equation 97 gives

$$n = (1 - a)/a, \qquad x_t = y_t = 0 \tag{102}$$

This last equation and Equation 100 give

$$a = -(h/H)/(2 + H/h), \qquad x_t = y_t = 0 \tag{103}$$

4. Case 4: Foundation of infinite width, water table of infinite width and soil below the foundation of infinite depth

For h, s, and S approaching infinity in the z-plane of Figure 3, the image points a, b, and f in the t-plane each approach infinity. We observe from Equation 97 that n approaches -1 as a approaches infinity. With n equal to -1, Equation 95 reduces to the indeterminate form of

ln 1 multiplied by an infinite h. Although we could evaluate the limit, it is easier to start with a new Schwartz-Christoffel transformation.

The appropriate transformation is similar to Equation 41 and has the terms t - a and t - b omitted. The transformation is

$$z(t) = M' \int \left(\frac{t - o'}{t - 1}\right)^{1/2} + N' \tag{104}$$

Using eq. 195.04 and 195.01 of Dwight, we find

$$z(t) = M\{(t - 1)(t - o') + (1 - o')\ln[(t - 1)^{1/2} + (t - o')^{1/2}]\} + N \tag{105}$$

By Figure 3 we have $z_{t=1} = -iH$ and $z_{t=o'} = 0$, from which Equation 105 gives

$$M[(1 - o')\ln(1 - o')^{1/2}] + N = -iH \tag{106a}$$

and

$$M[(1 - o')\ln(o' - 1)^{1/2}] + N = 0 \tag{106b}$$

Using the identity

$$\ln(o' - 1)^{1/2} = \ln(1 - o')^{1/2} + i\pi/2 \tag{107}$$

we can solve for M and N from Equations 106a and 106b finding

$$M = (2H/\pi)/(1 - o') \tag{108}$$

$$N = -iH - (2H/\pi)\ln(1 - o')^{1/2} \tag{109}$$

which when substituted in Equation 105 give

$$z(t) = (2H/\pi)\left\{\frac{(t - 1)(t - o')}{(1 - o')} + \ln\left[\frac{(t - 1)^{1/2} + (t - o')^{1/2}}{(1 - o')^{1/2}}\right]\right\} - iH \tag{110}$$

The parameter o' in Equation 110 can be determined from Equation 101 if the location of the tile center is specified.

5. Case 5: Foundation of finite width, water table of finite width and soil below the foundation of infinite depth

If in the z-plane of Figure 3 the permeable soil extends to a great depth, we see h approaches infinity and the image points a and f in the t-plane will coincide. For s and S finite and h approaching infinity, the exterior angle at point A will approach π in the z-plane. The Schwartz-Christoffel transformation mapping the interior of the resulting pentagon ABO'DEA onto the upper half of the t-plane by Equation 16 will now be

$$z(t) = M' \int (t - a)^{-1}(t - b)^{-1/2}(t - o')^{1/2}(t - 1)^{-1/2}dt + N \qquad (111)$$

To evaluate the integral in Equation 111, we may use eq. 237.02 of Byrd and Friedman (1954) and find

$$z(t) = M\,\pi(m,n,\sigma) + N, \qquad \sigma = \sigma(t) \qquad (112)$$

with

$$m^2 = \frac{o' - b}{1 - b} \qquad (113)$$

$$n = -\frac{o' - a}{1 - a} \qquad (114)$$

$$\sigma = \arcsin\left(\frac{t - 1}{t - o'}\right)^{1/2} \qquad (115)$$

Since b is less than o' and o' is less than 1, we observe from Equation 113 that m^2 lies between 0 and 1. Similarly, we can show that n lies between -1 and $-m^2$ from which it follows that the third order elliptic integral $\pi(m,n,\sigma)$ of Equation 112 is of the circular case as discussed under 17.7.9 of Abramowitz and Stegun (1964) with their n equal to our -n. We observe from Abramowitz and Stegun that $\pi_o(m,n)$ is real for our range of m and n.

The correspondence between points of the z and t-planes in Figure 3 reveals

$$z(1) = -iH \tag{116a}$$

$$\lim_{t \to \infty} z(t) = S - iH \tag{116b}$$

$$z(o') = 0 \tag{116c}$$

$$z(b) = -s \tag{116d}$$

The above four relations together with Equations 112, 113, 114, and 115 give

$$M\,\pi(m,n,0) + N = -iH \tag{117a}$$

$$M\,\pi(m,n,\pi/2) + N = S - iH \tag{117b}$$

$$M\,\pi(m,n,\sin^{-1}\infty) + N = 0 \tag{117c}$$

$$M\,\pi(m,n,\sin^{-1}[1/m]) + N = -s \tag{117d}$$

By Equation 49, Equation 117a reduces to

$$N = -iH \tag{118}$$

Use of -iH for N in Equation 117b and the definition of $\pi_o(m,n)$ from Equation 51 give

$$M = S/\pi_o(m,n) \tag{119}$$

Eq. 28c of Appendix B of Harr (1962) is the same as

$$\pi(m,n,\sin^{-1}\infty) - \pi(m,n,\sin^{-1}[1/m]) = -K + \pi_o(m,m^2/n) \tag{120}$$

Subtracting Equation 117d from Equation 117c and use of Equation 120 gives

$$M[-K + \pi_o(m,m^2/n)] = s \tag{121}$$

The last equation and Equation 119 give for the ratio S/s

$$S/s = \pi_o(m,n)/[\pi_o(m,m^2/n) - K] \tag{122}$$

Eq. 28b of Appendix B of Harr is

$$\pi(m,n,\sin^{-1}[1/m]) = \pi_o(m,n) + im^2\pi_o(m',n')/(n + m^2) \tag{123}$$

This identity along with Equation 117d and Equation 118 gives

$$M[\pi_o(m,n) + \frac{im^2\pi_o(m',n')}{n + m^2}] - iH = -s \tag{124}$$

which by use of Equation 119 is

$$[S/\pi_o(m,n)]\frac{im^2\pi_o(m',n')}{n + m^2} = -(s + S) + iH \tag{125}$$

where m' and n' are defined as in Equations 55 and 56

$$m'^2 = 1 - m^2$$

$$n' = -nm'^2/(m^2 + n)$$

from which we deduce n' is less than -1 and $\pi_o(m',n')$ has both a real and imaginary part (n lies between -1 and $-m^2$). For n' less than -1, Equation 82 reduces to

$$\pi_o(m',n') = -\pi_o(m',m'^2/n') + K' \pm (i\pi/2)/[-(n' + 1)(1 + m'^2/n')]^{1/2} \tag{126}$$

where the sign of the imaginary part would have to be determined. Use of the real part of the r.h.s. of Equation 126 for the real part of $\pi_o(m',n')$ in Equation 125 gives

$$H/S = (\frac{m^2}{n + m^2})\frac{K' - \pi_o(m',m'^2/n')}{\pi_o(m,n)} \tag{127}$$

Using the negative sign for the imaginary part of $\pi_o(m',n')$ from Equation 126, the real part of Equation 119 reduces to Equation 122 which adds no new information.

A third ratio can be obtained by multiplying each side of Equation 122 by each side of Equation 127:

$$H/s = -(\frac{m^2}{n + m^2})\frac{\pi_o(m',m'^2/n') - K'}{\pi_o(m,m^2/n) - K} \tag{128}$$

Any two of Equations 122, 127 and 128 are independent of each other and may be used to solve for m and n.

To apply Equation 112, we need to evaluate o' of Equation 115 as well as M, m and n. Assuming m and n have been determined, as discussed in the previous paragraph, we can find o' by specifying the tile center coordinates x_t and y_t in the z-plane. From Equation 115 we find

$$(\sin \sigma)_{t=0} = (1/o')^{1/2}$$

which along with Equation 101 and Equation 112 gives

$$[S/\pi_o(m,n)]\ \pi(m,n,\arcsin[1/o']^{1/2}) - iH = x_t + iy_t \tag{129}$$

6. Case 6: Foundation of infinite width, water table of finite width and soil below the foundation of infinite depth

If in the z-plane of Figure 3 the foundation width s approaches infinity, and the soil depth approaches infinity, we see that point B of the t-plane will approach point A. We assume the water table to be of finite width. Examining Equations 113 and 114, we observe for b equal to a, m^2 and -n are the same, that is, the limit as s approaches infinity of n is

$$\lim_{s \to \infty} n = -m^2 \tag{130}$$

We have by Equations 78 and 119 for $n = -m^2$ the relation

$$M = m'^2 S/E \tag{131}$$

Eq. 111.06 of Byrd and Friedman in our notation is

$$\pi(m,-m^2,\sigma) = [E(m,\sigma) - m^2 \sin\sigma \cos\sigma/(1 - m^2\sin^2\sigma)]/m'^2 \tag{132}$$

From Equations 112, 118, 130, 131, and 132, we have, for z(t), the limit, as s approaches infinity, the relation

$$z(t) = (S/E)[E(m,\sigma) - m^2 \sin\sigma \cos\sigma/(1 - m^2\sin^2\sigma)^{1/2}] - iH, \quad \sigma = \sigma(t) \quad (133)$$

where σ and m are given by Equations 113 and 115.

We now investigate the values of the r.h.s. of Equation 133 as t approaches o'. We do this to evaluate the parameter m. As t approaches o', sin σ approaches ∞ by Equation 113. This gives the limiting case of Equation 133 as sin σ approaches ∞ as

$$(S/E) \underset{\sin\sigma \to \infty}{\text{limit}} [E(m,\sigma) - m^2 \sin\sigma \cos\sigma/(1 - m^2\sin^2\sigma)^{1/2}] = iH \quad (134)$$

Eq. 115.03 of Byrd and Friedman enables us to prove

$$\underset{\sin\sigma \to \infty}{\text{limit}} [E(m,\sigma) - m^2 \sin\sigma \cos\sigma/(1 - m^2\sin^2\sigma)^{1/2}] = i(K' - E') \quad (135)$$

which along with Equation 134 yields

$$(S/E)(K' - E') = H$$

or

$$H/S = (K' - E')/E \quad (136)$$

The last equation may be solved to determine m corresponding to a specified value of H/S. Figure 6 is a plot of H/S as a function of m.

Since the origin of the t-plane of Figure 3 corresponds to the coordinates x_t, y_t of the z-plane, Equations 101 and 133 give

$$(S/E)\{E(m,\arcsin[1/o']^{1/2}) - m^2[\frac{o' - 1}{o'(o' - m^2)}]^{1/2}\} - iH = x_t + iy_t \quad (137)$$

In Equation 137 the second order elliptic integral $E(m,\arcsin[1/o']^{1/2}$ is as defined by Equation 73 and may be evaluated by eq. 115.03 of Byrd and Friedman or eq. 17.4.9 of Abramowitz and Stegun depending on whether o' is positive or negative. Examination of the z and t-planes of Figure 3

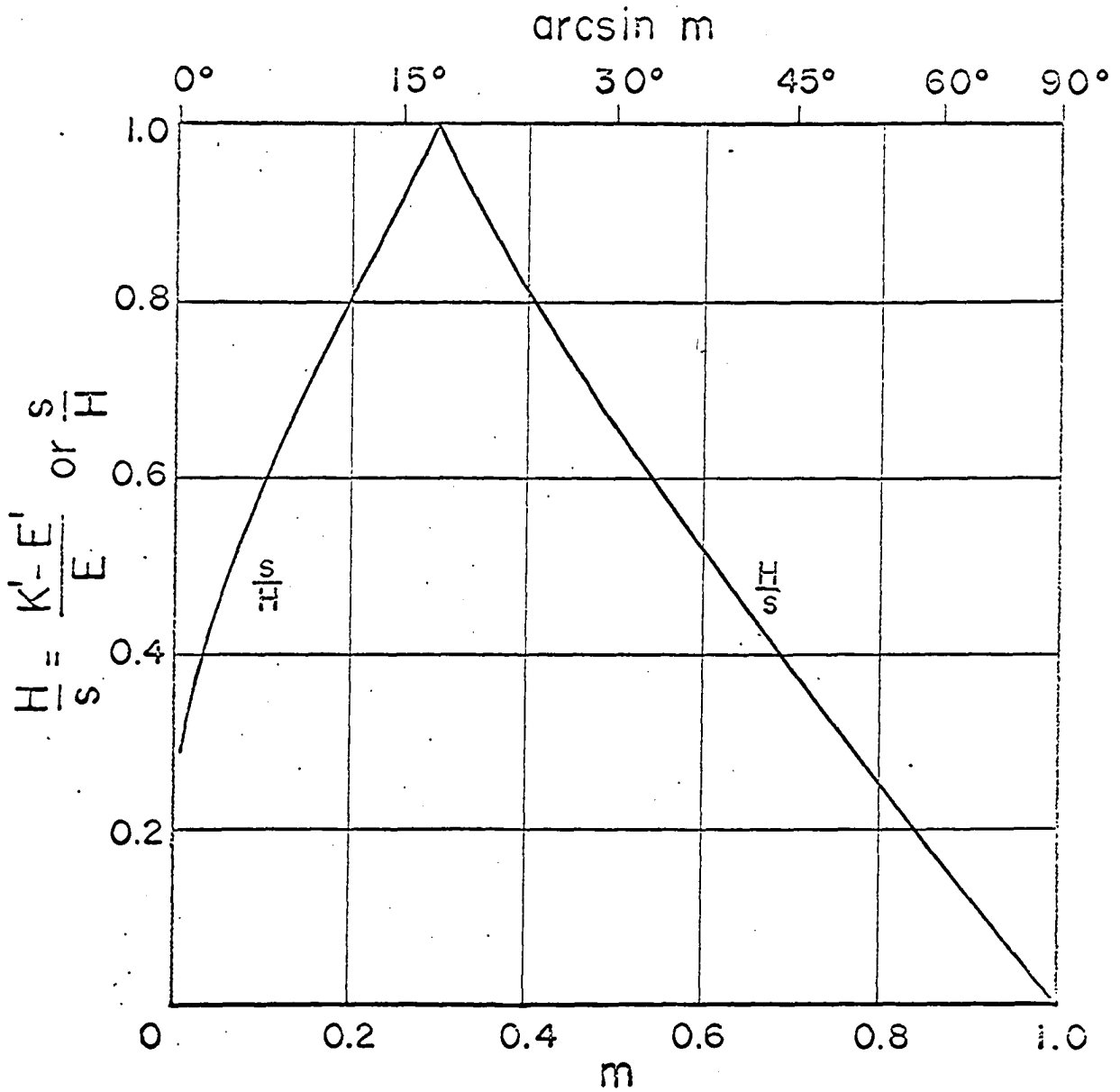

Figure 6. The graphical relationship of the elliptic modulus m to $(K' - E')/E$ used for Case 6.

shows if C is on the negative x-axis ($y_t = 0$), o' is positive; if C is on the negative y-axis ($x_t = 0$), o' is negative.

7. Examples and calculations

Two examples of Case 2 are now considered to illustrate seepage when the coarse gravel layer of Figure 2 does not extend to the base of the foundation. Also, as in the Figure 2, the width of the base is finite, but the plane water table extends to infinity horizontally in each direction and the soil is now infinitely deep.

To apply the results of Case 2 the following steps were utilized:

(i) Specification of the height of the plane water table H, the semi-width of the foundation s, the radius of the drain tube r, the location of the drain tube center $x_t + iy_t$, and the depth of the horizontal impermeable soil layer h.

(ii) Determination of m^2 from Equation 85 or from Figure 4.

(iii) Determination of M by Equation 80.

(iv) Determination of the constant o' by Equations 86, 87, or 88.

(v) Evaluation of the drain tube image point u_r of the t-plane by Equation 81.

(vi) Evaluation of Q/2k by Equation 34.

(vii) Calculation of the coordinates x and y corresponding to a specified complex potential $k\emptyset + i\psi$ by solving for the intermediate value t by Equation 28 followed by application of Equation 81.

In carrying out the calculations it was necessary to evaluate numerous incomplete elliptic integrals of the first and second kinds, in many cases, with complex arguments. The basic formulas used to evaluate incomplete first and second kinds of elliptic integrals were eq. 902.00 and 903.00 of Byrd and Friedman (1954). For complex arguments these were supplemented

by eq. 115.02 and 115.03 as well as by 17.4.8, 17.4.9, 17.4.11, and 17.4.12 of Abramowitz and Stegun (1964). The complete elliptic integrals of the first and second kinds were evaluated by eq. 17.3.34 and 17.3.36 of Abramowitz and Stegun. The inverse sine of a complex number was evaluated by eq. 4.4.37 of Abramowitz and Stegun.

For this case (Figure 7), the height of the plane water table above the foundation floor was chosen to be $H = 0.5s$ and the radius of the drain tube, $r = 0.025s$, where s is the semi-width of the foundation. The tile center is on the foundation barrier at $x = -s$. The value of the needed modulus is determined from Equation 85 and was found to be $m = 0.81$. The flow Q/2 into the drain from the region shown is determined by Equation 34 and was found to be $Q/2 = 0.17ks$. If one takes $k = 0.1$ m/hr and $s = 3$ m, there would result $Q/2 = 0.05$ $m^3/hr/m$.

Since $p/\rho g = \phi - y$, the potential is equal to the pressure head for $y = 0$, in particular, one has $p/\rho g = \phi$ along the negative x-axis. Observing the equipotential lines along the negative x-axis, we find that the pressure head varies from about $0.85H$ at $x = 0$ to zero at the tile surface. We can verify that the potential at the origin is $0.85H$ by using Figure 4. To use Figure 4 we need the values $u_r = 0.0003$ and $(u)_{t=0'} = 0.66$ which are determined from Equation 133. Interpolating between the solid curves of Figure 4 labeled $u_r = 0.001$ and $u_r = 0.0001$, we find the pressure head for $u = 0.66$ as $p/\rho g = 0.85H$ which agrees with our previous value $0.85H$ obtained directly from the equipotentials of Figure 7.

Figure 8 is a flow net for a geometry identical to that of Figure 7, except that the tile center is taken at the origin rather than at $x = -s$.

Figure 7. Flow net for Case 2 when the drain tube center is at $x/s = -1, y = 0$.

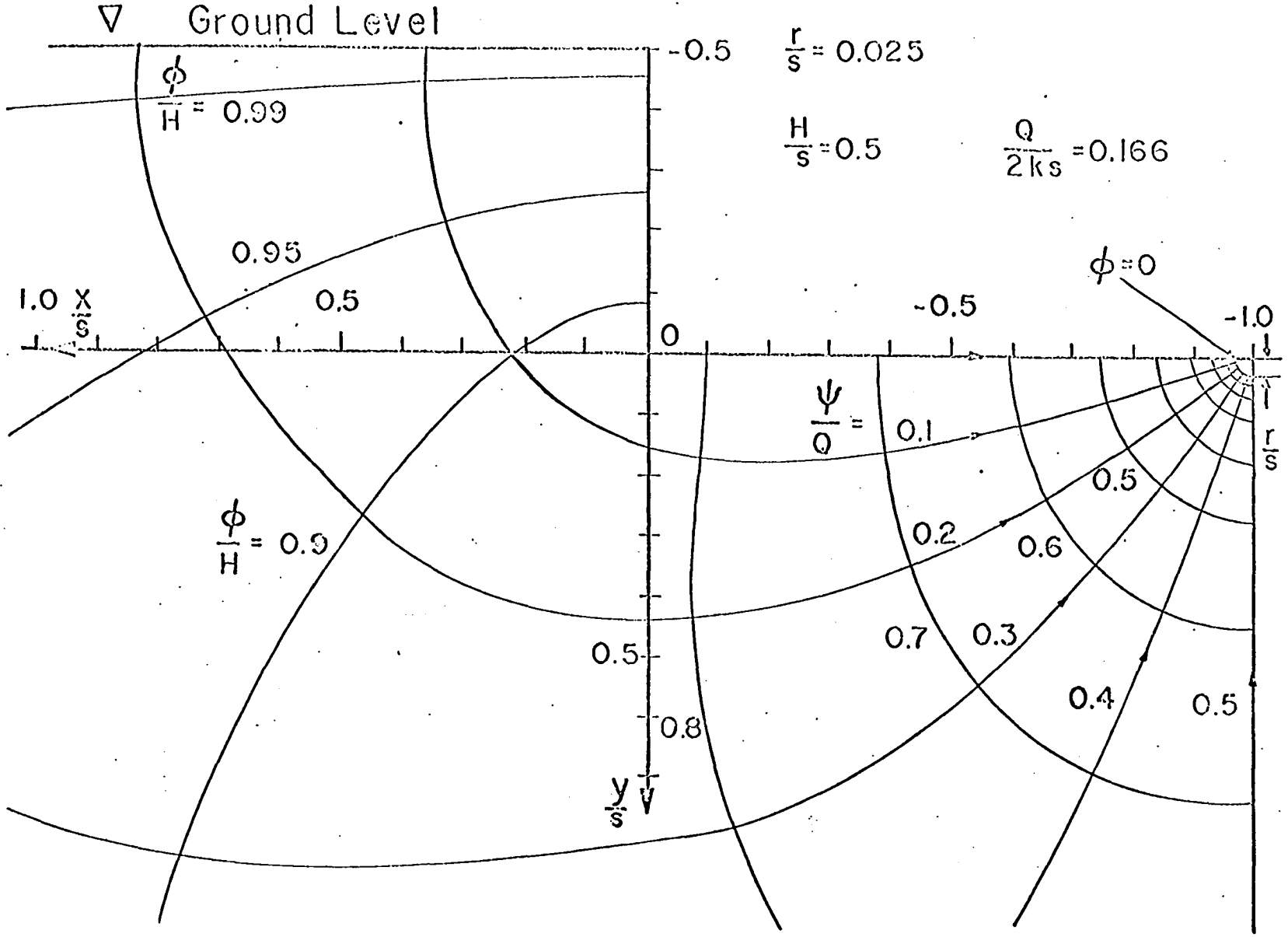
∇ Ground Level
-0.5
r/s = 0.025
φ/H = 0.99
H/s = 0.5
Q/2ks = 0.166
0.95
φ=0
1.0 X/s
0.5
0
-0.5
-1.0
ψ/Q = 0.1
0.5
0.2
0.6
r/s
φ/H = 0.9
0.7
0.3
0.5
0.4
0.5
0.8
y/s

Figure 8. Flow net for Case 2 when the drain tube center is at $x/s = 0, y = 0$.

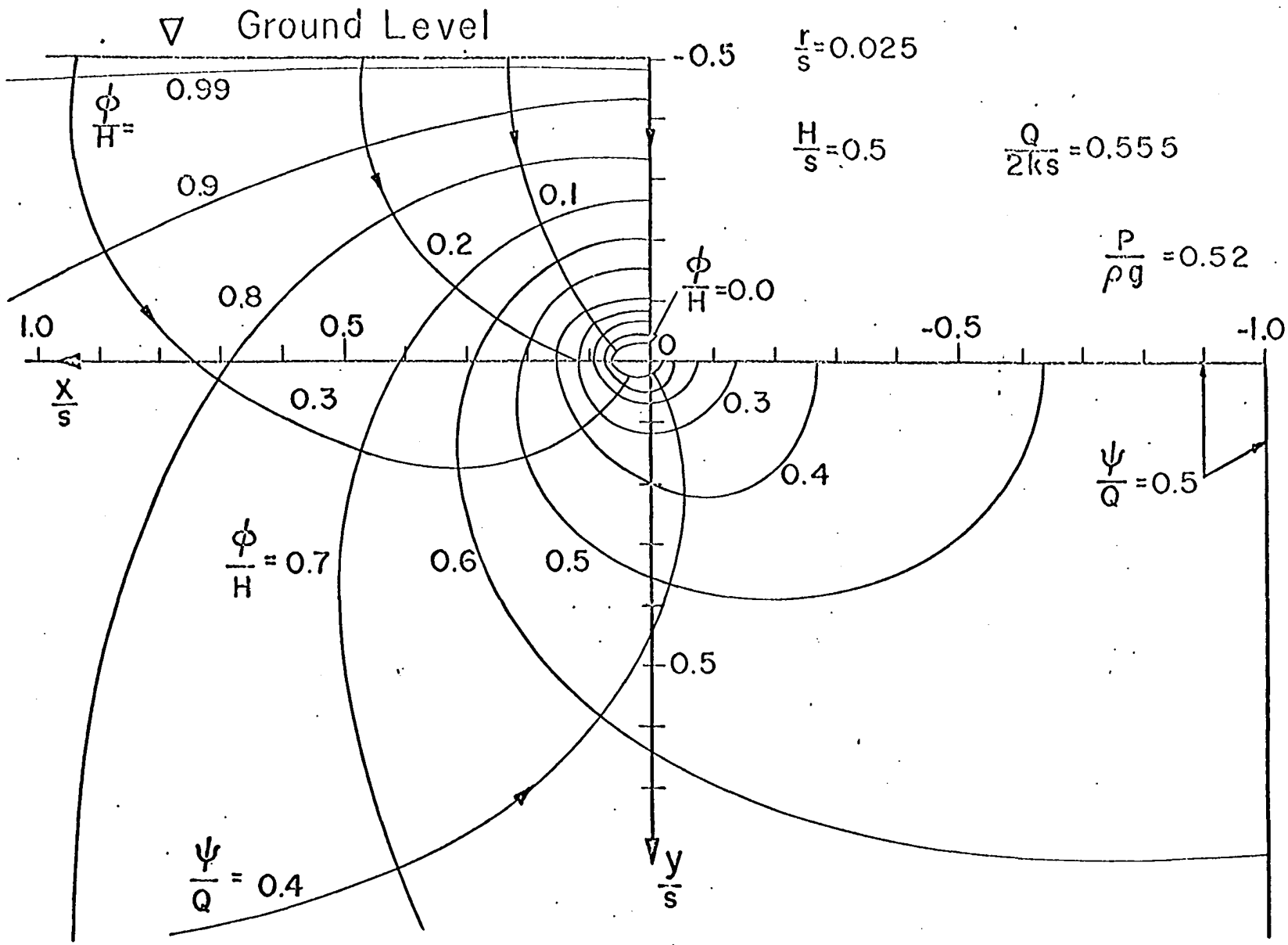
Ground Level
-0.5
r/s=0.025
H/s=0.5
Q/2ks=0.555
P/ρg=0.52
φ/H=
0.99
0.9
0.8
0.5
0.3
0.2
0.1
φ/H=0.0
1.0
0
-0.5
-1.0
X/s
0.3
0.4
ψ/Q=0.5
φ/H=0.7
0.6
0.5
-0.5
ψ/Q=0.4
y/s

The value of Q/2ks is 0.56 compared to 0.17 for the previous example of Figure 7. Thus, the flow rate to a tile located at the corner of the foundation is about three times that to the same size of a tile which is located at the center of the base of the foundation. The equipotential $\phi = 0.6H$ of Figure 8 intersects the $x = -s$ line at about $0.8s$ and the equipotential $\phi = 0.5H$ intersects the negative x-axis at $x = -0.63s$. Thus, the potential at $x = -s$, $y = 0$ must lie between $\phi = 0.5H$ and $\phi = 0.6H$. We can calculate ϕ at $x = -s$, $y = 0$ exactly by Equation 23. We will now do this since ϕ equals $p/\rho g$ along the foundation base and the pressure head is a maximum at $x = -s$. Examination of Figure 3 shows $x = -s$, $y = 0$ of the z-plane correspond to $u = b$, $v = 0$ of the t-plane. The calculations in preparing Figure 8 gave $b = -1.89$ from Equations 75 and 87 for $m = 0.81$. Substitution of $t = -1.89$ in Equation 23 gives

$$w(-1.89) = (iQ/\pi)\tan^{-1}(-2.89)^{1/2} + kH$$

Dwight (1962), eq. 408.18, gives

$$\tan(\pi/2 + i\ \coth^{-1}\gamma) = i\gamma$$

which is equivalent to

$$\tan^{-1}(i\gamma) = \pi/2 + i\ \coth^{-1}\gamma$$

Use of the last equation and the complex potential function w above gives

$$w(-1.89) = iQ/2 + kH[1 - (Q/2ks)(s/H)(2/\pi)\coth^{-1}(2.89)]$$

Recalling $w = k\phi + i\psi$, we find $\phi = 0.52H$ and $\psi = Q/2$. Thus a tile at the corner of the foundation gives a maximum pressure head along the base of $p/\rho g = 0.52H$ at the middle of the foundation base, whereas the tile located at the center gives a larger maximum pressure head of $p/\rho g = 0.85H$ found at the corner.

E. Coarse Gravel Layers at Each Side of a Foundation Extending to Depth of the Foundation

We choose in Figure 2 a finite value for the thickness δ of the coarse gravel and a value of zero for H. We observe under these conditions that the coarse gravel will extend to the base of the foundation as in Figure 9. Case 7 which follows is the most general case when gravel extends to the depth of the foundation, that is, s, S and h can each take any positive values whatever.

1. Case 7: Foundation of finite width, water table of finite width and soil below the foundation of finite depth

If the parameters h, s, and S of Figure 9 are all finite, the flow region as shown in the z-plane of Figure 10 is the rectangle ABEFA. The exterior angles of the rectangle in the z-plane are each $\pi/2$. If we map E at infinity in the t-plane of Figure 10, the Schwartz-Christoffel transformation Equation 15 mapping the interior of ABEFA to the upper half of the t-plane is

$$z(t) = M' \int (t - f)^{-1/2}(t - a)^{-1/2}(t - b)^{-1/2}dt + N \qquad (138)$$

where a, b, and f give the image points of A, B, and F of the z-plane. Using eq. 237.00 of Byrd and Friedman to evaluate the integral in Equation 138 gives

$$z(t) = M\, F(m,\sigma) + N, \qquad \sigma = \sigma(t) \qquad (139)$$

where M and N are constants to be determined, F is a normal elliptic integral of the first kind of modulus m and argument σ defined by Equation 72. The modulus and argument are given by

$$m = \left(\frac{a - f}{b - f}\right)^{1/2} \qquad (140)$$

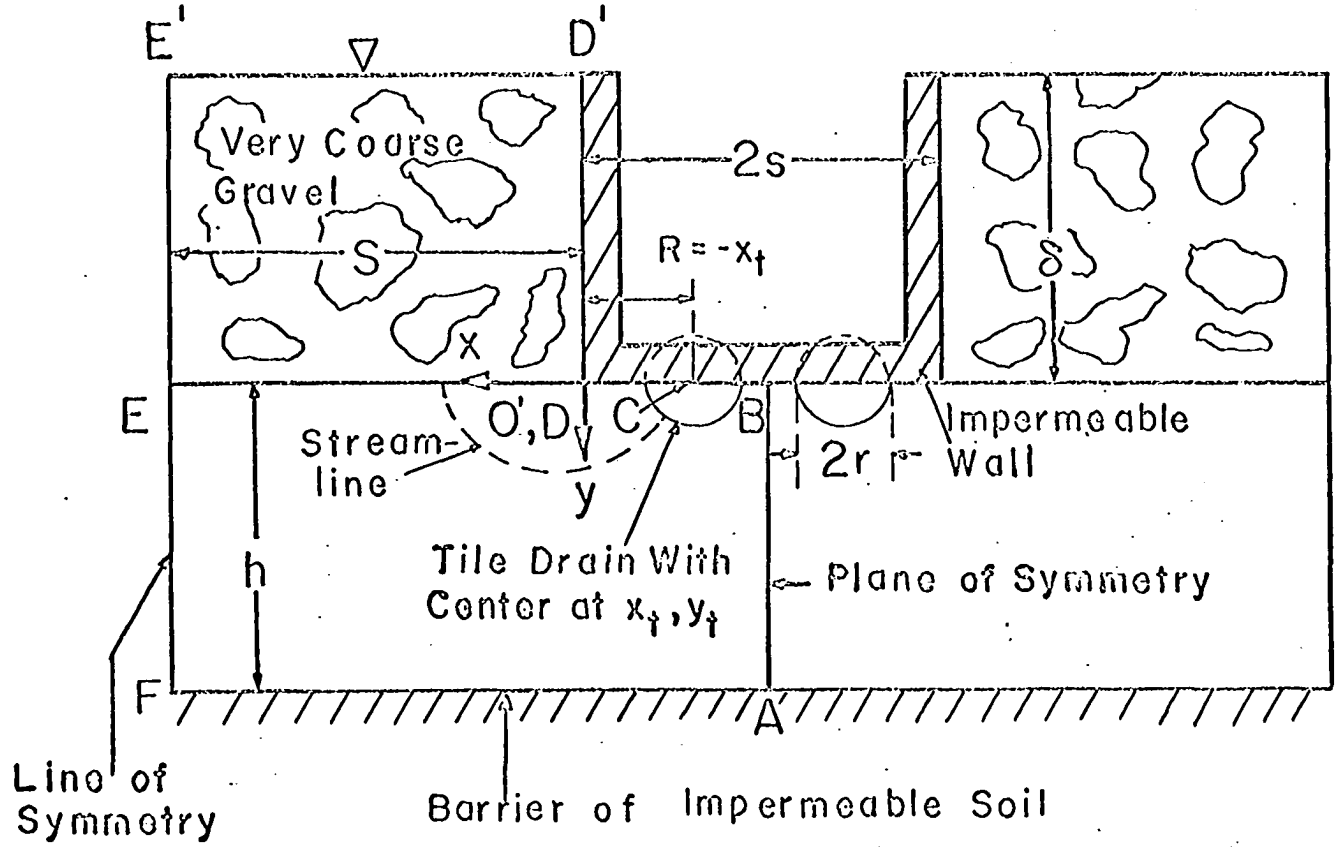

Figure 9. Flow geometry used for Cases 7-12 when a layer of coarse gravel extends alongside the foundation wall to the depth of the barrier.

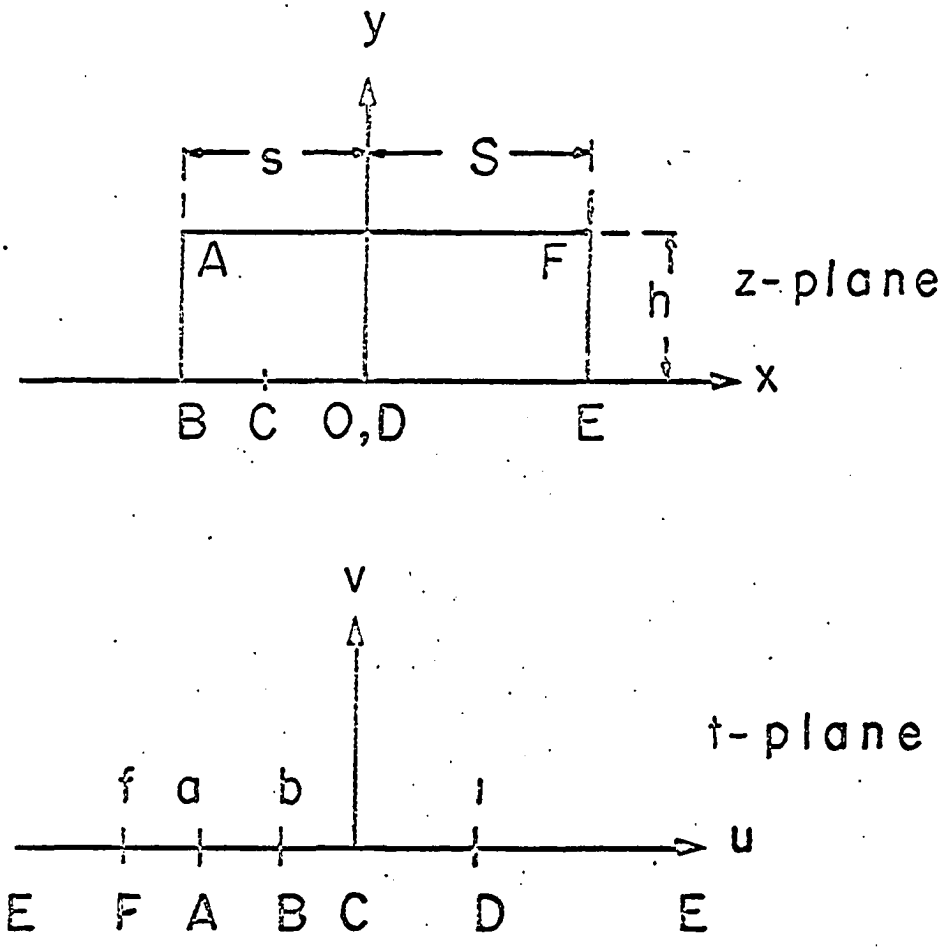

Figure 10. The z-plane and the t-plane for Cases 7-12.

and

$$\sigma = \sin^{-1}\left(\frac{t - b}{t - a}\right)^{1/2} \tag{141}$$

As the values f, a, and b of the t-plane correspond to the points F, A, and B of the z-plane, inspection of the z and t-planes of Figure 10 shows

$$z(f) = S + ih \tag{142a}$$

$$z(a) = -s + ih \tag{142b}$$

$$z(b) = -s \tag{142c}$$

Use of Equations 139, 140, and 141 gives from the last three equations

$$z(f) = M\,F(m,\sin^{-1}[1/m]) + N \tag{143a}$$

$$z(a) = M\,F(m,\sin^{-1}\infty) + N \tag{143b}$$

$$z(b) = M\,F(m,0) + N \tag{143c}$$

where $F(m,\sin^{-1}\infty)$ is the limiting value of $F(m,\sigma)$ as $\sin\sigma$ approaches infinity which by eq. 115.03 of Byrd and Friedman (1954) exists and is

$$F(m,\sin^{-1}\infty) = iK' \tag{144}$$

Eq. 8c of Appendix B of Harr (1962) is

$$F(m,\sin^{-1}[1/m]) = K + iK' \tag{145}$$

By Equation 72, F(m,0) is

$$F(m,0) = 0 \tag{146}$$

Use of Equations 144, 145 and 146 in Equations 143a, 143b, and 143c along with Equations 142a, 142b, and 142c give

$$M(K + iK') + N = S + ih \tag{147a}$$

$$iMK' + N = -s + ih \tag{147b}$$

$$M(0) + N = -s \tag{147c}$$

Solving the last three equations for M, N, and K/K', we find

$$M = h/K' \tag{148a}$$

or alternatively

$$M = (S + s)/K \tag{148b}$$

and

$$N = -s \tag{149}$$

Elimination of M from Equations 148a and 148b gives

$$K/K' = (S + s)/h \tag{150}$$

Since K and K' are functions of the modulus m, the value of m is implicitly defined by Equation 150. Figure 11 graphically gives the relationship between m and K/K'. Abramowitz and Stegun (1964) in Table 17.3 give m as a function of K'/K.

We may now write down the result for z(t) from Equations 139, 148, and 149 as

$$z(t) = (h/K')\ F(m,\sigma) - s, \qquad \sigma = \sigma(t) \tag{151}$$

where σ is defined by Equation 141 and m is determined from Equation 150 or from Figure 10. To determine a and b of Equation 141, we examine point C of the z and t-planes of Figure 10 and find

$$z(0) = x_t + i\ y_t \tag{152a}$$

$$z(1) = 0 \tag{152b}$$

where x_t and y_t are the x and y coordinates of the center of the tile drain. Before getting explicit equations for b and a, we shall solve Equation 151 for t in terms of z.

Solving Equation 151 for $F(m,\sigma)$, we find

$$F(m,\sigma) = (K'/h)(z + s) \tag{153}$$

Taking the Jacobian function "sn" of both sides, we find with the help of

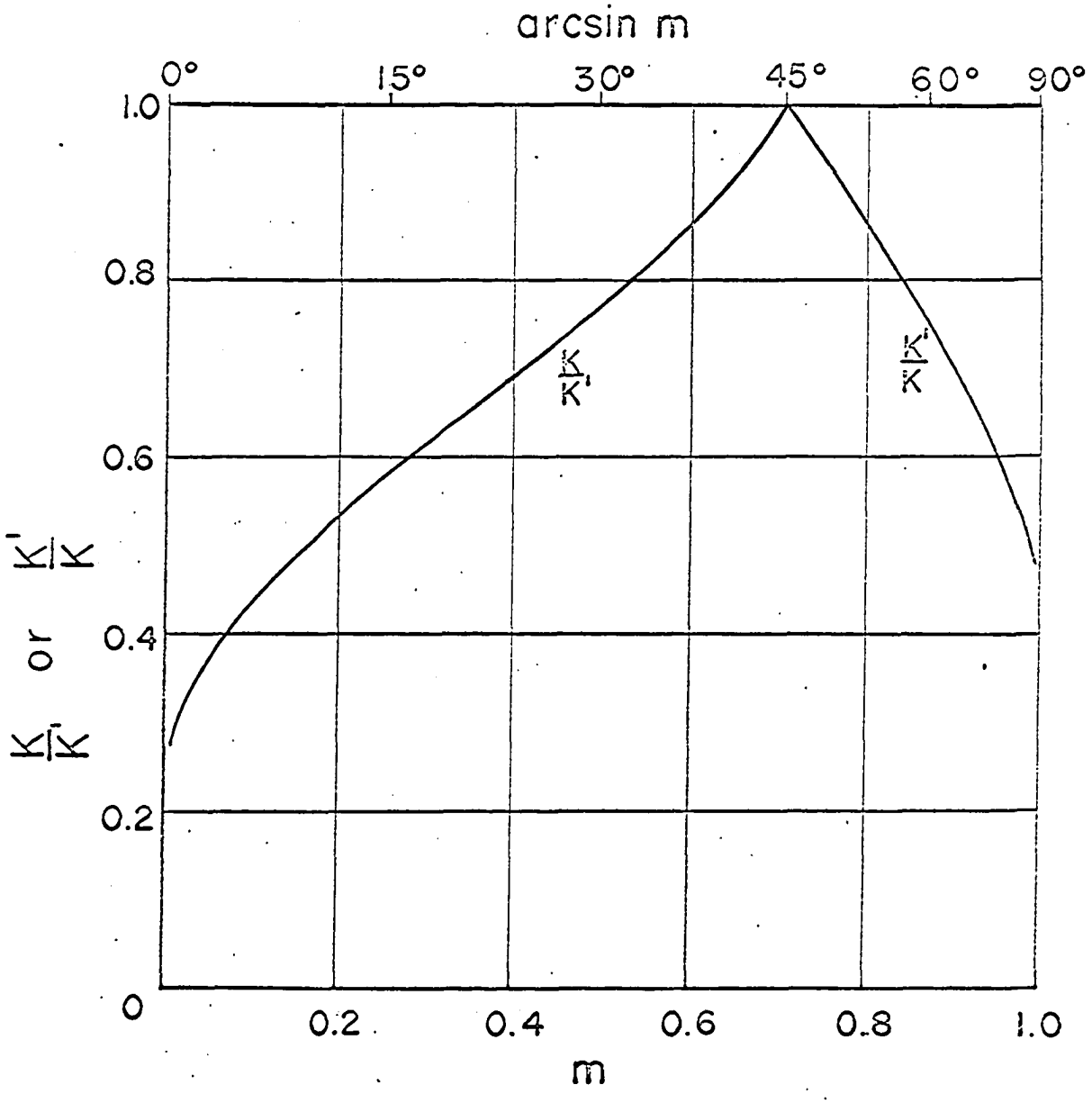

Figure 11. The graphical relationship of the elliptic modulus m to K/K' used for Case 7 and for the ditch drainage problems.

eq. 9b and 9e of Appendix B of Harr (1962), the relation

$$\sigma = \mathrm{sn}[(K'/h)(z + s)]$$

Use of Equation 141 and the last equation gives

$$\left(\frac{t - b}{t - a}\right)^{1/2} = \mathrm{sn}[(K'/h)(z + s)] \tag{154}$$

Squaring both sides of the last equation and solving for t yields

$$t = \frac{b - a\ \mathrm{sn}^2[(K'/h)(z + s)]}{1 - \mathrm{sn}^2[(K'/h)(z + s)]} \tag{155}$$

which is our needed result. Substitution of the r.h.s. of Equation 155 for u into Equations 40a and 40b would give the pressure distribution along the boundary of the flow system as a function of z.

We shall now find explicit relations for a and b. Use of Equations 152a and 152b along with Equation 155 leads to the two equations

$$b - a\ \mathrm{sn}^2[(K'/h)(x_t + s + i\ y_t)] = 0 \tag{156a}$$

and

$$\frac{b - a\ \mathrm{sn}^2(K's/h)}{1 - \mathrm{sn}^2(K's/h)} = 1 \tag{156b}$$

Solving the last two equations for a and b, we find

$$a = \frac{1 - \mathrm{sn}^2(K's/h)}{\mathrm{sn}^2[(K'/h)(x_t + s + i\ y_t)] - \mathrm{sn}^2(K's/h)} \tag{157a}$$

and

$$b = \frac{\mathrm{sn}^2[(K'/h)(x_t + s + i\ y_t)](1 - \mathrm{sn}^2(K's/h)}{\mathrm{sn}^2[(K'/h)(x_t + s + i\ y_t)] - \mathrm{sn}^2(K's/h)} \tag{157b}$$

2. Case 8: Foundation of finite width, water table of finite width and soil below the foundation of infinite depth

If the permeable soil extends to a great depth, then h of Figures 9 and 10 approaches infinity. Correspondingly, a approaches f in the t-plane. We consider s and S finite. Examination of Equation 150 gives

$$\lim_{h \to \infty} K/K' = 0 \tag{158}$$

It follows from the relationship of K/K' as shown in Figure 11 that m in the limit as h approaches ∞ must be zero:

$$\lim_{h \to \infty} m = 0 \tag{159}$$

Using Equations 139, 148, and 149 with $m = 0$, we find

$$z(t) = [S + s)/K]\, F(0, \arcsin[\frac{t - b}{t - a}]^{1/2}) - s \tag{160}$$

From the definition of $F(m,\sigma)$ in Equation 72, we find

$$F(0,\sigma) = \sigma \tag{161}$$

and

$$[K]_{m=0} = \pi/2 \tag{162}$$

The last two equations when used in Equation 160 give

$$z(t) = (2/\pi)(S + s) \arcsin(\frac{t - b}{t - a})^{1/2} - s \tag{163}$$

Solving the last equation for t, we find

$$t = \frac{b - a \sin^2[(\pi/2)(z + s)/(S + s)]}{1 - \sin^2[(\pi/2)(z + s)/(S + s)]} \tag{164}$$

which could perhaps more easily have been obtained from Equation 155 and use eq. 122.08 of Byrd and Friedman (1954) which gives

$$(\mathrm{sn}\ U)_{m=0} = \sin U \tag{165}$$

It is easily verified that use of Equation 165 and $(\pi/2)/(S + s)$ for K'/h in Equation 155 gives Equation 164 also. Similarly, explicit equations for a and b can be obtained by use of Equation 165 in Equations 157a and 157b.

3. Case 9: Foundation of finite width, water table of infinite width and soil below the foundation of finite depth

If the layer of gravel extends to an infinite width, the parameter S of Figure 9 approaches infinity. We keep h and s finite. An examination of Equation 150 shows in the limit as S approaches infinity, the relation

$$\lim_{S\to\infty} K'/K = 0 \tag{166}$$

Using the same reasoning for Equation 166 as for Equation 158 in the previous section, we conclude that K must be approaching infinity and that m must be approaching unity:

$$\lim_{S\to\infty} m = 1 \tag{167}$$

By use of Equations 148, 149 and 167, we find for Equation 139

$$z(t) = (2h/\pi)\, F(1,\sigma) - s, \qquad \sigma = \sigma(t) \tag{168}$$

where σ is given by Equation 141. Eq. 111.04 of Byrd and Friedman (1954) can be used to evaluate $F(1,\sigma)$ in terms of elementary functions to give for the last equation

$$z(t) = (2h/\pi)\, \ln(\tan\sigma + \sec\sigma) - s, \qquad \sigma = \sigma(t)$$

Use of Equation 141 to evaluate $\tan\sigma$ and $\sec\sigma$ in terms of t gives

$$z(t) = (2h/\pi)\, \ln\left[\left(\frac{t-b}{b-a}\right)^{1/2} + \left(\frac{t-a}{b-a}\right)^{1/2}\right] - s \tag{169}$$

An alternative form is found by observing the relation

$$\frac{t - a}{t - b} = \frac{t - b}{b - a} + 1 \tag{170}$$

and applying eq. 700.1 of Dwight (1961):

$$z(t) = (2h/\pi)\ \sinh^{-1}\left(\frac{t - b}{b - a}\right)^{1/2} - s \tag{171}$$

We now wish to solve Equation 171 for t in terms of z. Solving the last equation for t gives

$$t = (b - a)\ \sinh^2[(\pi/2h)(z + s)] + b \tag{172}$$

a result which could have been obtained from Equation 155 with the help of eq. 122.09 of Byrd and Friedman (1954) which gives

$$(\text{sn } U)_{m=1} = \tanh U \tag{173}$$

The constants a and b may be evaluated from Equations 157a and 157b by use of Equation 173 along with substitution of $\pi/2$ for K':

$$a = \frac{1 - \tanh^2(\pi s/2h)}{\tanh^2[(\pi/2h)(x_t + s + iy_t)] - \tanh^2(\pi s/2h)} \tag{174a}$$

$$b = \frac{\tanh^2[(\pi/2h)(x_t + s + iy_t)][1 - \tanh^2(\pi s/2h)]}{\tanh^2[(\pi/2h)(x_t + s + iy_t)] - \tanh^2(\pi s/2h)} \tag{174b}$$

One can verify that if point C of Figure 9 lies on the boundary DBAF, the coordinates x_t, y_t will give real values for a and b from Equations 174a and 174b.

4. Case 10: Foundation of infinite width, water table of finite width and soil below the foundation of finite depth

If the foundation extends to a great width, s of the z-plane of Figure 10 will approach infinity and a of the t-plane will approach b. We consider h and S finite. Examination of limits of Equations 140 and

141, as a approaches b as in the two previous sections, reveals Equation 139 would in this case be of an indeterminate form. It is, however, easy to develop a new t to z-plane transformation. The Schwartz-Christoffel transformation Equation 15 as s approaches infinity is

$$z(t) = M' \int (t - f)^{-1/2}(t - a)^{-1} dt + N \tag{175}$$

Use of eq. 192.11 of Dwight (1961) to evaluate the integral in Equation 175 gives

$$z(t) = M \ln\left[\frac{(t - f)^{1/2} - (a - f)^{1/2}}{(t - f)^{1/2} + (a - f)^{1/2}}\right] + N \tag{176}$$

The constants M and N may be evaluated by using Equation 176 and the limiting value of z = S as t approaches infinity. We find

$$N = S \tag{177}$$

Similarly, Equations 176, 177 and z(f) = S + ih yields for M

$$M = h/\pi \tag{178}$$

which when substituted in Equation 176 along with Equation 177 gives

$$z(t) = (h/\pi) \ln\left[\frac{(t - f)^{1/2} - (a - f)^{1/2}}{(t - f)^{1/2} + (a - f)^{1/2}}\right] + S \tag{179}$$

We may obtain an explicit form for t in terms of z by solving Equation 179 for t. We find

$$t = f + (a - f)\left\{\frac{1 + \exp[(\pi/h)(z - S)]}{1 - \exp[(\pi/h)(z - S)]}\right\}^2 \tag{180}$$

which is equivalent to

$$t = f + (a - f) \coth^2[(\pi/2h)(z - S)] \tag{181}$$

Use of Equations 152a and 152b in the last equation leads to

$$f + (a - f) \coth^2[(\pi/2h)(x_t - S + i\, y_t)] = 0 \tag{182a}$$

$$f + (a - f) \coth^2(-\pi S/2h) = 1 \tag{182b}$$

which can be solved for a and f. The results are

$$a = 1/\{1 - \operatorname{csch}^2(\pi S/2h)\ \sinh^2[(\pi/2h)(x_t - S + i\ y_t)]\} \tag{183}$$

and

$$f = 1/\{1 - \coth^2(\pi s/2h)\ \tanh^2[(\pi/2h)(x_t - S + i\ y_t)]\} \tag{184}$$

5. Case 11: Foundation of finite width, water table of infinite width and soil below the foundation of infinite depth

If the layer of gravel is of infinite width and the soil extends to a great depth, the parameters S and h of the z-plane of Figure 10 each approach infinity. If the foundation semi-width s is finite, the flow region of the z-plane will be the upper right quarter bounded by the y-axis and the vertical line $x = -s$.

The transformation of a quarter-plane to a half-plane is well known as in Chapter 6 of Kober (1957) or may be found by use of Equation 15 with $\pi/2$ for the exterior angle of B:

$$z(t) = M' \int (t - b)^{-1/2} dt + N$$

Evaluation of the integral gives immediately

$$z(t) = M(t - b)^{1/2} + N \tag{185}$$

As z(b) is -s and z(1) is 0, we have from the last equation

$$M = s/(1 - b)^{1/2} \tag{186}$$

$$N = -s \tag{187}$$

which when substituted back into Equation 185 give

$$z(t) = s[(\frac{t - b}{1 - b})^{1/2} - 1] \tag{188}$$

The constant b is evaluated by substituting $z = x_t + iy_t$ and $t = 0$ in Equation 185 to obtain

$$s[-b/(1 - b)]^{1/2} - s = x_t + iy_t \tag{189}$$

If we have $y_t = 0$ Equation 189 yields for b

$$b = \frac{(x_t/s + 1)^2}{(x_t/s + 1)^2 - 1}, \qquad y_t = 0 \tag{190}$$

Similarly, for $x_t = -s$, we find for b

$$b = (y_t/s)^2/[1 + (y_t/s)^2], \qquad x_t = -s \tag{191}$$

For $x_t = -s$ and $y = 0$, b is zero:

$$b = 0, \qquad x_t = -s, \; y_t = 0 \tag{192}$$

6. Case 12: Foundation of infinite width, water table of infinite width and soil below the foundation of infinite depth

Allowing h, s, and S of Figure 10 to all approach infinity is equivalent physically to having a base of great width, water table of great width, and a soil of great depth. The flow region is then geometrically and analytically very simple; it is the upper half of the z-plane of Figure 12. The coordinates of the tile center are $x = -R$, $y = 0$ and we have point C between O' and B, necessarily. The points B and E are at infinity and points O' and D coincide. The transformation from the z to the t-plane by inspection of Figure 12 is

$$t = 1 + z/R \tag{193}$$

The inverse is obtained by solving the last equation for z with the result

$$z = R(t - 1) \tag{194}$$

The complex potential plane w is also shown in Figure 12 and is identical to the w-plane of Figure 3.

A flow net will later be given for Case 12 and compared to flow net resulting when a vertical sheetpile extends downward from the origin of the z-plane of Figure 9.

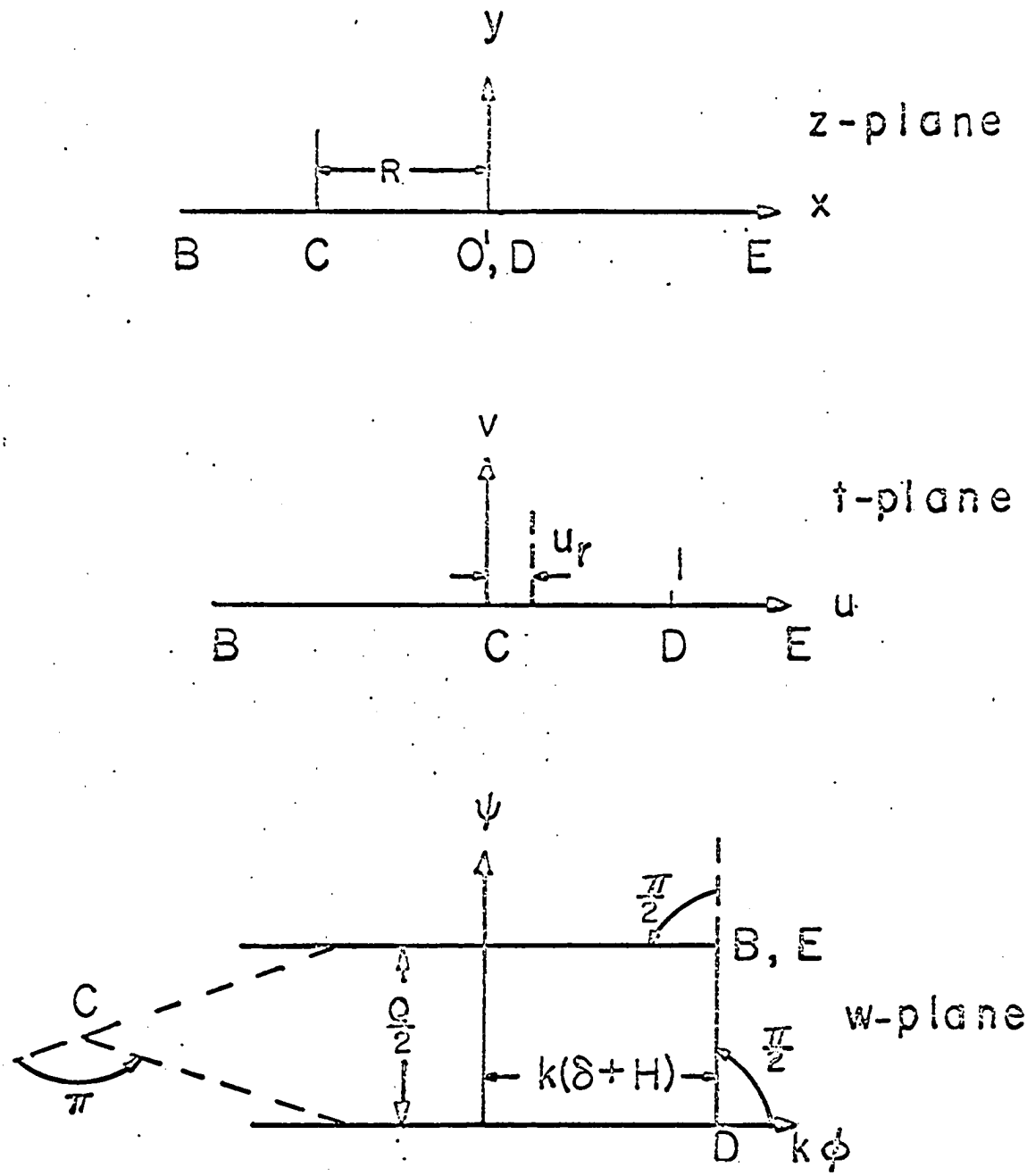

Figure 12. The z, t and w-planes for Case 12.

7. Examples and calculations

Two examples, one of Case 9 and one of Case 11, are now considered to illustrate seepage to a tile drain from a coarse gravel layer extending to the base of a foundation. In both examples the width of the base is finite and the width of the coarse gravel layer is infinite.

In applying the results for Case 9, the following steps are used:

(i) Specification of the parameters s, h, δ, r, x_t, and y_t.

(ii) Evaluation of a and b by Equations 174a and 174b.

(iii) Evaluation of u_r from Equation 171 with $z = x_t + r + iy_t$.

(iv) Determination of Q/2k by Equation 34.

(v) Calculation of the x and y values corresponding to specified values of ϕ and ψ by first solving for t by Equation 28 and then for z from Equation 171. This step yields a flow net.

In place of step (v), we could solve for the complex potential $k\phi + i\psi$ for a given value of $x + iy$ in the z-plane by solving for t from Equation 172 followed by Equation 23 for w.

In Figure 13, a flow net for Case 9, the coarse gravel is of thickness $\delta = 0.5s$, the tile radius $r = 0.025s$, and the impermeable soil layer is at a depth $h = 0.5s$ where s is the semi-width of the basement floor and can have any positive value. The calculated value of Q/2ks is 0.138. If we have k = 0.1 m/hr and s = 3 m, we find Q/2 = 0.041 m^3/hr/m. The values of r, δ, and h for the same system are 0.075, 1.5, and 1.5 m, respectively. The streamline labeled $\psi/Q = 0.4$ intersects the x-axis at $x = 0.38s$. Thus, most of the seepage takes place close to the foundation wall. The equipotential $k\phi = 0.88$ intersects the x-axis at $x = -0.18s$. Thus, a piezometer whose bottom was placed at $x = -0.18s$

Figure 13. Flow net for Case 9 when the drain tube center is at $x/s = -1$, $y/s = 0$.

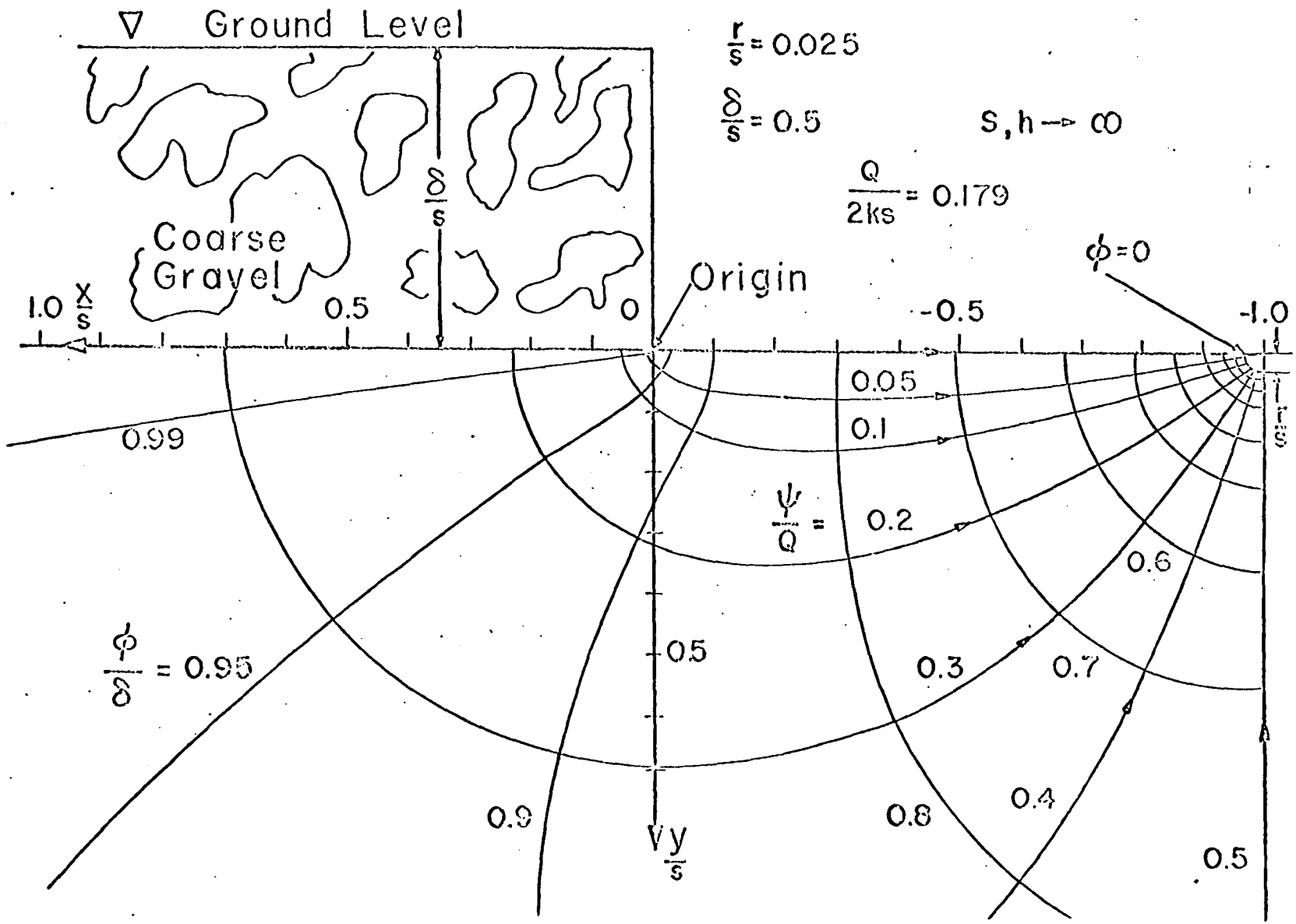
∇ Ground Level
r/s = 0.025
δ/s = 0.5
S, h → ∞
Q/2ks = 0.179
Coarse Gravel
δ/s
Origin
φ=0
1.0 x/s
0.5
0
-0.5
-1.0
0.05
0.1
0.2
0.6
0.99
ψ/Q =
φ/δ = 0.95
0.5
0.3
0.7
0.9
0.8
0.4
0.5
Vy/s

Figure 14. Flow net for Case 11 when the drain tube center is at $x/s = -1, y = 0$. The soil flow medium is infinitely deep.

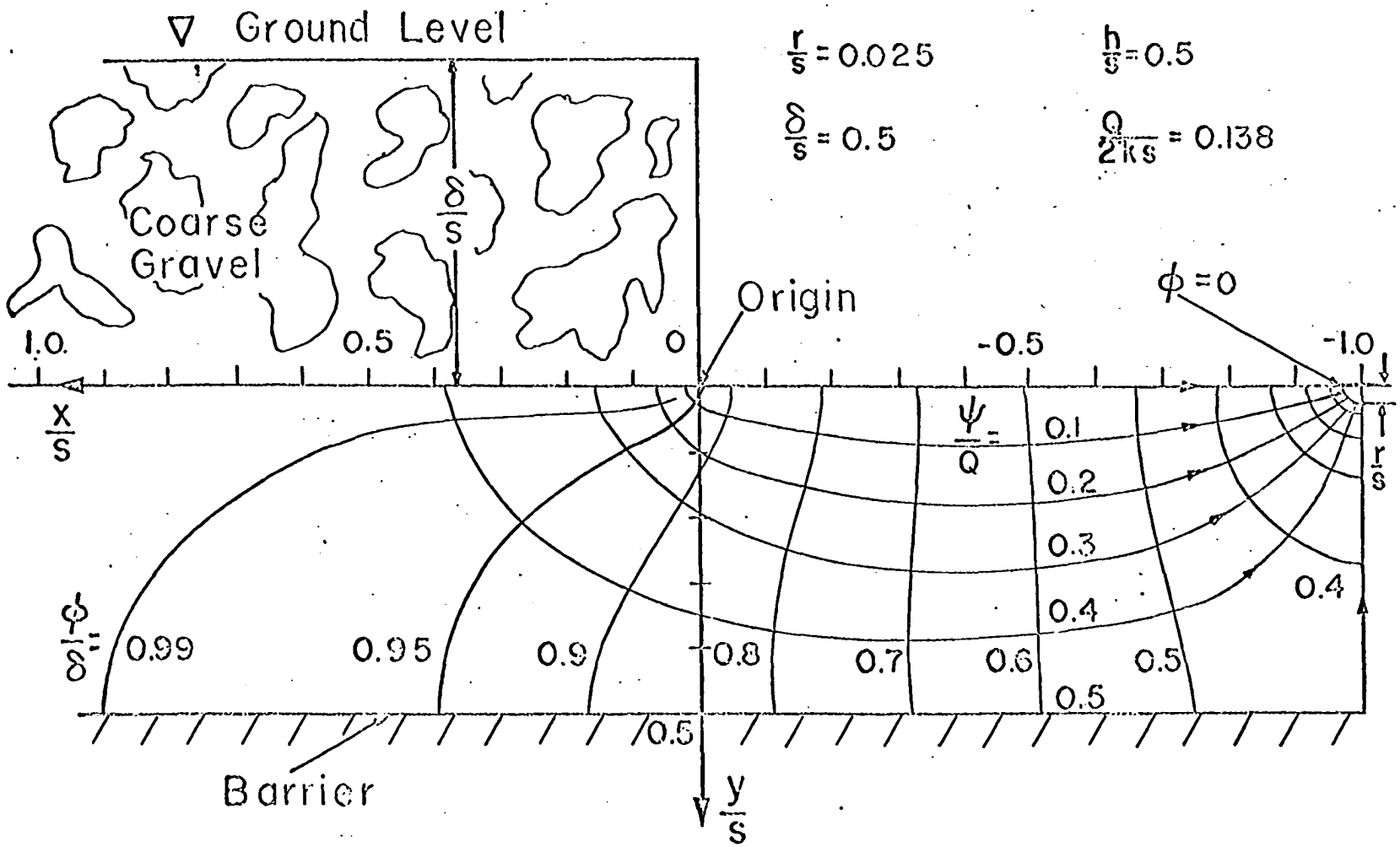
∇ Ground Level
r/s = 0.025
h/s = 0.5
δ/s = 0.5
Q/2πks = 0.138
Coarse Gravel
δ/s
Origin
φ = 0
1.0
0.5
0
-0.5
-1.0
x/s
ψ/Q
0.1
0.2
0.3
0.4
0.4
r/s
φ/δ =
0.99
0.95
0.9
0.8
0.7
0.6
0.5
0.5
0.5
Barrier
y/s

would have water standing in it to a height 0.8δ. The pressure head, which is the same as the total potential when y = 0 along the foundation, was a maximum, $p/\rho g = \delta$, at the origin and decreases to a value of 0 at the tile surface.

The flow system of Figure 14 is the same as that of the previous example, but with an infinite soil depth. For the infinite soil depth, the value of Q/2ks is 0.179. As the value of Q/2ks in the previous example was 0.138, we conclude the presence of an impermeable barrier at a depth h = 0.5s has reduced the flow by 23 percent compared with a barrier at infinite depth. A close comparison of the equipotentials of Figures 13 and 14 reveals the pressure head at most points along the basement floor is slightly higher when no barrier is present. For example, at x = -0.5δ, Figure 13 gives a potential of about 0.6δ and Figure 14 about 0.7δ. Although the difference in pressure head is significant for the steady-state problem, in corresponding unsteady-state cases with a falling water table, there would be less difference, as the system with no lower barrier would decrease the height of saturation in the coarse gravel layer at a faster rate which would drop the pressure all along the foundation base at a faster rate.

F. Sheetpile Extending Vertically Downward Below Foundation

Consider as in Figure 15 a thin sheetpile of length ε extending vertically downward along the y-axis. The flow region below BDD'O'E will be transformed to a t-plane as before. The corresponding t to w-plane transformation will be given by Equation 28. Although the z-plane geometry of Figure 14 is most like Case 12, the same method is

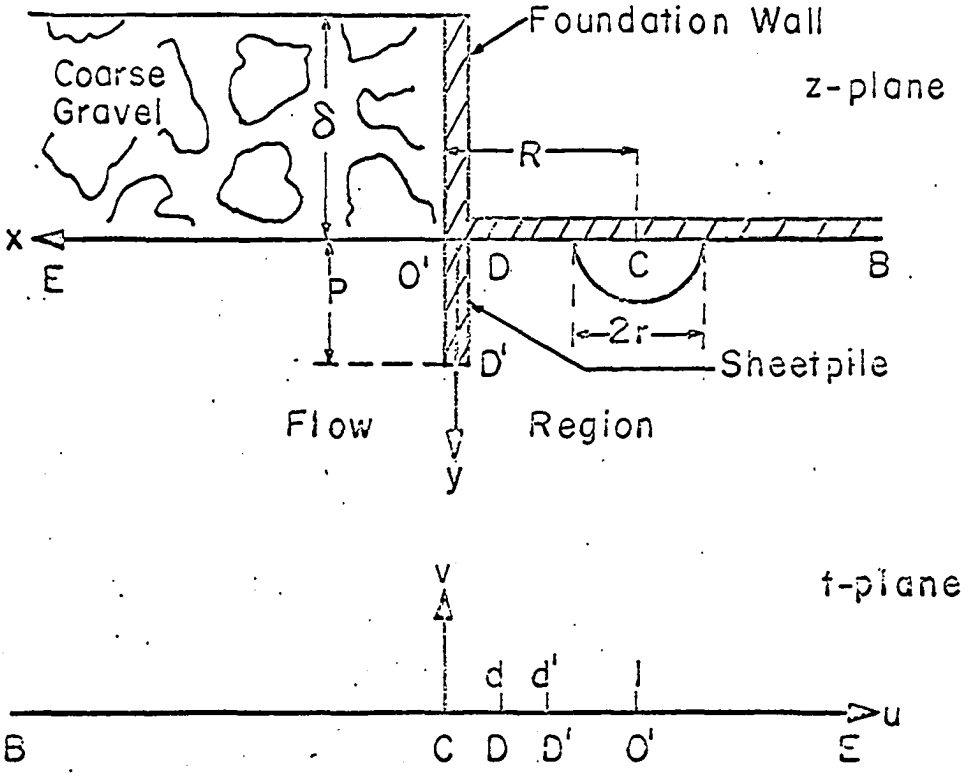

Figure 15. The z and t-planes used for a sheetpile extending vertically downward from the corner of an infinitely wide foundation.

applicable to any of the 12 cases described in the previous section with sheetpiling added. The same method could also be applied for a horizontal barrier extending along the positive x-axis to the left of the foundation wall of Figure 15.

The exterior angles at D, D', and O' of the z-plane of Figure 15 are $\pi/2$, $-\pi$, and $\pi/2$, respectively. The Schwartz-Christoffel transformation mapping the flow region BCDD'O'E to the upper half of the t-plane by Equation 15 is

$$z(t) = M \int (t - d)^{-1/2}(t - d')(t - 1)^{-1/2} dt + N \tag{195}$$

where D, D', and O' of the z-plane correspond to d, d', and 1 in the t-plane. Applying eq. 195.01 and 196.02 of Dwight (1961), we obtain

$$z(t) = M\{(t - 1)^{1/2}(t - d)^{1/2} - (2d' - 1 - d) \ln[(t - 1)^{1/2} + (t - d)^{1/2}]\} + N \tag{196}$$

As z(1) and z(d) are each zero, Equation 196 gives

$$-M(2d' - 1 - d)\ln(1 - d)^{1/2} + N = 0 \tag{197a}$$

$$-iM(2d' - 1 - d)[\ln(1 - d)^{1/2} + i\pi/2] + N = 0 \tag{197b}$$

from which we conclude if M is nonzero the coefficient $(2d' - 1 - d)$ is zero or d' is given by

$$d' = (1 + d)/2 \tag{198}$$

If $(2d' - 1 - d)$ is zero in Equation 197a, then N is given by

$$N = 0 \tag{199}$$

As z(d') is $i\varepsilon$, we have by Equations 196 and 199 the result

$$iM(1 - d')^{1/2}(d' - d)^{1/2} = i\varepsilon$$

or solving for M, we have

$$M = \varepsilon/[(1 - d')(d' - d)]^{1/2}$$

By use of the r.h.s. of Equation 198 for d', the last equation gives

$$M = 2\varepsilon/(1 - d) \tag{200}$$

Substituting Equations 199 and 200 and using Equation 198 in Equation 196, we find the z to t-plane transformation as

$$z(t) = \left(\frac{2\varepsilon}{1 - d}\right)(t - 1)^{1/2}(t - d)^{1/2} \tag{201}$$

In order to determine the inverse we square both sides of Equation 201 and rearrange to give a quadratic in t. The result is

$$t^2 - (1 + d)t + d - [z^2(1 - d)^2]\, 4\varepsilon^2 = 0$$

The solution of the quadratic is

$$t = (1 + d)/2 + \left\{(1 + d)^2 - 4\left[d - \frac{z^2(1 - d)}{4\varepsilon^2}\right]\right\}^{1/2}/2 \tag{202}$$

where the positive sign was chosen in the solution to give a t value of 1 for z values of 0 or d.

To apply Equation 201 the constant d must be evaluated. As the x-coordinate of the drain center is -R and the corresponding t-plane image is zero, we have from Equation 201

$$-R = \left(\frac{2\varepsilon}{1 - d}\right)(-1)^{1/2}(-d)^{1/2} \tag{203}$$

which may be solved for d:

$$d = \left(\frac{R^2 + 2\varepsilon^2}{R^2}\right)\left\{1 - \left[1 - \left(\frac{R^2}{R^2 + 2\varepsilon^2}\right)^2\right]^{1/2}\right\} \tag{204}$$

In order to solve for the amount of flow Q from Equation 34, it is necessary to evaluate u_r, the t-plane image of a point on the tile surface $x = -R + r$. If we define the equipotential passing through the x-axis at $x = -R + r$ as the tile surface and use u_r as its image on the u-axis of the t-plane, Equation 201 gives

$$-R + r = \left(\frac{2\varepsilon}{1 - d}\right)(u_r - 1)^{1/2}(u_r - d)^{1/2}$$

Squaring both sides of the last equation and substituting d/r^2 for $(1 - d)^2/4\varepsilon^2$ from Equation 203, we find

$$u_r^2 - (1 + d)u_r - (r/R)(2 - r/R) = 0$$

giving for u_r

$$u_r = \frac{1 + d - \{(1 + d)^2 - 4(r/R)d[2 - (r/R)]\}^{1/2}}{2} \qquad (205)$$

If the potential ϕ_r at the tile surface is zero and H = 0, the expression Equation 34 gives for Q/2 the amount of flow per unit time per unit length of tile as before

$$Q/2 = \pi k\delta/\ln\left[\frac{1 + (1 - u_r)^{1/2}}{1 - (1 - u_r)^{1/2}}\right], \qquad \phi = 0$$

which for small u_r is approximately the same as

$$Q/2 = \pi k\delta/\ln(4/u_r), \qquad 0 < u_r \ll 1$$

1. Numerical calculations for sheetpiling

The following series of steps were followed to investigate flow around a sheetpile for the geometry of the z-plane of Figure 15:

(i) Specification of the distance from the origin to the tile center R, the depth of the sheetpile ε, the height of the water table δ, and the drain radius r.

(ii) Calculation of the constant d by Equation 204 and M by Equation 200.

(iii) Determination of u_r by Equation 205 and Q/2k by Equation 34.

(iv) Evaluation of the x, y-coordinates for a given value of $k\phi + i\psi$ by using Equation 28 to evaluate t followed by the z-transformation Equation 201.

Instead of (iv) we could specify x + iy and determine the corresponding complex potential $k\phi + i\psi$ by use of Equations 23 and 202. The pressure

Figure 16. Flow net when a sheetpile extends vertically downward from a corner of an infinitely wide foundation.

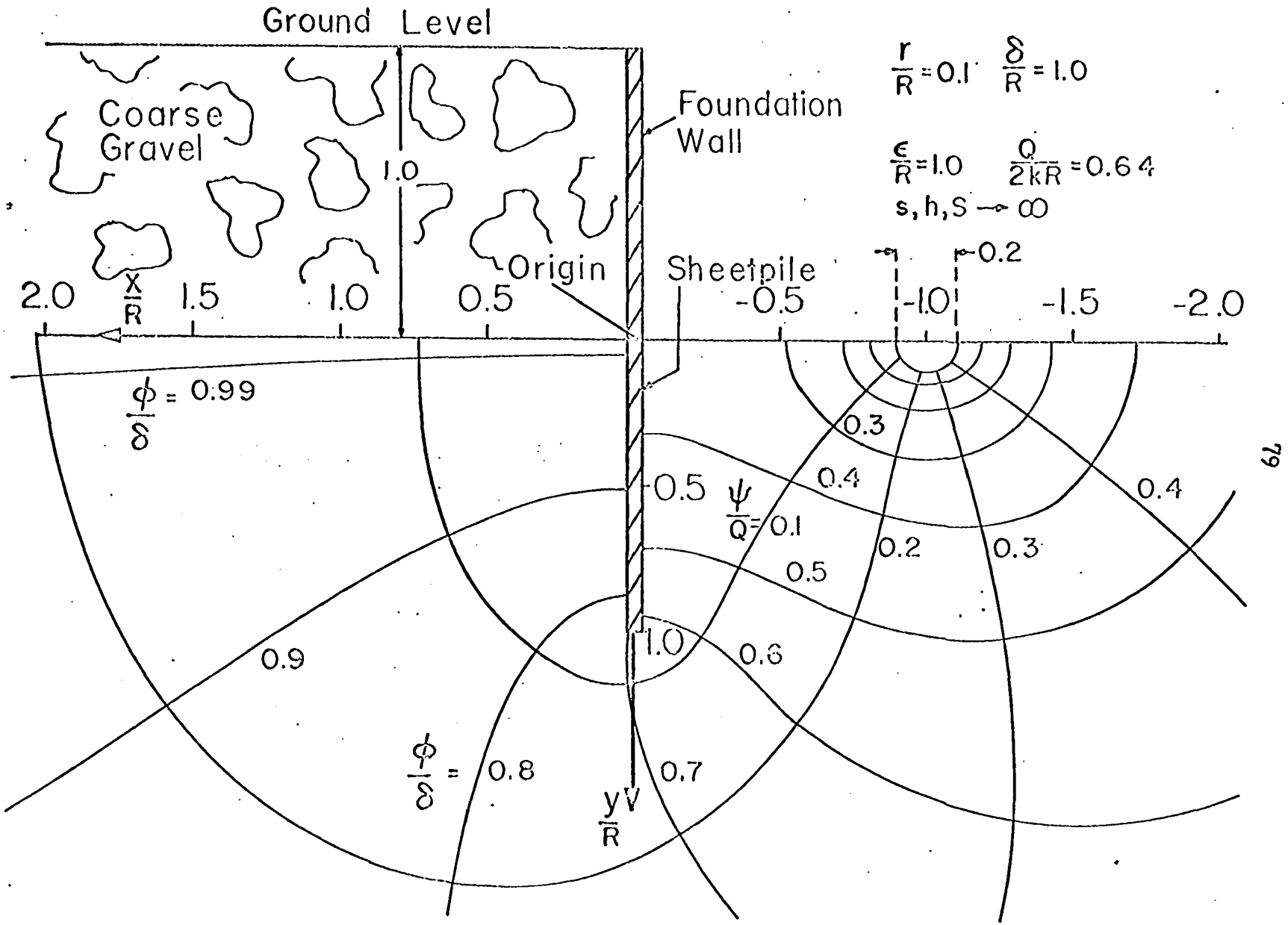
Ground Level
Coarse Gravel
Foundation Wall
Origin
Sheetpile
1.0
2.0
X/R
1.5
1.0
0.5
-0.5
-1.0
-1.5
-2.0
0.2
r/R = 0.1
δ/R = 1.0
ε/R = 1.0
Q/2kR = 0.64
s, h, S → ∞
φ/δ = 0.99
0.9
0.8
0.7
0.6
0.5
0.4
0.3
0.2
0.1
ψ/Q =
yV/R

head at any point is $\phi - y$.

Figure 16 is a flow net illustrating seepage around a sheetpile to a drain just below the basement floor. A layer of coarse gravel of thickness $\delta = R$ overlies an infinitely deep and wide isotropic soil. The sheetpile is assumed to be very thin and to extend to a depth $\varepsilon = R$. The tile drain is of radius $r = 0.1R$ which for $R = 1$ m would be 10 cm or approximately 4 in. The calculated value of $Q/2kR$ is 0.64. For $R = 1$ m and $k = 0.1$ m/hr the total flow to the drain per unit length of the drain would be $Q/2 = 0.064$ $m^3/hr/m$.

A flow net for Case 12 (a geometry identical to Figure 16 except that no sheetpile is present) is given as Figure 17 to compare with the last example. The value of $Q/2kR$ is 0.87 from which we conclude the sheetpile reduces the amount of flow by over 25 percent.

To determine the decrease in maximum pressure along the foundation base in the region between the tile and the sheetpile resulting from the sheetpile, we will utilize the generalized pressure curves of Figure 4. In order to use Figure 4, we need the value of u_r for the system of Figure 16 and the u value of Figure 15 corresponding to the point of maximum pressure of our problem. The maximum pressure will occur at $x = 0$, $y = 0$ to the right of the sheetpile. We observe from Figure 15 that the corresponding u value is $u = d$. By Equation 204, we calculate $d = 0.17$. We obtain u_r for $d = 0.17$ by Equation 205 and find $u_r = 0.029$. For $u = 0.17$ in Figure 4, we read from the solid curve labeled $u_r = 0.1$, a pressure head value $p/\rho g = 0.18$ R (where $y = 0$ and $\delta = R$). Similarly, the solid curve labeled $u_r = 0.01$ gives $p/\rho g = 0.43$ R. Interpolating linearly between the values gives for $u_r = 0.029$ a pressure head of

Figure 17. Flow net for Case 12. The geometry is identical to that of Figure 16, but without a sheetpile.

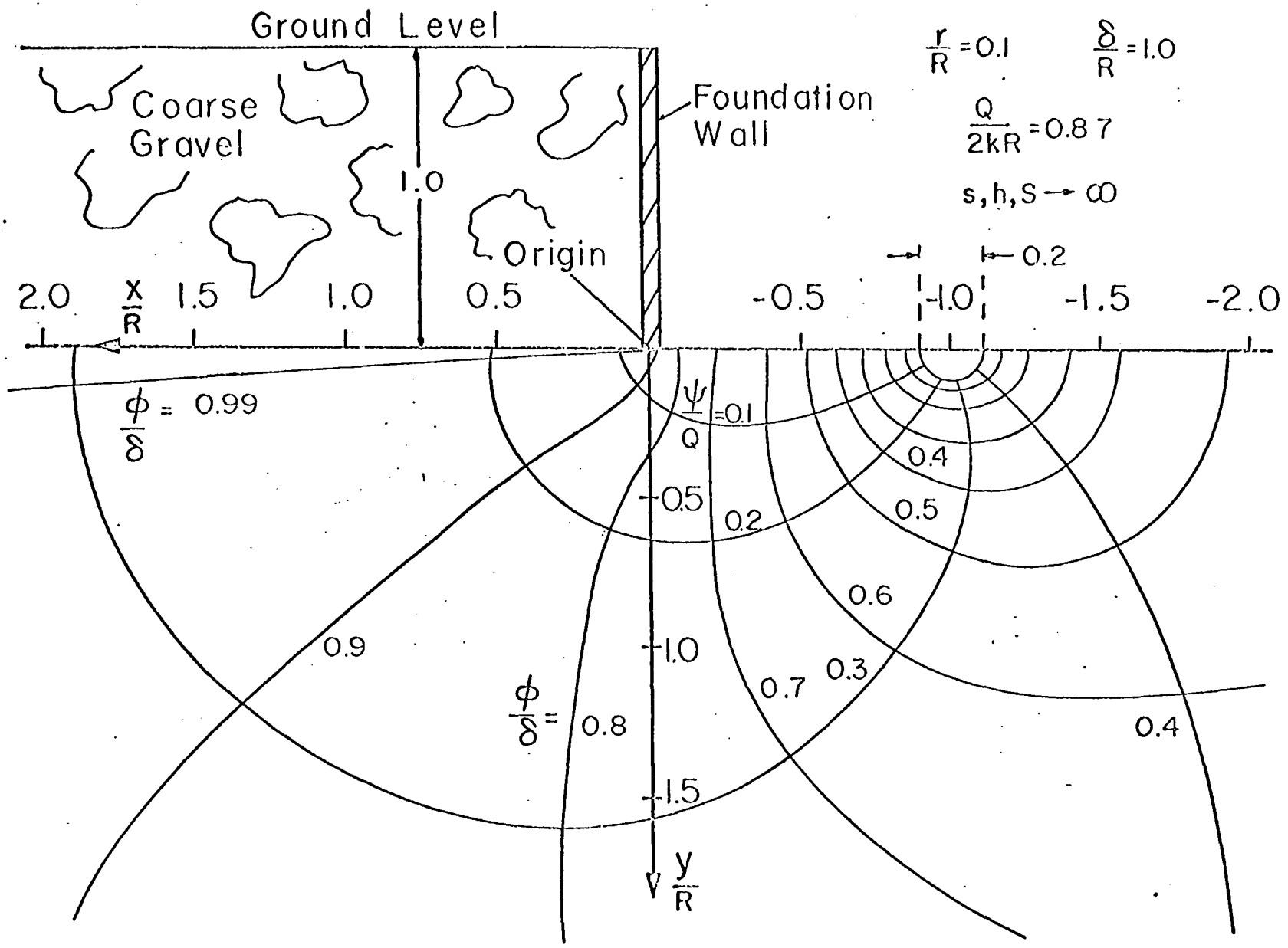
Ground Level
Coarse Gravel
Foundation Wall
1.0
Origin
r/R = 0.1
δ/R = 1.0
Q/2kR = 0.87
s, h, S → ∞
0.2
2.0
X/R
1.5
1.0
0.5
-0.5
-1.0
-1.5
-2.0
φ/δ = 0.99
Ψ/Q = 0.1
0.05
0.2
0.4
0.5
0.6
0.9
1.0
0.7
0.3
φ/δ = 0.8
0.4
1.5
y/R

$p/\rho g = 0.38R$. The pressure head value of $0.38R$ could have been closely estimated by examining the equipotentials $\phi/\delta = 0.3$ and $\phi/\delta = 0.4$ in the flow net of Figure 16. Thus, the sheetpile decreases the maximum pressure head along the floor left of the drain by $(1 - 0.38)R$, a relief of 62 percent. At a large distance to the right of the drain, the sheetpile will have no effect (nor will the tile). The pressure head at large distances to the right of the drain will be simply δ.

G. Multiple Drains Near the Foundation Barrier

In the previous sections we have solved problems of seepage from a stationary plane water table to a single tile drain or to a pair of symmetrically placed tile drains near the foundation. We now consider as in Figure 18 a problem differing from Case 12 only in that two drains are located near the floor of the foundation rather than one. A z to t-plane transformation for Figure 18 will be repeated, followed by the t to w (complex potential) plane transformation. The t to w-plane transformation will be applicable to the more complicated geometries of Cases 1 through 11 where two tiles rather than one are present in the half flow region considered. This would correspond to two, three, or four drains in the total flow region of Figure 2, depending on whether two, one, or none of the tiles are situated on the plane of symmetry AB.

Consider as in the z-plane of Figure 18 an infinitely wide layer of coarse gravel of thickness δ to the left of an infinitely wide foundation overlying a soil of saturated hydraulic conductivity k. An origin is located at O' where the coarse gravel, foundation, and permeable soil meet. The y-axis is vertically downward with the x-axis to the left. The centers of two tile drains of radius r_1 and r_2 are located at the

Figure 18. The z, t and w-planes used for the multiple drain systems. The z-plane shown is analogous to Case 12, but the t and w-planes could be used for the more complex Cases 1-11 when sheetpiling is added.

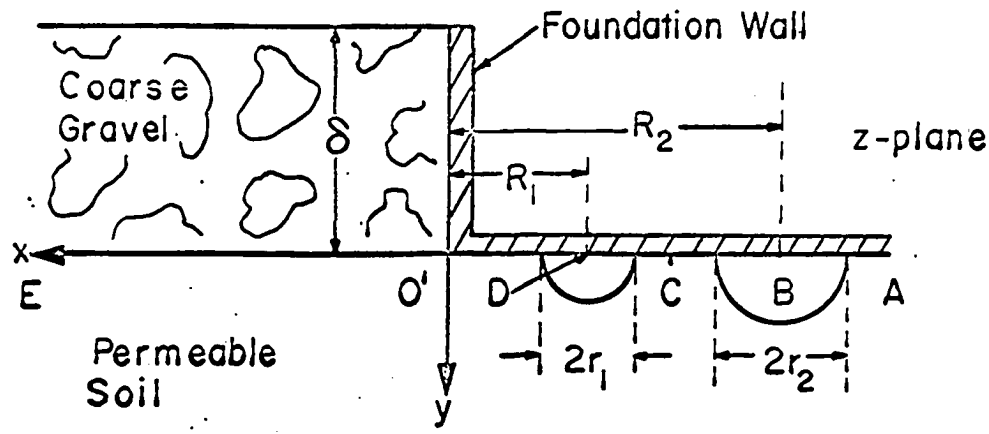
Foundation Wall
Coarse Gravel
δ
R2
R1
z-plane
x
E
O'
D
C
B
A
Permeable Soil
y
2r1
2r2

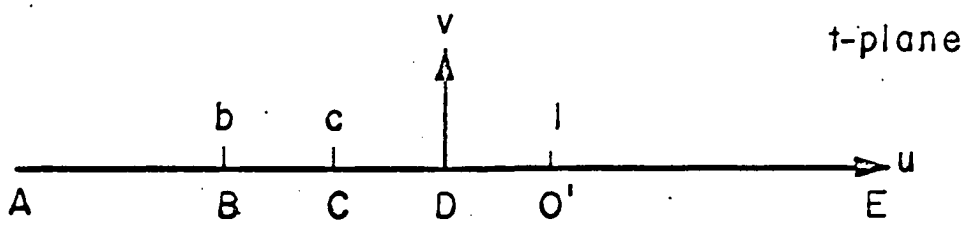
v
t-plane
b
c
1
u
A
B
C
D
O'
E

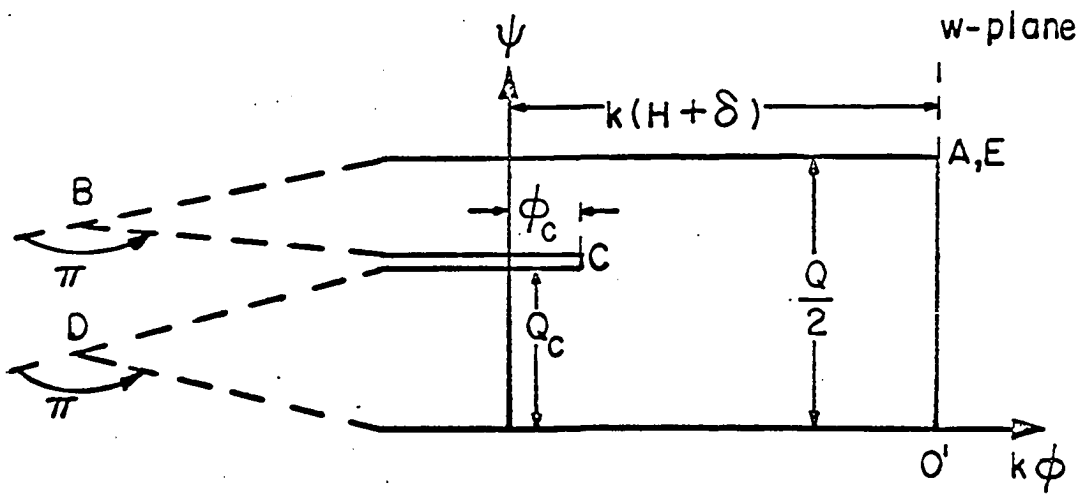
ψ
w-plane
k(H+δ)
A,E
B
π
φc
C
Q/2
D
π
Qc
O'
kφ

base of the foundation at points D and B which have x-coordinates of $-R_1$ and $-R_2$, respectively. The point C is the point of maximum potential between B and D. The transformation of the z-plane flow region to the upper half of the t-plane is, with $R = R_1$ in Equation 194, found as

$$z(t) = R_1(t - 1) \tag{206}$$

where the images of B, C, D, and O' of the z-plane are at b, c, 0, and 1, respectively. For $z(b) = -R_2$, the value of b determined by Equation 206 is

$$b = 1 - R_2/R_1 \tag{207}$$

a negative value. The inverse of Equation 206 is

$$t = z/R_1 + 1 \tag{208}$$

The flow region corresponds to the interior of the degenerate pentagon ABCDO'A in the w-plane of Figure 18 with B and D at $k\emptyset$ approaching $-\infty$. The infinite points A and E of the z and t-planes will have w-plane image points $k\emptyset = \delta + H$, $\phi = Q/2$ where Q/2 is the total flow to both of the drains per unit time per unit length of the drains. H is zero for the z-plane shown. The point C will be at $k\emptyset_c + iQ_c$ in the w-plane, a stagnation point. $\emptyset_c$ is the maximum potential between the two drains and Q_c is the amount of flow to the drain at D. The exterior angles for B, C, D, and O' are π, $-\pi$, π, and $\pi/2$, respectively. The Schwartz-Christoffel transformation mapping the pentagon in the w-plane to the upper half of the t-plane is by Equation 15

$$w(t) = M' \int \frac{(t - c)dt}{t(t - b)(t - 1)^{1/2}} + N \tag{209}$$

Defining u by

$$u = (t - 1)^{1/2} \tag{210}$$

we see Equation 209 becomes

$$w(t) = 2M' \int \frac{[(1 - c) + u^2]du}{(1 + u^2)[(1 - b) + u^2]} + N, \qquad u^2 = t - 1$$

Using partial fractions to express the integrand or using the third equation from the bottom of page 17 of Peirce (1956), we have

$$w(t) = (2M'/b)[c \int \frac{du}{1 + u^2} + (b - c) \int \frac{du}{1 - b + u^2} + N, \qquad u^2 = t - 1$$

Defining a new constant M and using eq. 48 of Peirce to evaluate the integrals, we find

$$w(t) = M[\tan^{-1}u + \frac{b - c}{c(1 - b)^{1/2}} \tan^{-1}[u/(1 - b)^{1/2}] + N, \qquad u^2 = t - 1$$

or by Equation 210, we find

$$w(t) = M[\tan^{-1}(t - 1)^{1/2} + \alpha \tan^{-1}(\frac{t - 1}{1 - b})^{1/2}] + N \tag{211}$$

where

$$\alpha = \frac{b - c}{c(1 - b)^{1/2}} \tag{212}$$

A comparison of the w and t-planes of Figure 18 shows

$$z(1) = k(H + \delta) \tag{213a}$$

$$\lim_{t \to \infty} z(t) = k(H + \delta) + iQ/2 \tag{213b}$$

The last two equations may be used to find M and N from Equation 211. The results are

$$M = (iQ/\pi)/(1 + \alpha) \tag{214}$$

$$N = k(H + \delta) \tag{215}$$

When the values for M and N are substituted back into Equation 211, the result is

$$w(t) = (iQ/\pi) \frac{1}{1 + \alpha}[\tan^{-1}(t - 1)^{1/2} + \alpha \tan^{-1}(\frac{t - 1}{1 - b})^{1/2}] + k(H + \delta) \tag{216}$$

To utilize Equation 216, it is necessary to determine Q and α. In a manner similar to that of Cases 1-12, we define an equipotential near each tile center as a tile surface. If in the z-plane of Figure 18 the equipotential passing through the x-axis at x equal to $-R_1 + r_1$ and x equal to $-R_2 - r_2$ is zero, the complex potential at these points will be

$$(w)_{x=-R_1+r_1} = 0 \tag{217}$$

$$(w)_{x=-R_2-r_2,y=0} = iQ/2 \tag{218}$$

which along with Equation 216 gives two equations from which the unknowns Q and α can be found. By Equation 208, we have for t - 1

$$t - 1 = z/R_1 \tag{219}$$

giving from Equation 216 for Equations 217 and 218:

$$(iQ/\pi)\frac{1}{1+\alpha}[\tan^{-1}i(1 - r_1/R_1)^{1/2} + \alpha \tan^{-1}i(\frac{R_1 - r_1}{R_1})^{1/2}] + k(H + \delta) = 0 \tag{220a}$$

and

$$(iQ/\pi)\frac{1}{1+\alpha}[\tan^{-1}i(\frac{R_2 + r_2}{R_1})^{1/2} + \alpha \tan^{-1}i(1 + r_2/R_2)^{1/2}] + k(H + \delta) = iQ/2 \tag{220b}$$

By eq. 408.18, 652.12, and 652.22 of Dwight (1961), we can verify

$$\tan^{-1}i\beta = i \tanh^{-1}\beta, \qquad 0 \leq \beta < 1 \tag{221}$$

$$\tan^{-1}i\beta = \pi/2 + i \coth^{-1}\beta, \qquad \beta > 1 \tag{222}$$

from which Equations 220a and 220b become

$$(Q/\pi)\frac{1}{1+\alpha}[\tanh^{-1}(1 - r_1/R_1)^{1/2} + \alpha \tanh^{-1}(\frac{R_1 - r_1}{R_2})^{1/2} = k(H + \delta) \tag{223a}$$

and

$$(iQ/\pi)\frac{1}{1+\alpha}\{\pi/2 + i\coth^{-1}(\frac{R_2+r_2}{R_1})^{1/2} + \alpha[\pi/2 + \coth^{-1}(1+r_2/R_2)^{1/2}]\} + k(H+\delta) = iQ/2 \qquad (223b)$$

The imaginary part of the last equation reduces to an identity. The real part gives

$$(Q/\pi)\frac{1}{1+\alpha}[\coth^{-1}(\frac{R_2+r_2}{R_1})^{1/2} + \alpha\coth^{-1}(1+r_2/R_2)^{1/2}] = k(H+\delta) \qquad (224)$$

Dividing Equations 223a and 223b by $(Q/\pi)/(1+\alpha)$ and equating the resulting left sides, we find

$$\tanh^{-1}(1-r_1/R_1)^{1/2} + \alpha\tanh^{-1}(\frac{R_1-r_1}{R_2})^{1/2} = \coth^{-1}(\frac{R_2+r_2}{R_1})^{1/2} + \alpha\coth^{-1}(1+r_2/R_2)^{1/2}$$

which gives for α

$$\alpha = \frac{\coth^{-1}[(R_2+r_2)/R_1]^{1/2} - \tanh^{-1}(1-r_1/R_1)^{1/2}}{\tanh^{-1}[(R_1-r_1)/R_2]^{1/2} - \coth^{-1}(1+r_2/R_2)^{1/2}} \qquad (225a)$$

or alternatively by eq. 702 and 703 of Dwight (1961)

$$\alpha = \frac{\ln\{\dfrac{[(R_2+r_2)^{1/2}+R_1^{1/2}][R_1^{1/2}-(R_1-r_1)^{1/2}]}{[(R_2+r_2)^{1/2}-R_1^{1/2}][R_1^{1/2}+(R_1-r_1)^{1/2}]}\}}{\ln\{\dfrac{[R_2^{1/2}+(R_1-r_1)^{1/2}][(R_2+r_2)^{1/2}-R_2^{1/2}]}{[R_2^{1/2}-(R_1-r_1)^{1/2}][(R_2+r_2)^{1/2}+R_2^{1/2}]}\}} \qquad (225b)$$

The flow Q/2 may be evaluated from Equations 223a or 223b once α is known. The result is

$$Q/2 = \frac{\pi(1+\alpha)k(H+\delta)}{2\tanh^{-1}(1-r_1/R_1)^{1/2} + \alpha\tanh^{-1}[(R_1-r_1)/R_2]^{1/2}} \qquad (226)$$

To solve for ϕ_c, the maximum potential along the t-plane between the two drains, and Q_c, the value of the stream function at C, we substitute c for t in Equation 216 and set the result equal to $k\phi_c + iQ_c$, finding

$$(iQ/\pi)\frac{1}{1+\alpha}[\arctan(c-1)^{1/2} + \alpha \arctan(\frac{c-1}{1-b})^{1/2} + k(H+\delta) = k\phi_c + iQ_c$$

In the t-plane of Figure 18 c is greater than b but less than zero, from which Equations 221, 222 and the last equation give

$$(iQ/\pi)\frac{1}{1+\alpha}[\pi/2 + i\coth^{-1}(1-c)^{1/2} + i\alpha \tanh^{-1}(\frac{1-c}{1-b})^{1/2} + k(H+\delta) = k\phi_c + iQ_c$$

Equating the real and imaginary parts of the last equation gives

$$Q_c = Q/[2(1+\alpha)] \tag{227}$$

$$\phi_c = (H+\delta) - (Q/k\pi)\frac{1}{1+\alpha}[\coth^{-1}(1-c)^{1/2} + \alpha \tanh^{-1}(\frac{1-c}{1-b})^{1/2}] \tag{228}$$

1. Numerical calculations for multiple drains

In Figure 19 water from a saturated coarse gravel layer of height δ equals R_1 seeps through underlying soil to a pair of tile drains, the centers of which lie just below the basement floor and at distances of R_1 and $3R_1$ from the basement wall along the negative x-axis. The tiles are each of radius $r_1 = r_2 = 0.125R_1$, although they could have been chosen of unequal size since the equations are not restricted to $r_1 = r_2$.

In applying the results from the preceding section the following steps were used:

(i) Specify the parameters r_1, r_2, R_1, R_2, and δ.

(ii) Solve for α and $Q/2k$ by Equations 225b and 226.

Figure 19. Flow net for a system of two equal sized tube drains below an infinitely wide foundation. The tiles are centered at $x/R_1 = -1, y/R_1 = 0$ and $x/R_1 = -3, y/R_1 = 0$.

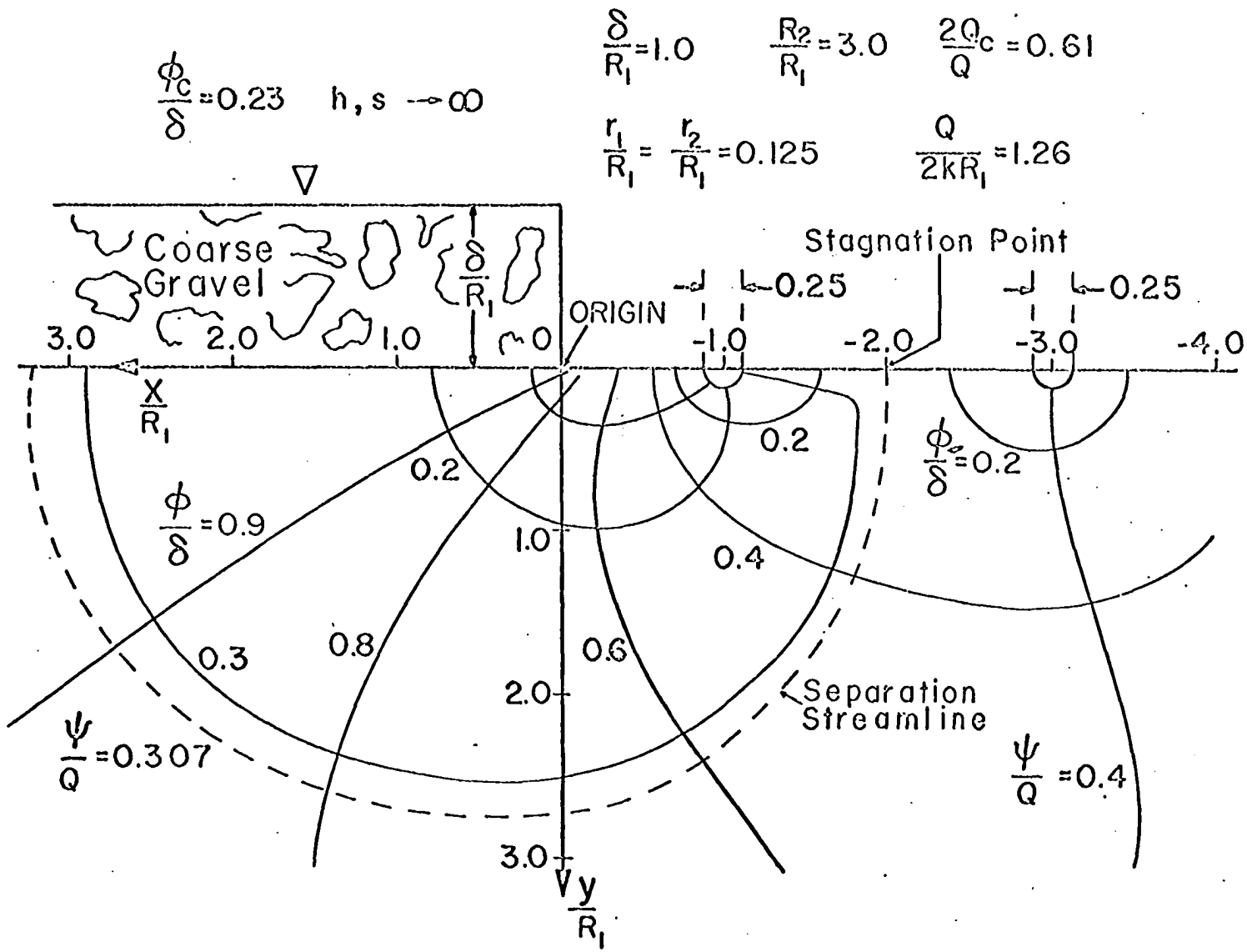
$\frac{\delta}{R_1}$=1.0
$\frac{R_2}{R_1}$=3.0
$\frac{2Q_c}{Q}$=0.61
$\frac{\phi_c}{\delta}$=0.23 h, s → ∞
$\frac{r_1}{R_1}$ = $\frac{r_2}{R_1}$=0.125
$\frac{Q}{2kR_1}$=1.26
Coarse Gravel
$\frac{\delta}{R_1}$
Stagnation Point
0.25
0.25
ORIGIN
3.0
2.0
1.0
0
-1.0
-2.0
-3.0
-4.0
$\frac{X}{R_1}$
0.2
0.2
$\frac{\phi_c}{\delta}$=0.2
$\frac{\phi}{\delta}$=0.9
1.0
0.4
0.3
0.8
0.6
2.0
Separation Streamline
$\frac{\psi}{Q}$=0.307
$\frac{\psi}{Q}$=0.4
3.0
$\frac{Vy}{R_1}$

(iii) Solve for Q_c/Q and ϕ_c from Equations 227 and 228.

(iv) Determine the complex potential $k\phi + i\psi$ for specified values of $x + iy$ by applying Equations 208 and 216.

The inverse transformation of Equation 216 giving z in terms of t and consequently of z in terms of w was not found, although an effort to do so was made. However, by repeating step (iv) several times the relationship of z to w can be established either by plotting ϕ and ψ on grid points in the z-plane or by interpolating graphically as did Warrick (1964) in his Figures 7 and 8.

The values of $Q/2kR_1$ and α for the system in Figure 19 are found to be $Q/2kR_1 = 1.26$ and $\alpha = 0.63$. If R_1 were 1 m and k were 0.1 m/hr, the total flow to the two drains would be Q/2 or 0.126 m^3/hr/m. The values of $2Q_c/Q$ and ϕ_c/δ were 0.61 and 0.23, respectively. The 0.61 value of $2Q_c/Q$ implies 61 percent of the seepage water goes to the drain which is closer to the coarse gravel and 39 percent to the farther drain of the same size. The dashed streamline labeled ψ equals 0.307 has special significance in that it separates the seepage to the first and second drains. The water seeping across the x-axis between the origin and $x = 3.2$ goes to the closer drain, that seeping across farther to the left (where the value of x is greater) goes to the second drain. The intersection of the 0.307 streamline and the negative x-axis is approximately at $x = -2$ which is a stagnation point and is of a potential $\phi_c = 0.236$.

IV. TWO-DIMENSIONAL SEEPAGE OF PONDED WATER TO A FULL DITCH DRAIN

We now consider the agricultural drainage problem of flow of ponded water to a ditch drain running full as indicated in semi-section in the z-plane of Figure 20. The solution is applicable when ponded water is drained by ditches or when salts are leached by ponding water for the special case that the ditch drains are running full. The distance between ditch centers is 2L and the depth from the ground surface to the barrier is h. Ponded water of thickness δ is on the surface and is prevented from overflowing directly into the ditch by an impermeable spoil bank whose base of width $(\varepsilon - s)$ extends along FE. The origin O' of the z-plane is chosen at the upper right hand corner with the x-axis to the left and the y-axis vertically downward. AB and O'C are planes of symmetry. We first consider that a vertical sink at a potential $-\phi_o$ and of length H exists along O'D. One of the equipotentials which will be given by our solution near the slot O'D may then be set equal to zero and used as the side of the "ditch" or ϕ_o itself may be set to zero and the slot considered as a very narrow ditch. For the special case when H = h, the equipotential O'D may be considered as a ditch wall for any width of ditch. The semi-width of the "ditch" at its top is taken to be s, the distance from the origin to where the zero equipotential intersects the x-axis.

The boundary conditions for ϕ and ψ are

Boundary Condition 1: $\psi = 0$ along FEO'
Boundary Condition 2: $\phi = \delta$ along AF
Boundary Condition 3: $\psi = Q/2$ along ABCD
Boundary Condition 4: $\phi = -\phi_o$ along DO'

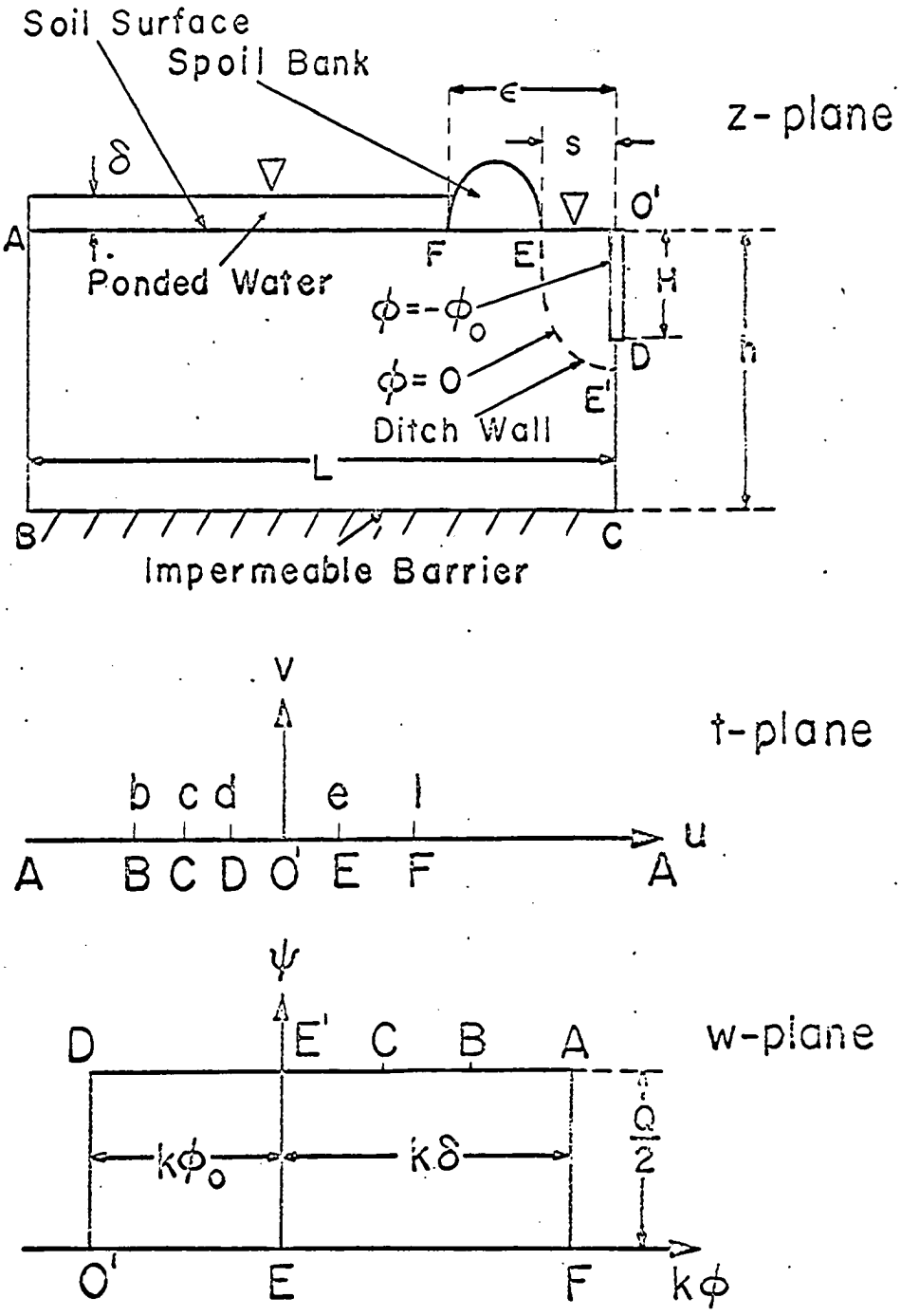

Figure 20. The z, t and w-planes for two-dimensional seepage of ponded water to a full ditch drain.

A. The z to t-Plane Transformation

In Figure 20 we observe that the exterior angles of the z-plane at B, C, and O' are each $\pi/2$. The Schwartz-Christoffel transformation from Equation 15 that maps the interior of the rectangle ABCO'A onto the upper half of the t-plane of Figure 20 is

$$z(t) = M_1' \int (t - b)^{-1/2}(t - c)^{-1/2}t^{-1/2}dt + N_1' \tag{229}$$

where the image points of A, B, C, and O' of the z-plane are at ∞, b, c, and 0, respectively. The image points of D and E are chosen to be at d and 1, respectively. Use of eq. 237.00 of Byrd and Friedman (1954) to evaluate the integral gives

$$z(t) = M_1 F(m_z,\sigma_z) + N_1, \qquad \sigma = \sigma(t) \tag{230}$$

with

$$m_z^2 = 1 - c/b \tag{231}$$

$$\sigma_z = \sin^{-1}[t/(t - c)]^{1/2} \tag{232}$$

We use the subscript "z" to designate the modulus and amplitude of the elliptic function for the z(t) transformation.

Comparing the z and t-planes of Figure 20, we find

$$z(0) = 0 \tag{233a}$$

$$z(b) = L + ih \tag{233b}$$

$$z(c) = ih \tag{233c}$$

which along with Equations 230, 231 and 232 give

$$M_1 F(m_z,0) + N_1 = 0 \tag{234a}$$

$$M_1 F(m_z,\sin^{-1}[1/m_z]) + N_1 = L + ih \tag{234b}$$

$$M_1 F(m_z,\sin^{-1}\infty) + N_1 = ih \tag{234c}$$

where $F(m_z, \sin^{-1}\infty)$ is the limiting value of $F(m_z,\sigma_z)$ as $\sin\sigma_z$ approaches infinity.

Since by Equation 72 $F(m_z,0)$ is 0, Equation 233a yields immediately

$$N_1 = 0 \tag{235}$$

Use of Equation 145 to evaluate $F(m_z,\sin^{-1}[1/m_z])$ gives from Equation 233b

$$M_1(K_z + iK_z') + N_1 = L + ih \tag{236}$$

Assuming M_1 is real and equating real and imaginary parts of Equation 236 with $N_1 = 0$, we find

$$M_1K_z = L \tag{237a}$$

$$M_1K_z' = h \tag{237b}$$

or

$$L/h = K_z/K_z' \tag{238}$$

In the last equation K_z' is the complementary complete elliptic integral of the first kind of modulus m_z. The prime is not a superscript of z. If L/h is specified, m_z can be evaluated from Equation 238 or by using Figure 11. Either Equation 237a or Equation 237b can be used to find M_1:

$$M_1 = L/K_z \tag{239a}$$

$$M_1 = h/K_z' \tag{239b}$$

Use of Equations 235 and 239a in Equation 230 gives

$$z(t) = (L/K_z)F(m_z,\sigma_z), \qquad \sigma_z = \sigma_z(t) \tag{240}$$

We can verify that Equation 233c is satisfied by Equation 240. Byrd and Friedman (1954) eq. 115.03 gives

$$\lim_{\sin\sigma_z \to \infty} F(m_z,\sigma_z) = iK_z' \tag{241}$$

Use of Equations 238 and 241 in Equation 240 gives

$$z(c) = ih$$

which is identical to Equation 233c and verifies our assumption that M_1 was real in Equation 236.

To find the inverse relationship we first solve Equation 240 for $F(m_z,\sigma_z)$. The result is

$$F(m_z,\sigma_z) = (K_z/L)z \tag{242}$$

Eq. 750 and 751.3 of Dwight (1961) give

$$\sin \sigma = sn(m,U) \tag{243}$$

with

$$U = F(m,\sigma) \tag{244}$$

We take the elliptic sine "sn" of each side of Equation 242 and use Equations 232, 243 and 244 in the result to find

$$[t/(t - c)]^{1/2} = sn(m_z,K_z z/L)$$

Squaring both sides of the last equation and solving for t yields

$$t = \frac{-c\ sn^2(m_z,K_z z/L}{1 - sn^2(m_z,K_z z/L)} \tag{245}$$

An alternative form may be obtained for the r.h.s. of Equation 245 by use of other elliptic functions. Use of the relationships

$$sn^2(m,U) + cn^2(m,U) = 1 \tag{246}$$

and

$$tn(m,U) = \frac{sn(m,U)}{cn(m,U)} \tag{247}$$

reduces Equation 245 to

$$t = -c\ tn^2(m_z,K_z z/L) \tag{248}$$

where tn(m,U) is the elliptic tangent.

In order to apply Equation 240 we need to evaluate c. The values of e and d will also be needed later in our analysis. Using Figure 20, we observe that the t-values of 1, e, and d correspond to z-values of ε, s, and iH respectively. These correspondences and Equation 245 yield

$$c = \frac{sn^2(m_z, \varepsilon K_z/L) - 1}{sn^2(m_z, \varepsilon K_z/L)} \tag{249}$$

$$e = \frac{-c\ sn^2(m_z, sK_z/L)}{1 - sn^2(m_z, sK_z/L)} \tag{250}$$

$$d = \frac{-c\ sn^2(m_z, iHK_z/L)}{1 - sn^2(m_z, iHK_z/L)} \tag{251a}$$

An alternative form for d in terms of real arguments only may be obtained using Byrd and Friedman eq. 125.02. From their equation we find

$$d = \frac{c\ tn^2(m_z, HK_z/L)}{1 + tn^2(m_z, HK_z/L)} \tag{251b}$$

Use of Equations 240 and 247 to simplify the last equation results in

$$d = c\ sn^2(m_z', HK_z/L) \tag{251c}$$

Still another form for d may be obtained by use of Equation 238 and the last equation. The result is

$$d = c\ sn^2(m_z', K_z'H/h) \tag{251d}$$

Equations 243 and 244 give

$$sn(m,K) = 1 \tag{252}$$

from which we verify Equation 251d will give d = c for H/h equal to 1.

B. The Complex Potential Function

The flow region of the z-plane of Figure 20 maps into the complex potential plane w as a rectangle of height Q/2 and width $k(\delta + \phi_o)$ where Q/2 is the amount of water seeping into the ditch from the flow region per unit time per unit length of the ditch and k is the saturated hydraulic conductivity. The images of A, D, O', and F of the z-plane each form a corner of the rectangle in the w-plane as shown in Figure 20. The Schwartz-Christoffel transformation Equation 15 mapping the interior of ADO'FA of the w-plane to the upper half of the t-plane is

$$w(t) = M_2' \int (t - d)^{-1/2} t^{-1/2} (t - 1)^{-1/2} dt + N_2' \qquad (253)$$

where d, 0, 1, and ∞ are the image points for D, O', F, and A of the w-plane.

Use of eq. 237.00 of Byrd and Friedman again gives

$$w(t) = M_2 F(m_w, \sigma_w) + N_2 \qquad (254)$$

with

$$m_w^2 = -d/(1 - d) \qquad (255)$$

$$\sigma_w = \arcsin\left(\frac{t - 1}{t}\right)^{1/2} \qquad (256)$$

A comparison of the w and t-planes of Figure 20 shows

$$w(1) = k\delta \qquad (257a)$$

$$w(0) = -k\phi_o \qquad (257b)$$

$$w(d) = -k\phi_o + iQ/2 \qquad (257c)$$

The last three equations along with Equation 254 give

$$M_2F(m_w,0) + N_2 = k\delta \tag{258a}$$

$$M_2F(m_w,\sin^{-1}\infty) + N_2 = -k\phi_o \tag{258b}$$

$$M_2F(m_w,\sin^{-1}[1/m_w]) + N_2 = -k\phi_o + iQ/2 \tag{258c}$$

Use of $F(m_w,0) = 0$ in Equation 258a gives

$$N_2 = k\delta \tag{259}$$

Use of Equation 241 to evaluate $F(m_w,\sin^{-1}\infty)$ and use of $N = k\delta$ in Equation 258b gives

$$iM_2K_w' = -k(\phi_o + \delta)$$

which gives for M_2

$$M_2 = ik(\phi_o + \delta)/K_w' \tag{260}$$

In the last equation K_w' is the complementary complete elliptic integral of the first kind of modulus m_w. The prime is not a superscript of w. Substituting the r.h.s. of Equations 259 and 260 for M_2 and N_2 in Equation 242, we find

$$w(t) = ik[(\phi_o + \delta)/K_w']F(m_w,\sigma_w) + k\delta, \qquad \sigma_w = \sigma_w(t) \tag{261}$$

with m_w and σ_w as defined in Equations 255 and 256 and K_w'. The value of m_w may be determined by using the r.h.s. of Equation 255 with d from Equation 251d. We can use Equation 257c to evaluate our unknown amount of flow Q/2. From Equation 145 we have $F(m_w,\arcsin[1/m_w]) = K_w + iK_w'$ which along with Equations 259 and 260 gives from Equation 254

$$ik[(\phi_o + \delta)/K_w'](K_w + iK_w') + k\delta = -k\phi_o + iQ/2$$

The real part is an identity and adds no new information, but the imaginary part yields

$$Q/2 = k(\phi_o + \delta)(K_w/K_w') \tag{262}$$

To find t in terms of w from Equation 261, first we solve Equation 261 for $F(m_w,\sigma_w)$ giving

$$F(m_w,\sigma_w) = (iK_w'/k)(\frac{k\delta - w}{\phi_o + \delta})$$

Use of Equations 243, 244, and 256 gives

$$(\frac{t - 1}{t})^{1/2} = sn[m_w,(iK_w'/k)(\frac{k\delta - w}{\phi_o + \delta})]$$

which when solved for t yields

$$t = 1/\{1 - sn^2[m_w,(iK_w'/k)(\frac{k\delta - w}{\phi_o + \delta})]\} \tag{263a}$$

An alternate form may be obtained by using eq. 120.02 and 121.00 of Byrd and Friedman (1954),

$$t = nc^2[m_w,(iK_w'/k)(\frac{k\delta - w}{\phi_o + \delta})] \tag{263b}$$

In order to solve for ϕ_o corresponding to a ditch width of s, we compare the w and t planes of Figure 20 and find

$$w(e) = 0 \tag{264}$$

which along with Equations 256 and 261 gives

$$\delta + i[(\phi_o + \delta)/K_w']F(m_w,\sin^{-1}[\frac{e - 1}{e}]^{1/2}) = 0 \tag{265}$$

As e is positive but less than 1, we may use Abramowitz and Stegun (1964) to obtain

$$F(m,\sin^{-1}[\frac{e - 1}{e}]^{1/2}) = iF(m_w',\sin^{-1}[1 - e]^{1/2}) \tag{266}$$

Substitution of the r.h.s. of Equation 266 into Equation 265 and solving for ϕ_o gives

$$\phi_o = \delta\{\frac{K_w'}{F(m_w',\sin^{-1}[1 - e]^{1/2})} - 1\} \tag{267}$$

where e is known by Equation 250.

By substituting the r.h.s. of Equation 263a or Equation 263b for t in Equation 240, we have an explicit relationship of z in terms of $\emptyset$ and ϕ.

C. An Infinitely Deep Flow Medium

If, in the z-plane of Figure 20, h approaches infinity, correspondingly the image points b and c in the t-plane will approach each other. Thus, we have by Equation 231 the limiting value of m_z as

$$\lim_{h \to \infty} m_z = 0 \tag{268}$$

For m equal to zero, inspection of Equation 72 shows $F(0,\sigma) = \sigma$ and $K_{m_z=0} = \pi/2$. Use of these last two relationships and Equation 232 gives for Equation 240 as h approaches infinity

$$z(t) = (2L/\pi)\sin^{-1}[t/(t - c)]^{1/2} \tag{269}$$

The inverse is

$$t = -c \tan^2(\pi z/2L) \tag{270}$$

The values of c, d, and e are found analogously to Equations 249, 250, and 251d and are

$$c = -\cot^2(\pi\varepsilon/2L) \tag{271}$$

$$e = -c \tan^2(\pi s/2L) \tag{272}$$

$$d = c \tanh^2(\pi H/2L) \tag{273}$$

D. Numerical Calculations for the Ponded Water Problems

To investigate seepage of ponded water to a full ditch drain when an impermeable barrier is present as in the z-plane of Figure 20, the following steps were used to get the results of this section:

(i) Specification of the semi-width of the flow medium L, the depth to the impermeable barrier h, the length of the vertical sink H, the semi-width of the ditch s, the width of the soil bank $\varepsilon - s$, and the depth of the ponded water δ.

(ii) Determination of the modulus m_z by use of Equation 238 or Figure 11.

(iii) Determination of c, e, and d from Equations 249, 250 and 251d.

(iv) Evaluation of m_w by Equation 255.

(v) Evaluation of ϕ_o by Equation 267.

(vi) Evaluation of Q/2k by Equation 262 or Q/2 if k is specified.

(vii) Determination of the x,y-coordinates for a given complex potential $k\phi + i\psi$ by applying Equation 203a followed by Equation 230.

In place of (vii) we could calculate the complex potential $k\phi + i\psi$ for a specified value of $x + iy$ by using Equation 245 followed by Equation 261. The pressure head would then be given by $\phi - y$.

The basic series used for evaluating the first order incomplete elliptic function was eq. 902.01 of Byrd and Friedman (1954) supplemented by eq. 115.02 and 115.03 and by eq. 17.4.8 and 17.4.11 of Abramowitz and Stegun (1964) when the imaginary part of the arguments were non-zero. The elliptic sine, sn(m,u), for all types of arguments was evaluated using eq. 908.01 of Byrd and Friedman modified as described in our Appendix 2.

Figure 21 is a flow net illustrating seepage of ponded water of depth $\delta = 0.025L$ to a full ditch drain whose top is of semi-width $s = 0.05L$ where L is the semi-width of the flow medium. A horizontal impermeable barrier is at a depth of $h = 0.2L$. A spoil bank of width $0.075L$ prevents the ponded water from overflowing directly into the

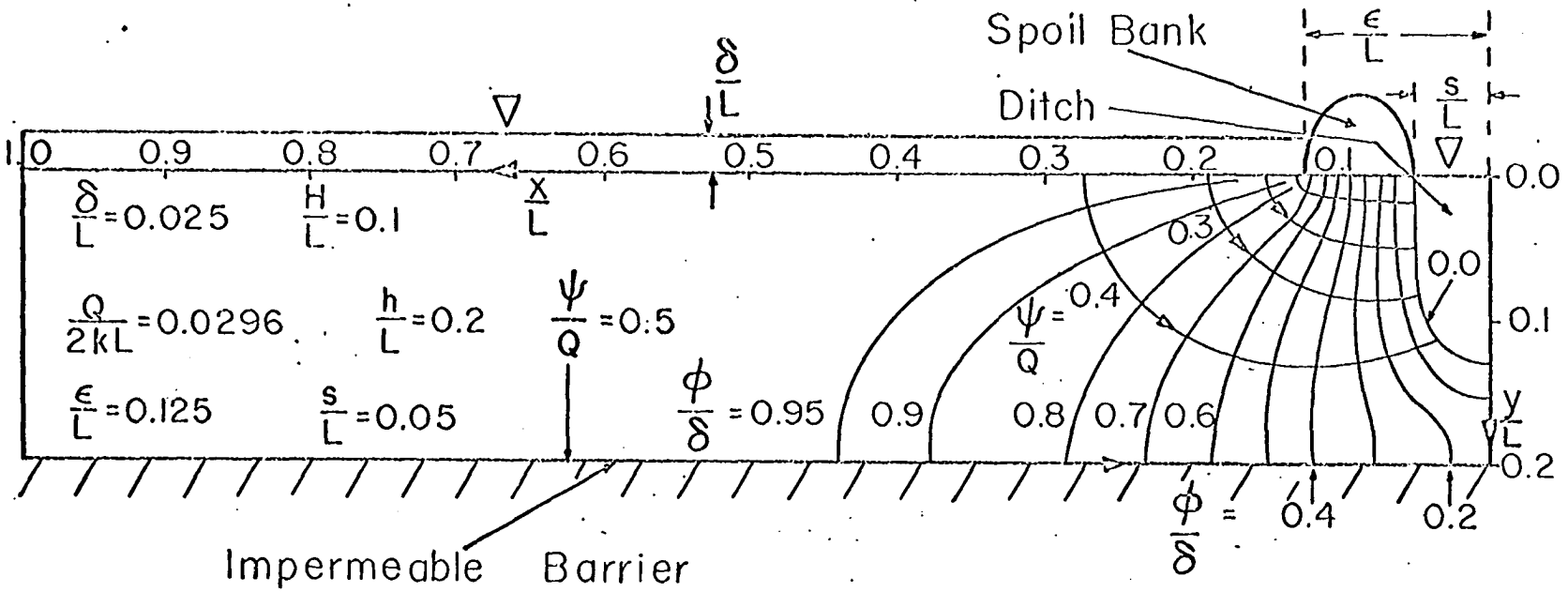

Figure 21. Flow net of two-dimensional seepage of ponded water to a full ditch drain when an impermeable barrier is at depth h/L = 0.2. L is the width of the semi-system shown.

top of the ditch. The vertical sink chosen was of length 0.1L along the y-axis and resulted in the zero equipotential simulating the ditch wall to be of approximate depth 0.13L. If L = 6 meters the corresponding values of ponded water depth, semi-width of ditch, depth to impermeable barrier and soil bank width are, in meters, ö = 0.15, s = 0.3, h = 1.2, and ε - s = 0.45. The values of m_z^2, m_w^2, and ϕ_o/L were calculated and were $[1 - (8)(10)^{-6}]$, 0.2901, and 0.0112, respectively.

The rate of dimensionless flow rate was found to be Q/2kL = 0.0296. If L were 6 m and k were 0.18 m/hr (a value of conductivity given by Harr (1962) as a typical value for a sandy loam), Q/2 would be 0.032 m^3/hr/m. This would correspond to an average infiltration rate of 0.005 m/hr (about 4 in/day).

It is observed in Figure 21 that the streamline labeled $\phi/Q = 0.4$ intersects the x-axis at x = 0.28L. As the maximum value of ϕ/Q of the flow medium is 0.5, we calculate 80 percent of the seepage originates at the soil surface between x = 0.125L and 0.28L. If the ponded water were being used to leach salts from the soil medium, the consequence would be relative ineffectiveness in the region beyond x = 0.3. If the ditch were being used to remove excess water only, the velocity distribution of seepage water intake would not be as important. If one were leaching salts, he would ordinarily want to keep the water in the ditch at a low level.

Figure 22 is a flow net for parameters differing from Figure 21 only in that there is no impermeable barrier present, that is, the depth to the impermeable barrier h is infinity. The length of the vertical

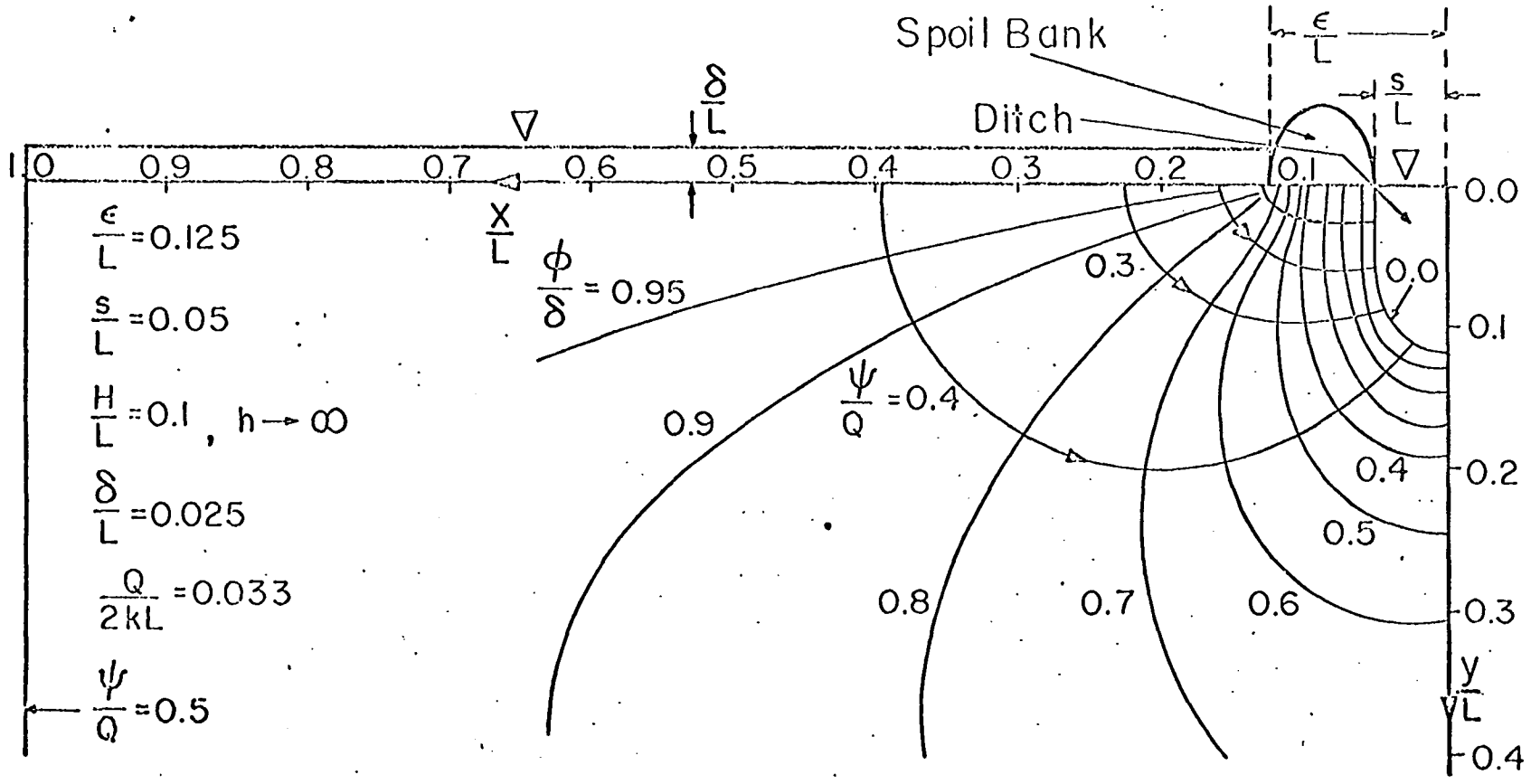

Figure 22. Flow net of two-dimensional seepage of ponded water to a full ditch drain when no lower impermeable soil barrier is present. L is the width of the semi-system shown.

sink was chosen as 0.1L as in the previous example, but resulted in a slightly shallower ditch of 0.12L compared with 0.13L. The value of Q/2kL is 0.033 compared to 0.0296 for the previous example with the impermeable barrier, implying the barrier at 0.2L resulted in a 13 percent reduction in rate of flow. The streamline labeled $\phi/Q = 0.4$ intercepts the x-axis at $x = 0.39L$ compared to $x = 0.28L$ for the previous example. Thus, the seepage velocities at points far away from the ditch are relatively as well as absolutely less when a barrier is present. Values of m_w^2 and ϕ_o/L were determined to be 0.380 and 0.0118, respectively, for the system of Figure 22.

V. GENERAL DISCUSSION

Two types of seepage problems have been considered. The first type of problems were for two-dimensional flow from a stationary plane water table to tile drains near a foundation barrier and were analyzed for 14 different flow geometries. The second type of problems were for two-dimensional agriculture drainage of ponded water to a full ditch drain where an impermeable soil barrier was present at a finite depth and later when the barrier was at an infinite depth. The first type of problems will now be discussed.

Figure 4 is a nomograph that was presented to determine potential and pressure heads along the foundation for the first 13 problems solved. By integrating the pressure along the foundation base, one could determine total uplift force on the foundation which could occur at an eventual crack.

The effect of a vertical sheetpile near a foundation perhaps deserves more attention than is given to it in this thesis. For the geometry of Figure 16, the vertical sheetpile reduced the maximum pressure head along the foundation and between the wall and the drain by 62 percent from the pressure head when no sheetpile was present. It would be relatively easy to study the effectiveness of a shorter sheetpile and also the influences of different tile placings.

The multiple drain problem the last foundation problem worked could be expanded to include many more drains. Perhaps, the results obtained by Grover, Ligon, and Kirkham (1960) on the edge effects of a drainage system could be analyzed theoretically. The problem of flow to a crack rather than to a tube could be considered. An infinitely long crack running perpendicular to the two-dimensional system studied would have

the same solution as for a small slot sink. The small slot sink would be equivalent to a tube drain of an appropriate size.

Another problem which could probably be solved using the same methods as those of the first section would be that of seepage to drains under a foundation on a right-angled terrace. The two-dimensional cross-section of the flow region might be similar to a step function with the side and floor of the foundation forming a barrier and the rest of the boundary being plane free surfaces.

Drainage problems with subsurface artesian water sources could be worked out using the methods of this thesis for both the foundation and agriculture drainage problems. In solving artesian flow problems by this method, it would be necessary to assume the potential (or the flux) was constant along a horizontal plane.

All examples considered have been steady-state systems. Perhaps corresponding nonsteady-state problems could be solved by assuming equivalence to a series of steady-state cases in a manner similar to that used by Ligon, Johnson, and Kirkham (1964). The assumption of equivalence to a series of steady-state cases would seem to be particularly appropriate for the ponded water problems since the driving potential gradients are small, the flow velocities are low, and the systems would change slowly with time.

VI. SUMMARY

This thesis presents a theoretical treatment of seepage into drain facilities located near barriers of two types, foundation barriers as of buildings and impermeable soil barriers preventing natural deep drainage of land. In the foundation problems 14 situations are analyzed. In the first 12 foundation drainage problems there are one or two drains located next to the foundation forming a symmetric system; in particular, for one drain it is at the center of the foundation base and for two drains they must be equidistant from a plane of symmetry. In all cases, the drain tubes are considered to be infinitely permeable, which, in practice, is equivalent to surrounding them with gravel or another highly permeable material. A special problem is considered with the drains at the edge of the foundation. In problem 13 sheetpiling extends vertically downward at the edge of the foundation. In problem 14, called the multiple drain problem, a two-drain unsymmetric system was studied. In all 14 foundation problems, a layer of water-saturated coarse gravel was assumed to have been located at the sides of the foundation. This gravel extended fully or partially down the foundation sides. In some problems, ponded water was assumed to exist at the soil surface at the foundation sides.

There were two agricultural field drainage problems solved. In each of the problems, ponded surface water contained between parallel ditch banks seeped through the soil and under the banks into parallel equally spaced drainage ditches. In the first problem, drainage ditches extended vertically downward part way to an impermeable horizontal

soil barrier that prevents natural deep seepage. The second agricultural drainage problem differed from the first only in that the barrier was taken to be at great depth, mathematically at infinity.

In all problems, the foundation and field drainage problems, the flow for analytic purposes was assumed to be two-dimensional and conformal transformations were used. In the conformal transformation procedure the Schwartz-Christoffel transformation was utilized. The physical flow region in the z-plane was transformed to an auxilliary t-plane. Then a rectilinear flow net plane (the complex potential plane) was transformed to the same auxilliary t-plane so that finally the complex potential plane could be transformed to the physical flow plane. Nine flow nets were worked out and drawn. The numerical calculations were made with the aid of a high speed digital computer. The flow nets provided the hydraulic head and the value of the stream function for points in the flow medium. Of particular interest was the hydraulic head along the base of the foundation in the foundation problems. The hydraulic head was the same as the pressure head along the foundation and gave the maximum pressure at an eventual crack in the foundation. In one example given, a single tube at the center of the foundation reduced the maximum pressure head along the foundation base by 15 percent. Two tubes, one at each corner and of the same size, reduced the maximum pressure by 48 percent. In the example, gravel did not extend down to the base of the foundation. At the drain tubes themselves the pressure was reduced to zero.

In the analyses and in the drawn flow nets the drain tubes of

the foundations were often taken to be of semicircular cross-section with their diameters touching a plane barrier. If the radius of the semicircular tube is a, then the equivalent circular tube is of a smaller radius $2a/\pi$.

VII. LITERATURE CITED

Abramowitz, M. and Stegun, I. A., eds. 1964. Handbook of Mathematical functions. National Bureau of Standards Applied Mathematics Series No. 55. Washington, D.C., U.S. Department of Commerce.

Adams, E. P. 1935. Electrical distributions on circular cylinders. American Philosophical Society Proceedings 75: 11-70.

Asseed, M. and Kirkham, D. 1966. Depth of barrier and water table fall in a tile drainage model. Soil Science Society of America Proceedings 30: 292-298.

Beer, C. E., Johnson, H. P. and Roth, F. W. 1963. What can you do about a wet basement. Iowa Farm Science 18: 13-16.

Bewley, L. V. 1948. Two-dimensional fields in electrical engineering. New York, New York, The Macmillan Company.

Bouwer, H. and van Schilfgaarde, J. 1963. Simplified method of predicting fall of water table in drained land. American Society of Agricultural Engineers Transactions 6: 288-291.

Byrd, P. F. and Friedman, M. D. 1954. Handbook of elliptic integrals for engineers and physicists. Berlin, Germany, Springer-Verlag.

Childs, E. C. 1943. The water table, equipotentials, and streamlines in drained land. I. Soil Science 56: 317-330.

Childs, E. C. 1945a. The water table, equipotentials, and streamlines in drained land. II. Soil Science 59: 313-327.

Childs, E. C. 1945b. The water table, equipotentials, and streamlines in drained land. IV. Soil Science 59: 405-415.

Childs, E. C. 1946. The water table, equipotentials, and streamlines in drained land. IV. Soil Science 62: 183-192.

Churchill, R. V. 1960. Complex variables and applications. 2nd ed. New York, New York, McGraw-Hill Book Company, Inc.

Creasy, L. R. 1963. Watertight concrete basements. Structural Concrete 1: 109-134.

DeBoer, D. 1963. Model study of basement and footing drains. National Student Journal of American Society of Agricultural Engineers 1963: 14-16.

DeJong, G. D. 1965. A many-valued hodograph in an interface problem. Water Resources Research 1: 543-555.

Dwight, H. B. 1961. Tables of integrals and other mathematical data. 4th ed. New York, New York, The Macmillan Company.

Fukuda, H. 1957. Underdrainage into ditches in soil overlying an impervious substratum. American Geophysical Union Transactions 38: 730-739.

Grover, B. L. and Kirkham, D. 1964. Solving tile drainage problems by using model data. Iowa Agricultural and Home Economics Experiment Station Research Bulletin 523.

Grover, B. L., Ligon, J. T., and Kirkham, D. 1960. Operational characteristics of the laterals near the edge of a tile drainage system. Journal of Geophysical Research 65: 3733-3738.

Harr, M. E. 1962. Groundwater and seepage. New York, New York, McGraw-Hill Book Company, Inc.

Harvard Computation Laboratory. 1949. Tables of the function arcsin z. Cambridge, Massachusetts, Harvard University Press.

Hinesly, T. D. and Kirkham, D. 1966. Theory and flow nets for rain and artesian water seeping into soil drains. Water Resources Research 2: 497-511.

Jolley, L. B. W. 1961. Summation of series. 2nd ed. New York, New York, Dover Publications, Inc.

Kirkham, D. 1947. Reduction in seepage to soil underdrains resulting from their partial embedment in, or proximity to, an impervious substratum. Soil Science Society of America Proceedings 12: 54-59.

Kirkham, D. 1949. Flow of ponded water into drain tubes in soil overlying an impervious layer. American Geophysical Union Transactions 30: 369-385.

Kirkham, D. 1958. Seepage of steady rainfall through soils into drains. American Geophysical Union Transactions 39: 892-908.

Kirkham, D. 1966. Steady-state theories for drainage. Journal of the Irrigation and Drainage Division, American Society of Civil Engineers 92, No. IR1: 19-39.

Kober, H. 1957. Dictionary of conformal representations. New York, New York, Dover Publications, Inc.

Lamb, H. 1945. Hydrodynamics. 6th ed. New York, New York, Dover Publications, Inc.

Lazarr, T. R. L. 1965. Waterproofing below the ground line. Civil Engineering, American Society of Civil Engineers 35: 73.

Leliavsky, S. 1955. Irrigation and hydraulic design. Volume 1. London, England, Chapman and Hall Ltd.

Ligon, J. T., Kirkham, D. and Johnson, H. P. 1964. The falling water table between open ditch drains. Soil Science 97: 113-118.

List, E. J. 1964. The steady flow of precipitation to an infinite series of tile drains above an impervious layer. Journal of Geophysical Research 69: 3371-3381.

Luthin, J. N., ed. 1957. Drainage of agricultural lands. Madison, Wisconsin, American Society of Agronomy.

Luthin, J. N. 1966. Drainage engineering. New York, New York, John Wiley and Sons, Inc.

Maasland, M. 1953. Tile drainage in anisotropic soil. Unpublished M.S. thesis. Ames, Iowa, Library, Iowa State University of Science and Technology.

Muskat, M. 1946. The flow of homogeneous fluids through porous media. Ann Arbor, Michigan, J. W. Edwards, Inc.

Peirce, B. O. 1956. A short table of integrals. 4th ed. Waltham, Massachusetts, Blaisdell Publishing Company.

Polubarinova-Kochina, P. Y. 1962. Theory of ground water movement. Princeton, New Jersey, Princeton University Press.

Powers, W. L., Kirkham, D. and Snowden, G. 1967. Seepage of steady rainfall through soil into ditches of unequal water level height. Soil Science Society of America Proceedings 31: 307-312.

Powers, W. L., Kirkham, D. and Snowden, G. ca. 1968. Orthonormal function tables and the seepage of steady rain through soil bedding. [To be published in the Journal of Geophysical Research.]

Tice, L. M. 1965. Stop plant basement leaks. Plant Engineering 19: 152-154.

Toksoz, S. and Kirkham, D. 1961. Graphical solution and interpretation of a new drain-spacing formula. Journal of Geophysical Research 66: 509-516.

Van Deemter, J. J. 1949. Results of mathematical approach to some flow problems connected with drainage and irrigation. Applied Scientific Research A2: 33-53.

Van Deemter, J. J. 1950. Bijdragen tot de kennis van enige natuurkundige grootheden van de grond, 11, theoretische en numerieke behandeling van ontwatering-en infiltratie-stromingsproblemen. Verslagen Van Landbouwkundige Onderzoekingen No. 56.7.

Van Schilfgaarde, J., Kirkham, D. and Frevert, R. K. 1956. Physical and mathematical theories of tile and ditch drainage and their usefulness in design. Iowa Agricultural and Home Economics Experiment Station Research Bulletin 436.

Warrick, A. W. 1964. Theory of soil water seepage near tile drains for a curved water table. Unpublished M.S. thesis. Ames, Iowa, Library, Iowa State University of Science and Technology.

Warrick, A. W. 1966. A discussion of Kirkham's "steady-state theories for drainage". Journal of Irrigation and Drainage Division, American Society of Civil Engineers 35, No. IR4: 84-88.

Wesseling, J. 1964. The effect of using continually submerged drains on drain spacing. Journal of Hydrology 2: 33-43.

Whipple, F. J. W. 1920. Equal parallel cylindrical conductors in electrical problems. Royal Society of London Proceedings, Series A, 96: 465-475.

VIII. ACKNOWLEDGEMENTS

This investigation was supported by Public Health Service Research Grants WP-00070-03, 04, and 05 under Project 998 of the Iowa Agricultural and Home Economics Experiment Station, Ames, Iowa.

The author expresses his sincere appreciation to Dr. Don Kirkham for his advice and assistance throughout his degree program and in the preparation of this manuscript. Special thanks are also given to the Soil Physics graduate students for their help, suggestions and encouragement.

The author also wishes to thank his wife, Shan, and family for their help, encouragement and patience.

IX. APPENDIX 1: DETERMINATION OF EQUIVALENT RADII FOR HALF-TUBE AND WHOLE-TUBE DRAINS IN CONTACT WITH AN IMPERMEABLE BARRIER

We consider as in Figure 23 a half-tube drain ABCDEOA of radius a with a semicircular cross-section. The diameter EOA is in contact with the barrier (the x-axis). Also in Figure 23 is a circular whole-tube drain OBFDO of radius b, and whose center is at H, which is tangent to the x-axis at the origin. If b is larger than a/2 then the two tubes must intersect at B and D as shown. Below the x-axis are image drains AB'C'D'EOA and OB'F'D'O which are symmetric with respect to the barrier. We assume the walls of the tubes are at a potential $\phi = 0$ and are infinitely permeable, an assumption which does not lead to serious error if the tubes are surrounded by an envelope of gravel.

We wish to compare the potential about the half-tube drain with that of the whole-tube drain in the upper z-plane. A constant radii ratio a/b will be sought which results in the same amount of flow to either the half-tube or the whole-tube when the potential distribution at some distance away from the tubes is the same in both cases. If there exists such a constant radii ratio a/b giving the same flow, then solutions for problems using a half-tube in contact with a barrier, or equivalently a single whole-tube whose diameter is on the barrier, would be applicable for whole-tubes tangent to a barrier or to a pair of whole-tubes touching each other at the barrier, such as OBFDO and its image tube OB'F'D'O. Kirkham (1949), in a similar problem, compared flows from the same boundary sources to different types of tubes on a barrier. He established an inequality, proving that a whole-tube of

Figure 23. A half-tube drain ABCDEOA of radius a and an equivalent whole-tube drain OBFDO of smaller radius $b = 2a/\pi$. Each tube is in contact with the barrier along the x-axis. The images below the x-axis are shown.

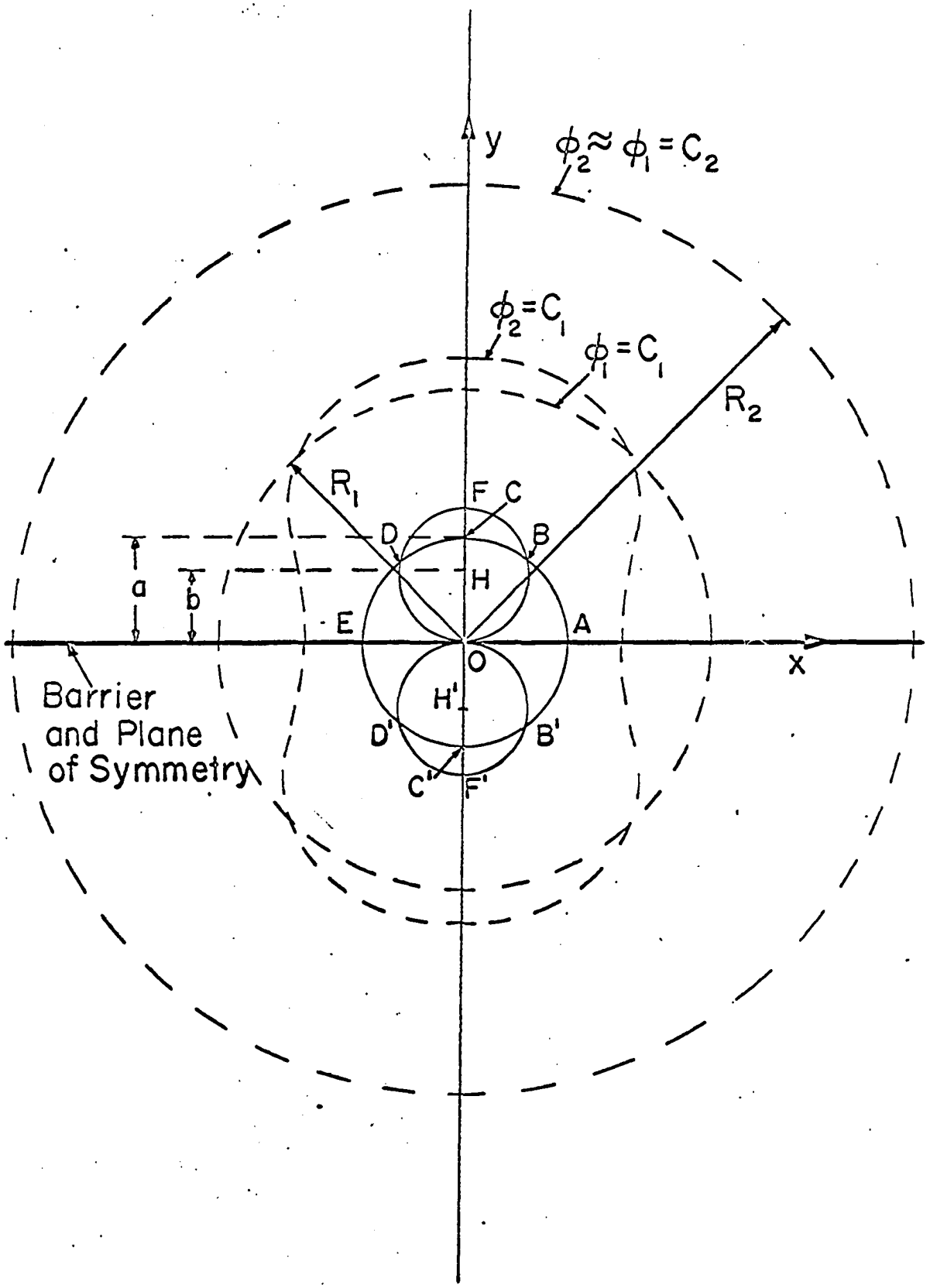
y
$\phi_2 \approx \phi_1 = C_2$
$\phi_2 = C_1$
$\phi_1 = C_1$
R_2
R_1
F
C
D
B
H
a
b
E
A
O
X
H'
D'
B'
C'
F'
Barrier
and Plane
of Symmetry

radius r which is tangent to the barrier has more flow going to it than the quantity of flow into a half-tube of radius r whose diameter is on the barrier, but less than flow into an equipotential resulting from a point sink at a point r from the barrier and whose outside surface passes through a point 2r from the barrier. In our case, we find an equivalent circular tube to provide the same flow as a semicircular tube.

Let Q be the amount of flow into the half-tube ABCDEOA of Figure 23 which is at a potential of $\phi_1 = 0$ and whose surrounding equipotentials are semicircles such as those shown of radius R_1 and R_2. The potential function is the same as if the center of the tile were a point sink and is given by eq. 3, page 64 of Lamb (1945) or is easily shown to be

$$\phi_1 = (Q/k\pi) \ln(r/a) \tag{274}$$

where

$$r^2 = x^2 + y^2 \tag{275}$$

and where Q is taken to be positive in sign.

Whipple (1920) and Adams (1935) each solved electrical problems with infinitely long, parallel charged circular cylinders which may be adapted to give the potential for the whole tile OBFDO. Whipple considered pairs of parallel cylinders of equal size which for a special case could be touching and would be analogous to our problem. Adams (1935) considered touching charged circular cylinders of unequal size, but which in the special case of equal sized cylinders would correspond to our problem. We adapt Adams' problem to our situation.

By choosing the radii of the touching cylinders equal of Adams (1935), his eq. 12 gives the complex potential w_E of the electrostatic problem

for our coordinates as

$$w_E = 4\pi iQ - 4Q \cosh^{-1}\csc(i\pi b/z) \tag{276}$$

where 2Q is the total charge on both of the cylinders per unit length and the surfaces of the cylinders are of a potential $\phi = 0$. The flux lines extend outward to infinity.

Replacing his value of Q by our $-Q/4\pi$, we find, by analogy, the complex potential about the whole-tube OBFDO of Figure 23 as

$$k\phi_2 + i\psi = -iQ + (Q/\pi) \cosh^{-1}\csc(i\pi b/z) \tag{277}$$

The real part of the last equation is the hydraulic head ϕ_2,

$$\phi_2 = \text{Real}\{(Q/k\pi) \cosh^{-1}\csc(i\pi b/z)\} \tag{278}$$

where "real" on the r.h.s. denotes the real part of the expression in braces.

Use of eq. 701 of Dwight (1961) gives the identity

$$\cosh^{-1}\csc \alpha = \ln[\csc \alpha + (\csc^2\alpha - 1)^{1/2}]$$

By 400.14, 403.02 and 403.5 of Dwight, the last equation reduces to

$$\cosh^{-1}\csc \alpha = \ln \cot(\alpha/2)$$

The last equation and Equation 278 give

$$\phi_2 = \text{Real}\{(Q/k\pi) \ln \cot(i\pi b/2z)\} \tag{279}$$

We define the polar angle θ by

$$z = r\, e^{i\theta} \tag{280}$$

where

$$e^{i\theta} = \cos\theta + i \sin\theta \tag{281}$$

Use of Equation 280 gives for ϕ_2 from Equation 279

$$\phi_2 = \text{Real}\{(Q/k\pi) \ln \cot[(i\pi b/2r)e^{-i\theta}]\} \tag{282a}$$

or alternatively by Equation 281, the last equation is

$$\phi_2 = \text{Real}\{(Q/k\pi)\ \ln \cot[(\pi b/2r)(\sin\theta + i\cos\theta)]\} \tag{282b}$$

We can use eq. 408.19 of Dwight and the last equation to give

$$\phi_2 = \text{Real}\{(Q/k\pi)\ \ln(A + iB)\} \tag{283}$$

where A and B are given by

$$A = \frac{\sin[(\pi b/r)\ \sin\theta]}{\cosh[(\pi b/r)\ \cos\theta] - \cos[(\pi b/r)\ \sin\theta]} \tag{284}$$

and

$$B = -\frac{\sinh[(\pi b/r)\ \cos\theta]}{\cosh[(\pi b/r)\ \cos\theta] - \cos[(\pi b/r)\ \sin\theta]} \tag{285}$$

Since the real part of a logarithm of a complex number is equal to the logarithm of the modulus of the complex number, we have by Equation 283 the result

$$\phi_2 = (Q/k\pi)\ \ln(A^2 + B^2)^{1/2} \tag{286}$$

which is the potential function for the whole-tube OBFDO of Figure 23. We note for the special cases of $x = 0(\theta = \pi/2)$ and $y = 0(\theta = 0)$ that A and B of Equations 284 and 285 simplify giving for Equation 286

$$(\phi_2)_{x=0} = (Q/k\pi)\ \ln \cot(\pi b/2r) \tag{287a}$$

$$(\phi_2)_{y=0} = (Q/k\pi)\ \ln \coth(\pi b/2r) \tag{287b}$$

which are the minimum and maximum values, respectively, for ϕ_2 at a given value of r (see the equipotential $\phi_2 = C_1$ of Figure 23). By Dwight 415.04 and 657.4, we observe for large values of r that the last two equations become

$$(\phi_2)_{x=0} = (Q/k\pi)\ \ln[(2r/\pi b) - (1/3)(\pi b/2r)], \qquad r >> 1 \tag{288a}$$

$$(\phi_2)_{y=0} = (Q/k\pi)\ \ln[(2r/\pi b) + (1/2)(\pi b/2r)], \qquad r >> 1 \tag{288b}$$

where the error in the argument of the logarithm terms is of the order

of r^{-3}. For large values of r, each of the last two equations approaches the value of ϕ_1 of Equation 274 provided $(2r/\pi b) = r/a$ or if a and b are related by

$$a = \pi b/2 \tag{289}$$

Thus, the sought for ratio of radii $a/b = \pi/2$ and the maximum difference in ϕ_1 and ϕ_2 for a given r may be determined by Equations 274, 288a and 288b.

We shall now obtain an approximation of Equation 286 similar to Equation 288a and Equation 288b, but good for all values of θ. We consider the cotangent term in Equation 282a and define D by

$$D = 2r/\pi b \tag{290}$$

Use of Equation 290 and Dwight 408.13 gives from Equation 282a

$$\phi_2 = (Q/k\pi) \ln\left|-i \coth(e^{-i\theta}/D)\right| \tag{291}$$

Dwight 657.4 gives

$$\coth^{-1}(e^{-i\theta}/D) = (D + 1/3D) \cos\theta + i(D - 1/3D) \sin\theta, \qquad D >> 1$$

Neglecting terms of the order D^{-2}, we find for the modulus of $i \coth(e^{-i\theta}/D)$ from the last equation as

$$\left|i \coth(e^{-i\theta}/D)\right| = D[1 + (\cos 2\theta)/3D^2], \qquad D >> 1$$

The last equation along with Equation 291 gives an approximation of ϕ_2 which neglects terms of the order r^{-3} in the argument of the logarithm as

$$\phi_2 = (Q/k\pi) \ln\{(2r/\pi b)[1 + (\pi b/2r)^2 \frac{\cos 2\theta}{3}]\}, \qquad 2r/\pi b >> 1 \tag{292}$$

We note the last equation reduces to Equation 288a for $\theta = \pi/2$ and to Equation 288b for $\theta = 0$.

In Figure 23 the curves labeled $\phi_1 = C_1$ and $\phi_2 = C_2$ are schematic equipotentials resulting from a half-tube ABCDEOA of radius a and the whole-tube OBFDO of radius $b = (2a/\pi)$, respectively. The $\phi_1 = C_1$ equipotential must be a semicircle of the radius R_1. The $\phi_2 = C_2$ equipotential will be at a greater distance from the origin along the y-axis, will be at the same distance for θ approximately $\pi/4$ and $3\pi/4$, and will be at a lesser distance along the x-axis. At the greater distance R_2 from the origin the $\phi_1 = C_2$ and $\phi_2 = C_2$ equipotentials will for practical purposes coincide.

The resulting ratio of radii $a/b = \pi/2$ is appropriate to interchange the solution for the half-tube and for the whole-tube for all types of boundary geometries where the equipotentials may be regarded as nearly circular for a distance of $r = 3a$ or more from the center of the tile. To verify this, we use Equations 287a and 287b to determine ϕ_2 exactly for $r = 3a$ and $b = \pi a/2$ as

$$(\phi_2)_{x=0,y=3a} = 1.06(Q/k\pi)$$

$$(\phi_2)_{x=3a,y=0} = 1.13(Q/k\pi)$$

The corresponding value of ϕ_1 by Equation 274 is

$$(\phi_1)_{r=3a} = 1.10(Q/k\pi)$$

Thus, the maximum difference at $r = 3a$ between ϕ_1 and ϕ_2 is less than 4 percent. Similarly, for $r = 2a$ the maximum difference between ϕ_1 and ϕ_2 is less than 13 percent.

X. APPENDIX 2: EVALUATION OF sn(m,u) FOR u COMPLEX

Eq. 908.01 of Byrd and Friedman (1954) gives

$$sn(m,u) = (\pi/mK) \sum_{odd}^{\infty} \frac{\sin(n\pi u/2K)}{\sinh(n\pi K'/2K)} \tag{293}$$

where "odd" denotes n is to take on all positive odd integer values. We consider m to be real. The series is convergent if the imaginary part of u is less than the complementary complete elliptic integral of the first kind K'.

Defining the real and imaginary parts of u by A and B, we may write

$$u = A + iB \tag{294}$$

We can use eq. 408.16 of Dwight (1961) to separate the real and imaginary parts of Equation 293 giving

$$sn(m,A + iB) = (\pi/mK)[\sum_{odd}^{\infty} \frac{\cosh(n\pi B/2K)}{\sinh(n\pi K'/2K)} \sin(n\pi A/2K)$$

$$+ i \sum_{odd}^{\infty} \frac{\sinh(n\pi B/2K)}{\sinh(n\pi K'/2K)} \cos(n\pi A/2K)] \tag{295}$$

We now shall show that faster converging series than Equation 295 can be developed by subtracting an appropriate exponential from each hyperbolic ratio and adding back the same exponential in a separate summation for which an analytic expression is known. We may write from Equation 295 the identity

$$sn(m,A + iB) = (\pi/mK) \sum_{odd}^{\infty} \{\frac{\cosh(n\pi B/2K)}{\sinh(n\pi K'/2K)} - \exp[-n\pi(K' - B)/2K]\} \sin(n\pi A/2K)$$

$$+ i(\pi/mK) \sum_{odd}^{\infty} \{\frac{\sinh(n\pi B/2K)}{\sinh(n\pi K'/2K)} - \exp[-n\pi(K' - B)/2K]\} \cos(n\pi A/2K)$$

$$+ (\pi/mK)(S_1 + iS_2) \tag{296}$$

where S_1 and S_2 are given by

$$S_1 = \sum_{\text{odd}}^{\infty} \exp[-n\pi(K' - B)/2K] \sin(n\pi A/2K) \tag{297a}$$

$$S_2 = \sum_{\text{odd}}^{\infty} \exp[-n\pi(K' - B)/2K] \cos(n\pi A/2K) \tag{297b}$$

We define a by

$$a = \exp[-\pi(K' - B)/2K] \tag{298}$$

Using the easily verified relationship

$$\sum_{\text{odd}}^{\infty} f(n) = \sum_{n=1}^{\infty} f(n) - \sum_{n=1}^{\infty} f(2n) \tag{299}$$

where f(n) is the nth term of an arbitrary convergent series, we have for Equations 297a and 297b

$$S_1 = \sum_{n=1}^{\infty} a^n \sin(n\pi A/2K) - \sum_{n=1}^{\infty} (a^2)^n \sin(n\pi A/K) \tag{300a}$$

$$S_2 = \sum_{n=1}^{\infty} a^n \cos(n\pi A/2K) - \sum_{n=1}^{\infty} (a^2)^n \cos(n\pi A/K) \tag{300b}$$

Application of eq. 499 and 500 of Jolley (1961) gives for S_1 and S_2

$$S_1 = \frac{a \sin(\pi A/2K)}{1 - 2a \cos(\pi A/2K) + a^2} - \frac{a^2 \sin(\pi A/K)}{1 - 2a^2 \cos(\pi A/K) + a^4} \tag{301a}$$

$$S_2 = \frac{1 - a \cos(\pi A/2K)}{1 - 2a \cos(\pi A/2K) + a^2} - \frac{1 - a^2 \cos(\pi A/K)}{1 - 2a^2 \cos(\pi A/K) + a^4} \tag{301b}$$

where a is defined by Equation 298. Equations 296, 301a and 301b were used for calculating t from Equation 263a.